THE ASTROPHYSICAL JOURNAL

An International Review of Spectroscopy and Astronomical Physics

VOLUME 79

JANUARY–JUNE 1934

THE UNIVERSITY OF CHICAGO PRESS
CHICAGO, ILLINOIS

THE CAMBRIDGE UNIVERSITY PRESS, LONDON
THE MARUZEN COMPANY LIMITED, TOKYO
THE COMMERCIAL PRESS, LIMITED, SHANGHAI

PUBLISHED JANUARY, MARCH, APRIL, MAY,
JUNE, 1934

COMPOSED AND PRINTED BY THE UNIVERSITY OF CHICAGO PRESS
CHICAGO, ILLINOIS, U.S.A.

CONTENTS

NUMBER I

NUMBER II

NUMBER III

NUMBER IV

NUMBER V

THE ASTROPHYSICAL JOURNAL

AN INTERNATIONAL REVIEW OF SPECTROSCOPY AND ASTRONOMICAL PHYSICS

VOLUME 79 JANUARY 1934 NUMBER 1

COLOR TEMPERATURES OF B-TYPE STARS AND RAYLEIGH SCATTERING

By O. STRUVE, P. C. KEENAN, and J. A. HYNEK

ABSTRACT

Observations of two red B stars indicate that their energy-curves are consistent with Planck's law for temperatures which are considerably lower than those usually attributed to normal B stars. The results are not in harmony with Rayleigh scattering, but do not disprove other types of scattering.

I

Several years ago the suggestion was made by H. N. Russell[1] that local selective absorption might be the cause of the abnormally yellow color of three B-type stars situated within 5° of one another, in a region full of diffuse nebulosity. In 1926 Struve[2] investigated the color excesses of early type stars, determined by Bottlinger,[3] and found several regions in the sky where the colors are systematically either too red or too blue. He made the suggestion that reddening in certain areas may be produced by light-scattering in dark nebulae or in calcium clouds. Recent investigations by Elvey,[4] Becker,[5] and

[1] *Proceedings of the National Academy of Sciences*, **5**, 398, 1919.

[2] *Astronomische Nachrichten*, **227**, 377, 1926.

[3] *Veröffentlichungen der Sternwarte Berlin-Babelsberg*, **3**, Part IV, 1923.

[4] *Astrophysical Journal*, **74**, 298, 1931; **75**, 354, 1932.

[5] *Veröffentlichungen der Sternwarte Berlin-Babelsberg*, **10**, Part III, 1933; *Zeitschrift für Astrophysik*, **5**, 101, 1932; J. Dufay and Ssu-Pin Liau, *Comptus rendus*, **196**, 1372, 1933.

Stebbins and Huffer[6] have added strong evidence to the hypothesis of a selectively scattering medium concentrated in Hubble's region of avoidance of extra-galactic nebulae, near the central line of the Milky Way. On the other hand, it is rather surprising that the correlation between color excess and intensity of interstellar calcium lines is as weak as Gerasimovič,[7] Struve,[8] and Miss Westgate[9] have found it to be. Both Elvey and Becker have suggested that the scattering medium may not be coexistent with the interstellar gas, but we have at present little information as to whether the type of reddening observed in B stars is consistent with the theory of Rayleigh scattering.[10] It is the purpose of this paper to find whether the energy-curves of some of the reddest B stars are in harmony with the hypothesis of Rayleigh scattering. Such tests have already been made by Trumpler[11] and by Gerasimovič.[12] The former measured the difference in photographic density, at various wave-lengths, between several red B stars in clusters and normal B's in the same region. The latter worked on a general program of early-type stars, referring the measured intensities to those of Ao comparison stars as standards.

II

Consider two stars of temperatures T_1 and T_2 which radiate as black bodies, and let the first star be affected by Rayleigh scattering. Then, using Wien's approximation to Planck's law, we have

$$E_1(\lambda)=c_1\lambda^{-5}e^{-\frac{c_2}{\lambda T_1}}e^{-\beta\lambda^{-4}H},$$

$$E_2(\lambda)=c_1\lambda^{-5}e^{-\frac{c_2}{\lambda T_2}},$$

where

$$\beta=\frac{32}{3}\frac{\pi^3(m-1)^2}{N},$$

[6] *Proceedings of the National Academy of Sciences*, **19**, 597, 1933.

[7] *Harvard Observatory Circular*, No. 339, 1929.

[8] *Naturwissenschaften*, **17**, 717, 1929.

[9] *Astrophysical Journal*, **78**, 65, 1933.

[10] O. Struve, *Popular Astronomy*, **41**, 423, 1933.

[11] *Publications of the Astronomical Society of the Pacific*, **42**, 267, 1930.

[12] *Loc. cit.*

m is the coefficient of refraction of the medium, and N is the number of particles per cubic centimeter.

The quantity actually measured is

$$\Delta m = -2.5 \log_{10} \frac{E_1}{E_2} = c\left(\frac{c_2}{\lambda T_2} - \frac{c_2}{\lambda T_1} - \frac{\beta H}{\lambda^4}\right). \tag{1}$$

Consequently, if Δm is plotted against $1/\lambda = \nu$, we obtain a straight line if $\beta = 0$ and a curved line depending upon $1/\lambda^3$ if $\beta \neq 0$. The spectrophotometric gradient used by Gerasimovič is

$$\text{Gradient} = \frac{d(\Delta m)}{d\frac{1}{\lambda}} = \frac{c_2}{T_2} - \frac{c_2}{T_1} - \frac{4\beta H}{\lambda^3}, \tag{2}$$

which is a constant if $\beta H = 0$. The error introduced in the discussion by the use of Wien's formula in place of the precise expression by Planck is insignificant because the observed energy-curves of the stars in the narrow range between λ 3500 and λ 6200 are not sufficiently accurate to make a distinction between the two expressions possible.

By measuring a red B star against a comparison star having a similar absorption-line spectrum, we obtain a curve which must be interpreted in the light of equation (2). It has usually been assumed that $T_1 = T_2$, and the coefficient βH has then been fitted as accurately as possible to the observations. This method is not entirely satisfactory, because it results in a large range in the values of Δm. If a red and a normal B star are exposed in such a manner that at λ 3500 the intensities of the continuous spectra are identical, the red star will be much stronger at λ 6200; there is always some uncertainty in the photometric measurement of a large Δm. Thus, in Trumpler's work Δm has a range of over 2.5 mag.

There is, however, no theoretical reason why the comparison should be limited to stars having similar absorption spectra. By varying T_2 it is possible to change the slope of the curve in such a manner as to reduce the total range of Δm, thereby increasing the precision of the measurements. In an ideal case we should measure Δm against a comparison star of later class, adjusting T_2 in such a

way that Δm is always small. Then the test of linearity of equation (2) can be easily demonstrated, and if $\beta H = 0$, then $T_2 = T_1$.

If βH is small, the deviation from a straight line will be insignificant. Therefore the test should be limited to B stars which are appreciably reddened.

III

Preliminary measures of color have been made on objective-prism spectrograms of two early-type stars known to be unusually red for their spectral classes: 55 Cygni ($20^h46^m, +45°45'$, H.D. sp. B2, mag. 4.89) and 13 Cephei($21^h52^m, +56°08'$, H.D. sp. B9p, mag. 6.01). The instrument employed was the Zeiss U.V. doublet of 14.5-cm aperture and 81-cm focus, fitted with a 30° prism.

Each plate contains the spectrum of one or more comparison stars placed close to that of the star to be measured, the exposures being timed to make the average densities of the several spectra about the same. Care was taken also to see that all of the stars compared were photographed at nearly the same zenith distance.

The exposures of 55 Cygni were made on both Wratten and Wainwright Hypersensitive Panchromatic and Imperial Eclipse Soft 850 plates in order to make available a range of wave-lengths from 3500 A to 6200 A. Because of its faintness, 13 Cephei was taken only on the blue sensitive plates. The emulsions of both types were calibrated photometrically by means of a tube sensitometer used without a filter. A separate series of sky spectra was taken with a small slit spectrograph provided with a rotating logarithmic sector, for the purpose of determining the corrections for variation of contrast with wave-length to be applied to the mean calibration-curve. Some evidence was found, in agreement with the results of others, that the contrast increases toward the red, particularly for the Panchromatic plates, where the change of slope may amount to as much as 10 per cent. However, since this is of the order of accuracy of the rather rough data on the stars, it was decided to use the mean curves for all reductions. For this reason it must be understood that the accompanying curves are only provisional, but in view of the smallness of the differences in density measured in most cases it is felt that the set of curves is not affected by serious systematic errors. In connection with the more extensive investigation of colors planned here, accurate heterochromatic calibration will necessarily be provided.

The colors of 55 Cygni and of 13 Cephei were obtained by measuring the relative brightnesses of their spectra with respect to those of the comparison stars, at several wave-lengths. Since the absolute values of the differences in magnitude depended entirely upon the conditions of exposure and had no significance, the differences at the intermediate wave-length of 4580 A were set equal to zero and the gradients determined by plotting Δm against wave-number in the usual manner.[13]

The comparison stars were so chosen as to have either the same Harvard spectral classification or the same color, on the basis of Bottlinger's color excesses, as the ones to be investigated. The star 55 Cygni turned out to be redder than we anticipated, so that the A2–A3 comparison stars still show a relative gradient in the same direction as that of the B2–B3 stars.

IV

The results are shown in Figures 1 and 2. It will be seen that the comparison stars of classes B3 and F5 give straight lines. Comparison stars of classes B9, A2, and A3 give straight lines between about λ 4000 and λ 6200; to the violet of λ 4000 they show a "hump," which is evidently identical with the phenomenon discovered by Gerasimovič and called by him "ultra-violet appendage." In agreement with Öpik,[14] we attribute this to the continuous absorption at the limit of the Balmer series of the comparison stars, not to a real increase of radiation in the red B stars. Evidently the strength of the continuous hydrogen absorption in late B stars and in most A stars renders them unsuitable for this type of work.

As long as we do not know the exact amount of the continuous hydrogen absorption, we shall have to doubt all parts of our curves to the violet of λ 4000. There is, however, a strong indication that the observed curves are in agreement with the hypothesis $\beta H = 0$ in equation (2). In other words, whatever the cause of the reddening may be, it converts the energy-curve of a B star into one agreeing, within errors of measurement, with Planck's curve for a definite but relatively low temperature, and disagreeing with the assumption of

[13] B. P. Gerasimovič, *Harvard Bulletin*, **857**, 15, 1928; H. Kienle, *Monthly Notices of the Royal Astronomical Society*, **88**, 700, 1928.

[14] *Harvard Observatory Circular*, No. 359, 1931.

Rayleigh scattering. To bring this latter conclusion out more clearly, we have shown in the diagrams the amount of curvature demanded by Rayleigh scattering. The curves were adjusted in such a way

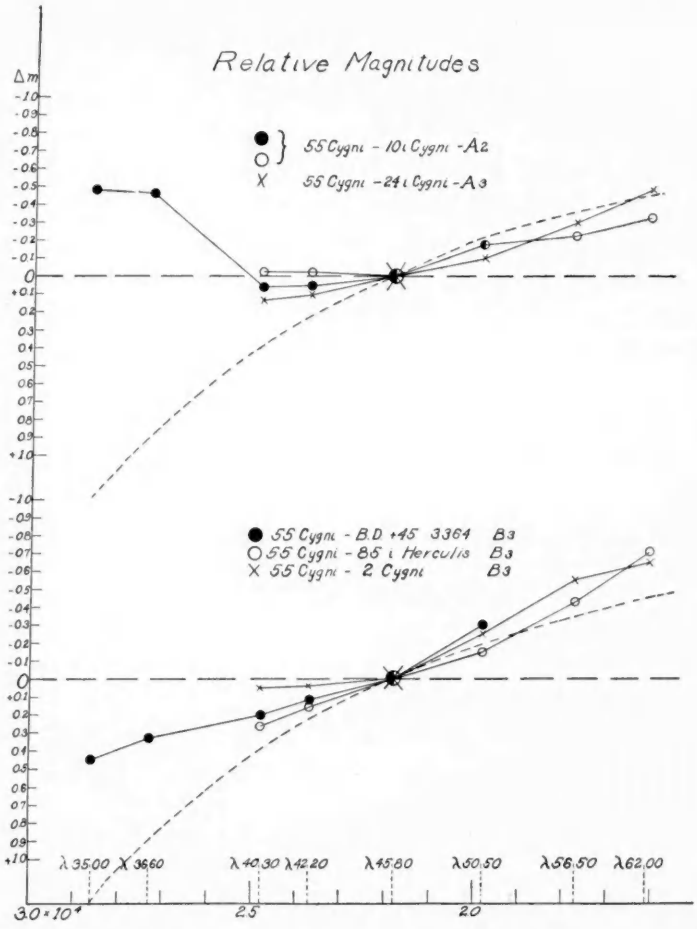

FIG. 1.—The curved broken line represents the effect of Rayleigh scattering

that the slope between λ 4500 and λ 5000 was about that indicated by the comparison stars of early class. In doing so we assume that $T_1 = T_2$ = ionization temperature of the red B star. It is clear that the observed points do not agree with the curve.

A similar uniform variation of Δm with wave-number has been

found in individual cases: by Gerasimovič[13] in P Cygni and by H. Kienle[13] in ζ Persei.

The linearity of the relation is especially striking in the case of 13 Cephei, whose energy-curve seems to be identical with that of a normal F5 star. Inasmuch as the colors of the comparison stars appear to be approximately normal for their spectral classes, we can use the slopes of the observed lines to estimate effective temperatures

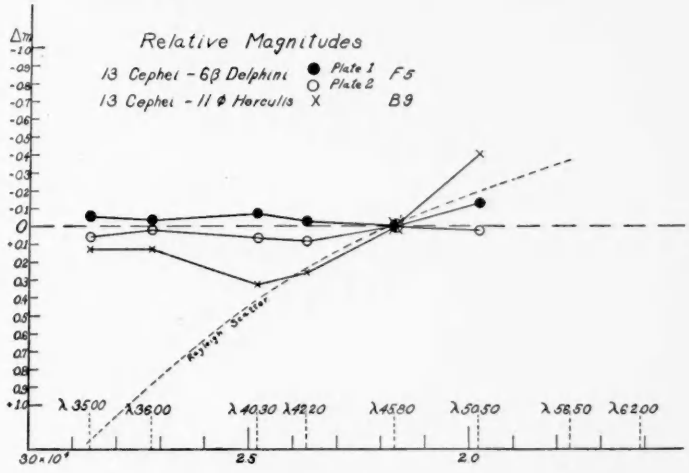

FIG. 2

for the abnormal stars. Adopting the scale of A. Brill,[15] we find an equivalent temperature of 7400° for 55 Cygni and of 7000° for 13 Cephei.

This does not necessarily mean that the temperatures of the red B stars are low, for there are types of scattering which do not introduce curvature. For example, if $\beta \propto \lambda^{-2}$, the observations would be represented. Öpik[16] has discussed this and other possible types of scattering, and Struve has discussed the consequences of our results elsewhere.[17]

YERKES OBSERVATORY
July 1933

[15] *Zeitschrift für Astrophysik*, **3**, 373, 1931.

[16] See n. 14.

[17] *Popular Astronomy*, **41**, 423, 1933.

THE DISTRIBUTION OF EXTRA-GALACTIC NEBULAE[1]

By EDWIN HUBBLE

ABSTRACT

The *object* of the investigation is to determine the distribution of extra-galactic nebulae to a faint uniform limiting magnitude. The *material* consists of counts of about 44,000 nebulae on 1283 plates with the 100-inch and 60-inch reflectors, distributed over the three-quarters of the sky north of $-30°$ Dec. The counts are reduced to the standard conditions of excellent one-hour exposures at the zenith on Eastman 40 plates with the 100-inch reflector.

In general no nebulae are found along the Milky Way. The *zone of avoidance*, representing local obscuration, is irregular and follows the general pattern of the known obscuring clouds. It is bordered by partial obscuration, which fades away into the regions of *normal distribution* where the frequency-curve of $\log N_m$ closely approximates a Gaussian error-curve.

Systematic *variations in longitude* are appreciable only in the lower latitudes, where obscuration appears to be conspicuously greater in the direction of the galactic center than in the opposite direction. There is a definite variation with *latitude*, which from the poles to about $\beta = 15°$ is represented by the *cosecant formula*

$$\log N_m = C - 0.15 \operatorname{cosec} \beta ,$$

indicating a total obscuration of 0.5 mag. from pole to pole with *no appreciable difference* between the two hemispheres.

With allowance for the effect of the red shift, the rate of increase of $\log N$ with exposure time suggests *uniform distribution in depth*.

The standard conditions represent a *threshold of identification* for nebulae at about 20.0 pg m. Corrected for red shift, the *number of nebulae* per square degree to magnitude m is

$$\log N_m = 0.6m - 9.12 ,$$

which leads to values for the *density of matter in space* of $\log \rho = -16.4$ to -16.8 in nebulae per cubic parsec, or -29.8 to -29.9 gr/cc, depending upon the value adopted for the mean absolute magnitude of nebulae.

PART I. RELATIVE DISTRIBUTION OF NEBULAE OVER THE SKY

The empirical approach to the problem of the structure of the physical universe consists in extrapolating the observed characteristics of the sample available for inspection. If the sample is fair and the characteristics are well determined, the method may be significant. Investigations have recently emerged from the stellar system and now range through a large volume of space whose inhabitants, the nebulae, are of the same general order as the stellar system itself. There are as yet no indications of a super-system of nebulae analogous to the system of stars. Hence, for the first time, the region now

[1] *Contributions from the Mount Wilson Observatory, Carnegie Institution of Washington*, No. 485.

observable with existing telescopes may possibly be a fair sample of the universe as a whole. This circumstance enhances the interest in, and possibly the value of, the determination of general characteristics.

The first reliable information concerning extra-galactic regions came from stars involved in the nearer nebulae, which provided rough methods of estimating distances—clues which have been rapidly exploited during the last decade until now we have a hasty sketch of some of the general features of the observable region as a unit. The next step was to follow the reconnaissance with a survey—to repeat carefully the explorations with an eye to accuracy and completeness. The program, with its emphasis on methods, will be a tedious series of successive approximations, but the procedure is necessary, since extrapolations beyond the frontiers will be significant only in proportion to the accuracy with which the trend of correlations has been established out to the frontier itself.

The present discussion is a contribution to the program in the form of an investigation of nebular distribution as observed with the large reflectors at Mount Wilson. The purpose is to delimit more closely the influence of local galactic obscuration and to sketch out the general background of normal distribution against which irregularities, local or systematic, may be further investigated. Few of the results are wholly new, but they are formulated more precisely than has hitherto been possible, in keeping with the character of the investigation as a second approximation toward the end in view.

Unless otherwise stated, the term "nebula" is used throughout the discussion to designate the extra-galactic nebulae alone. Latitude and longitude refer to galactic co-ordinates and are designated by β and λ, respectively.[2]

RECENT CONTRIBUTIONS TO THE SUBJECT

The first modern note in discussions of nebular distribution is found in an article by Hinks[3] published in 1911, urging the desira-

[2] The galactic co-ordinates are referred to the pole at R.A.$=12^h40^m$; Dec. $+28°$ (1900). The conversions from equatorial co-ordinates were made or checked with the aid of the tables by John Ohlsson (*Annals of the Observatory at Lund*, No. 3, 1932).

[3] A. R. Hinks, *Monthly Notices of the Royal Astronomical Society*, **71**, 588, 1911. The earlier literature on the subject is briefly summarized by Hinks.

bility of investigating the nebulae recorded on the Franklin-Adams plates. The gaseous nebulae, both planetary and diffuse, are recognized as galactic in the sense that they concentrate along the Milky Way. The complementary group, "the so-called white nebulae of which the large and better known examples are spirals," are called extra-galactic because

> in general they avoid the actual Milky Way zone. But they do it without imposing upon themselves symmetry in either galactic latitude or galactic longitude, and these results suggest that it will be prudent in the future to discuss spiral nebula distribution more on its own merits, and less with an eye to the galactic poles.

The data from the Franklin-Adams plates compiled by Hardcastle[4] and Fath's[5] study of plates of Selected Areas with the 60-inch reflector at Mount Wilson, both published in 1914, tended to confirm Hinks's conclusions. Curtis'[6] discussion of nebulae on the Crossley plates at Mount Hamilton contributed

> the valuable indication that the density of small nebulae persists to at least 60° from the galactic poles, with only a comparatively small diminution of the frequency of distribution which obtains about the two galactic poles.

This conclusion was confirmed and developed as far as the data permitted in Seares's[7] very thorough analysis of Fath's counts, published in 1925. In addition, Seares found suggestions of a complicated distribution in longitude with a band of high frequency apparently crossing the northern hemisphere in longitudes 50°–220°.

Wirtz,[8] in 1923–1924, discussed nebular distribution as indicated by the NGC, by the counts of Fath and of Curtis, and by his own extensive measures of surface brightness. He found no conspicuous dependence of surface brightness on latitude, but some indications of such a dependence on nebular density, in addition to the familiar concentration near the north pole. He concluded that distribution purely according to latitude is only a rough approximation. Well-defined centers of clustering are conspicuous, one of which is near the

[4] *Monthly Notices of the Royal Astronomical Society*, **74**, 699, 1914.

[5] *Astronomical Journal*, **28**, 75, 1914.

[6] *Publications of the Lick Observatory*, **13**, 11, 1918.

[7] *Mt. Wilson Contr.*, No. 297; *Astrophysical Journal*, **62**, 168, 1925.

[8] *Astronomische Nachrichten*, **222**, 33, 1924; **223**, 123, 1924; also *Meddelanden från Lunds Astron. Observatorium*, Ser. II, No. 29, 1923.

north pole. The fainter the nebulae, however, the less pronounced the concentration toward the pole and the more defined the tendency toward uniform distribution over the sphere.

Reynolds,[9] in 1923, discussed the distribution of the brighter nebulae and called attention, among other items, to apparent anomalies in the distribution in longitude. For instance, the large spirals and the globular star clusters tend to be mutually exclusive, congregating in opposite hemispheres whose poles are near the galactic plane. Moreover, he stated, "there is very definite evidence of a band, fairly widespread in the Ursa Major region, stretching past the pole beyond Virgo, the average size becoming smaller as the band passes beyond the pole."

The band is in the general region of that later suggested by Seares and represents the phenomenon described much earlier as the Milky Way of the nebulae.

Provisional results from the present survey were summarized[10] in 1931. Although the quantitative results have been revised in the present more detailed analysis, the general outlines of the picture remain unchanged and need not be restated.

In 1932 appeared the Harvard[11] survey of nebulae brighter than the thirteenth magnitude, which covers the entire sky in a homogeneous manner. The results concerning distribution were summarized as "the avoidance of low latitudes, the strong clustering in the northern galactic hemisphere, and the general unevenness of distribution." Later, in 1933, Shapley[12] discussed the distribution of nebulae to much fainter limits on the basis of approximately 100,000 nebulae photographed with the Bruce 24-inch refractor, stating that "there is no change with latitude north of $+25^\circ$; south of -25° the mean density increases, but the obstructing streamers of dark nebulosity in latitude -20° to -40° are probably largely responsible for the apparent increase." He further emphasized the apparent irregularities in distribution and the greater richness in the northern hemisphere.

[9] *Monthly Notices of the Royal Astronomical Society*, **83**, 147, 1922; **84**, 76, 1923.

[10] *Publications of the Astronomical Society of the Pacific*, **43**, 282, 1931; also *Science*, **75**, 24, 1932, and *Annual Report of the Mount Wilson Observatory*, 1930, 1931, and 1932.

[11] Shapley and Ames, *Harvard Annals*, **88**, Part II, 1932.

[12] *Proceedings of the National Academy of Sciences*, **19**, 389, 1933.

THE OBSERVATIONAL DATA FOR THE INVESTIGATION

With the broad features of nebular distribution thus outlined, it was evident that further reliable information could be expected only from large bodies of new data, reasonably complete and thoroughly homogeneous. An examination of the reflector plates available at Mount Wilson in 1926 proved them unsuitable for the particular purpose, owing to lack of uniformity in aperture, emulsion, development, exposure, distribution, etc. A special survey was therefore initiated, and current programs of direct photography were modified where possible to meet the new requirements. Extensive studies of threshold images were also undertaken, with especial attention to the comparison of plates taken with various instruments and under various exposure conditions, until now it is believed that a consistency has been attained in the treatment of nebular images which warrants a general discussion of the accumulated material.

At present about eighty thousand nebulae have been identified on Mount Wilson photographs, of which some sixty thousand are on plates in the writer's collection. Of the latter, about three-fourths[13] were observed under the standard conditions adopted for the present investigation. Both reflectors are represented indiscriminately, but, owing to differences in mounting, the 100-inch alone is generally used south of about $-20°$ Dec., and the 60-inch alone north of about $+60°$.

The standard conditions were Newtonian foci, full apertures, Eastman 40 plates—5×7 inches for the 100-inch and 4×5 inches for the 60-inch, and full development with a hydroquinone developer (X-ray). Minor variations in sky, mirrors, emulsions, and development were treated as accidental errors, but corrections were applied for atmospheric extinction, variations in definition, and exposure time. The nebular counts were first reduced to the equivalent of one-hour exposures, of excellent definition, at the zenith, with the 100-inch, and in this form were used for the investigation of relative distribution. Later the results were reduced to numbers of nebulae per square degree to a definite limiting magnitude for the purpose of

[13] The residue are about equally divided among plates of the great clusters; plates with the Ross correcting lens; plates with other apertures, emulsions, or development; and plates with the 10-inch camera.

deriving significant quantitative values for various characteristics of the observable region.

Each plate was examined at least three times with high and low power, the last examination being a continuous review of the entire collection in the light of accumulated experience for the purpose of improving the consistency of the counts and the estimates of quality. All images not definitely stars or obvious defects were marked as nebulae. Comparisons of pairs of duplicate plates indicate that mistakes tend to balance misses; hence, for statistical purposes, the counts appear to be fairly homogeneous.[14]

It is impossible, however, to identify all nebulae recorded on a plate from the appearance of the images alone. Numbers increase rapidly with diminishing size and brightness, and, in the faintest half-magnitude, where about one-half of the total may be expected, the nebulae tend to lose themselves among the stars. The threshold of identification varies with the type; open spirals fade out, while areas are still perceptible, and compact globular nebulae merge into the star images well above the limit of the plates. This effect can be treated as statistically uniform, since it depends upon the relative frequencies of nebular types and there is no reason to assume that the relations vary systematically over the sky. But the threshold of identification also varies with the criteria upon which different observers, consciously or unconsciously, base their judgments. This irregularity represents a personal equation which may attain consider-

[14] The accuracy of the counts was tested in various ways. Several dozen duplicates were included in the collection, but most of them represent plates discarded for particular reasons (usually poor seeing) and replaced by others of better quality. Fifteen duplicates, however, were judged suitable for comparison purposes, and these pairs of independent counts, when reduced to the standard system, show an average difference without regard to sign of about 0.05 in log N. Some of the difference can be attributed to uncertainties in the reduction, especially in the corrections for quality, which exhibit a considerable range.

A more detailed investigation of these fifteen pairs (six with the 60-inch, four with the 100-inch, and five with both telescopes), together with eight two-hour exposures with the 100-inch (not included in the discussion), of fields covered by hour exposures with either telescope, indicated that among about 1020 identifications on plates included in the survey, 42 were mistakes representing defects and stars, while 56 nebulae were missed, although above the threshold of identification. A ratio of this order is assumed to hold for the entire body of data. The relative number of nebulae actually recorded, but below the threshold of identification, is discussed later.

able proportions and must be calibrated before counts by various observers can be compared. The personal equation may also be expressed as the difference between the limiting magnitude of the nebular counts and the limiting magnitude of the star images on the plates—a quantity which varies with the observer as well as the instrumental equipment. Calibration of the present counts has been attempted in some detail, since the writer believes that the interpretation of most of the published counts is seriously restricted or even confused by the omission of this important feature.

The observational data, together with log N reduced to a homogeneous system, are listed in Tables I–IV.

Table I gives the survey data. The 765 plates, about equally divided between the two reflectors, are distributed along circles of latitude 5° apart, the galactic equator itself being omitted. From $\beta = 5°$ to 60°, the longitude intervals are 10°; for $\beta = 65°$ and 70°, the intervals are 20°; for $\beta = 75°$ and 80°, they are 30°; for $\beta = 85°$, they are 60°. With the exception of six fields,[15] the survey is complete to Dec. $= -30°$ and hence covers three-fourths of the sphere, including both galactic poles and about two-thirds of the Milky Way. The northern hemisphere is complete from the pole to and including $\beta = +40°$. The corresponding southern cap, $\beta = -40°$ to $-90°$, is about 60 per cent complete.

Uniform exposures of one hour were used for 690 plates, and half-hour exposures for 74 plates scattered along the latitude circles at $\beta = 35°, 45°, 55°$, and 65°. The half-hour exposures, which are marked with an asterisk in Table I, were included primarily for use in determining the manner in which numbers of nebulae increase with exposure time. For the same reason a 45-minute exposure was included and marked with a double asterisk. The last column of the table gives the values of log N reduced to the uniform conditions of one-hour exposures of excellent quality at the zenith with the 100-inch. Log N is simply the sum of log N_1 (the number of nebulae ac-

[15] The exceptions are $\beta = +20°$, $\lambda = 310°$; $-25°$, 200°; $-45°$, 190°; $-55°$, 190°; $-65°$, 190°, and 350°. The plates were rejected for various reasons and attempts to repeat them have failed. Counts on the rejected plates are considered uncertain, but they indicate no remarkable deviations from normal distribution; hence their omission is not very material.

TABLE I*

SURVEY FIELDS

β	λ		Z	Q	N_1	I	log N	β	λ		Z	Q	N_1	I	log N
+90°	.....	h	39°	E	71	6	1.90	+65°	140°	s*	7°	E	14	2	1.71
									160	s*	19	GE	14	2	1.76
85	0°	h	29	FG	60	7	1.98		180	h	32	F	37	5	1.88
	60	h	20	E	50	2	1.71		200	s	19	E	67	6	2.00
	120	h	41	E	37	3	1.63		220	s	30	E	84	12	2.11
	180	h	34	F	80	4	2.22		240	h*	28	E	26	2	1.83
	240	h	15	E	51	4	1.71		260	s	32	FG	36	4	1.93
	300	h	11	E	60	10	1.78		280	h	34	GE	48	4	1.76
									300	h*	33	F	11	2	1.75
80	0	h	11	FG	41	4	1.79		320	h	33	GE	86	5	2.00
	30	s	51	G	44	5	2.00		340	s*	17	E	16	1	1.77
	60	s	41	E	43	9	1.85								
	90	s	42	FG	23	5	1.76	60	0	s	21	E	58	12	1.93
	120	s	37	F	19	1	1.76		10	s	28	G	54	4	2.01
	150	s	39	E	77	7	2.10		20	s	42	G	35	5	1.86
	180	h	23	GE	54	5	1.78		30	s	13	GE	39	6	1.79
	210	s	55	G	32	7	1.90		40	s	43	F	14	2	1.65
	240	h	43	FG	44	4	1.88		50	s	19	G	31	5	1.76
	270	h	41	G	62	5	1.95		60	s	18	G	28	4	1.72
	300	h	49	G	72	5	2.05		70	s	37	G	25	3	1.70
	330	s	43	GE	76	9	2.14		80	s	32	G	46	6	1.95
									90	s	24	GE	40	1	1.81
75	0	h	34	E	90	10	1.99		100	s	42	GE	79	14	2.16
	30	s	16	E	58	10	1.93		110	s	21	GE	85	12	2.14
	60	s	7	F	22	1	1.78		120	s	30	GE	31	2	1.72
	90	s	34	E	54	6	1.93		130	h	43	FG	52	8	1.96
	120	s	23	E	30	7	1.65		140	s	30	G	31	6	1.78
	150	s	29	E	39	2	1.77		150	h	26	GE	145	23	2.22
	180	h	8	E	97	9	1.99		160	h	28	GE	37	3	1.63
	210	h	32	GE	67	2	1.90		170	h	7	GE	37	9	1.61
	240	s	30	G	83	5	2.21		180	h	34	FG	50	5	1.92
	270	h	35	GE	63	7	1.88		190	h	17	GE	64	8	1.86
	300	h	33	E	73	12	1.90		200	s	45	F	31	3	2.00
	330	h	22	FP	27	2	1.89		210	h	29	E	120	8	2.10
									220	s	36	E	67	13	2.03
70	0	s	43	G	44	5	1.96		230	h	41	E	88	7	2.00
	20	h	39	G	43	4	1.78		240	s	37	E	36	6	1.76
	40	s	28	F	31	5	1.95		250	h	40	GE	77	7	1.98
	60	s	34	G	29	2	1.76		260	h	36	GE	41	5	1.69
	80	h	41	G	76	7	2.04		270	s	42	E	77	10	2.11
	100	h	41	G	36	6	1.72		280	s	46	GE	34	2	1.81
	120	s	26	G	51	2	1.99		290	s	45	E	76	12	2.11
	140	s	44	GE	44	6	1.91		300	s	33	GE	35	6	1.77
	160	s	35	E	52	12	1.92		310	h	50	G	65	7	2.01
	180	s	20	FG	36	7	1.91		320	s	36	GE	53	9	1.96
	200	s	37	E	69	3	2.04		330	h	52	FG	56	7	2.04
	220	s	49	FG	33	3	1.95		340	s	20	GE	74	9	2.08
	240	h	33	GE	75	8	1.95		350	s	43	G	35	3	1.86
	260	h	37	FG	43	5	1.85								
	280	h	38	G	35	1	1.69	+55	0	h*	25	E	39	5	2.01
	300	h	37	FG	44	5	1.86		10	s	8	GE	380	32	2.78
	320	h	29	FG	40	4	1.80		20	s*	17	E	20	2	1.87
	340	h	21	G	38	5	1.71		30	s*	25	E	16	1	1.78
									40	s*	25	GE	17	3	1.85
+65	0	s*	13	E	18	5	1.82		50	s*	23	GE	16	3	1.81
	20	s*	19	E	12	1	1.65		60	s*	25	GE	22	2	1.96
	40	s*	19	E	17	3	1.80		70	s*	43	E	37	6	2.19
	60	s*	23	E	12	0	1.65		80	s	35	GE	57	8	2.00
	80	s*	10	F	13	1	1.95		90	s*	29	F	7	1	1.71
	100	s	35	E	51	3	1.91		100	s	39	GE	58	5	2.01
	120	s*	14	E	17	3	1.79		110	s*	26	E	33	5	2.10

* Symbols are: β, λ=galactic latitude and longitude; "h"=100-inch, "s"=60-inch, Z=zenith distance at mid-exposure, Q=quality of plate, N_1=number of nebulae actually counted, I=number within central circle (diameter 10′ for 100-in., 13′.8 for 60-in.); corrections from Tables VI, VII, and IX, added to log N_1, give log N, N being the number of nebulae for an hour's exposure of excellent quality at the zenith with the 100-inch. All exposures are 60^m except those for which "h" or "s" are starred. A single star indicates a 30^m exposure and a double star (one field only, $\beta=+55°$, $\lambda=130°$), a 45^m exposure.

Two fields of quality P ($\beta=+35°$, $\lambda=300°$; $\beta=-15°$, $\lambda=140°$) are included for which the quality factor, $\Delta Q=0.70$, is not evaluated in the text but represents a result of low weight indicated by a dozen rejected P plates.

TABLE I—*Continued*

β	λ		Z	Q	N_1	I	log N	β	λ		Z	Q	N_1	I	log N
+55°	120°	s*	23°	F	13	1	1.96	+45°	110°	s*	33°	F	11	0	1.91
	130	s**	16	GE	19	3	1.66		120	s*	27	E	30	3	2.06
	140	s*	14	E	15	4	1.74		130	s*	21	GE	27	6	2.04
	150	s*	16	G	10	4	1.67		140	s*	15	FG	15	3	1.92
	160	s*	16	G	14	3	1.82		150	s*	12	E	26	3	1.97
	170	h	10	F	33	8	1.80		160	s*	11	E	16	3	1.76
	180	s	33	GE	53	7	1.95		170	h	27	FP	23	1	1.83
	190	s	25	GE	59	9	1.99		180	s*	17	E	16	3	1.77
	200	h	22	G	76	8	1.99		190	h	27	F	30	4	1.78
	210	s	28	GE	44	4	1.86		200	h*	28	GE	21	1	1.78
	220	h	34	FP	31	4	1.98		210	s*	35	G	31	6	2.19
	230	s*	34	E	27	1	2.03		220	s	43	E	31	5	1.71
	240	s*	42	F	8	0	1.80		230	s*	44	F	7	2	1.76
	250	s*	40	E	32	2	2.12		240	s*	48	G	15	2	1.93
	260	s*	47	GE	17	2	1.91		250	s*	49	G	11	2	1.79
	270	s	41	GE	75	14	2.14		260	s*	51	FG	9	3	1.79
	280	s	42	GE	77	9	2.15		270	s	51	GE	48	3	1.98
	290	h*	41	FG	15	0	1.82		280	s	51	GE	31	1	1.79
	300	s	40	FG	35	3	1.93		290	s*	49	GE	20	5	1.99
	310	h*	36	G	22	2	1.88		300	h	47	FG	26	4	1.67
	320	s	31	GE	75	6	2.11		310	h	48	G	42	6	1.81
	330	h*	30	GE	35	3	2.01		320	h	50	FG	36	2	1.84
	340	s	28	GE	72	9	2.08		330	h	42	FG	48	4	1.92
	350	h*	23	G	21	4	1.83		340	h	38	GE	110	9	2.13
									350	h*	42	G	20	2	1.86
50	0	h	14	FG	66	8	2.00								
	10	h	19	G	60	6	1.89	40	0	h	29	F	50	6	2.00
	20	h	31	FG	61	3	2.00		10	h	40	F	44	6	1.97
	30	s	14	G	22	1	1.60		20	h	35	FG	56	3	1.97
	40	s	17	G	33	4	1.79		30	s	17	G	44	4	1.91
	50	s	35	G	38	1	1.88		40	s	13	GE	37	7	1.77
	60	s	37	E	30	1	1.68		50	s	25	GE	48	9	1.90
	70	s	36	G	33	2	1.82		60	s	30	GE	24	2	1.61
	80	s	41	GE	22	3	1.60		70	s	38	FG	24	4	1.77
	90	s	41	G	40	5	1.92		80	s	41	GE	34	8	1.79
	100	s	37	G	23	2	1.66		90	s	44	FG	45	4	2.06
	110	s	41	GE	32	2	1.77		100	s	42	FG	21	2	1.72
	120	s	45	GE	36	3	1.83		110	s	38	E	50	7	1.91
	130	s	35	GE	58	12	2.00		120	s	34	G	32	6	1.81
	140	s	22	GE	29	2	1.67		130	s	26	E	77	15	2.07
	150	h	37	F	26	2	1.73		140	s	25	FP	21	5	1.95
	160	h	23	FP	29	1	1.92		150	s	8	F	32	5	1.95
	170	h	26	F	49	7	1.99		160	h	31	G	107	23	2.16
	180	h	21	FG	53	5	1.91		170	s	31	GE	47	6	1.90
	190	h	37	FP	23	4	1.85		180	h	48	F	31	2	1.86
	200	h	25	F	35	7	1.84		190	h	50	F	24	4	1.76
	210	s	35	G	84	16	2.22		200	s	42	F	28	9	1.95
	220	s	40	GE	42	4	1.87		210	s	45	G	91	15	2.29
	230	s	40	GE	41	4	1.86		220	h	43	FG	95	11	2.22
	240	s	47	GE	32	3	1.79		230	h	51	FP	23	4	1.91
	250	s	44	GE	28	5	1.72		240	h	52	F	16	1	1.59
	260	s	47	FG	21	1	1.74		250	h	54	FG	31	5	1.79
	270	s	50	G	37	7	1.93		260	h	56	FG	25	1	1.72
	280	s	43	GE	24	5	1.64		270	h	57	FG	61	7	2.12
	290	h	47	F	40	4	1.96		280	h	56	FG	34	1	1.85
	300	h	43	F	51	7	2.05		290	h	54	FG	46	4	1.96
	310	h	40	FP	19	0	1.78		300	h	52	FG	48	2	1.97
	320	h	46	F	32	5	1.87		310	h	48	FG	27	4	1.70
	330	h	34	FP	22	0	1.83		320	h	43	FG	48	6	1.92
	340	h	31	F	45	3	1.96		330	h	37	FP	13	3	1.60
	350	h	39	FP	32	1	2.01		340	h	43	FP	10	1	1.51
									350	s	34	E	37	5	1.77
+45	0	h*	45	G	42	0	2.19								
	10	h	15	E	65	13	1.81	+35	0	h	32	G	30	0	1.61
	20	h	3	GE	67	10	1.87		10	h	16	GE	55	3	1.79
	30	h	29	GE	72	6	1.92		20	h	5	GE	30	4	1.52
	40	s	21	G	50	5	1.97		30	s	18	GE	43	4	1.84
	50	s	35	GE	94	7	2.21		40	s	23	FG	17	2	1.58
	60	s	48	G	39	7	1.94		50	s	27	FG	9	1	1.31
	70	s	53	FG	25	5	1.86		60	s	30	F	24	2	1.81
	80	s	52	F	17	3	1.78		70	s	39	GE	33	5	1.77
	90	s	41	F	20	2	1.80		80	s	44	G	22	2	1.67
	100	s*	39	E	50	5	2.31		90	s	51	GE	43	6	1.93

TABLE I—*Continued*

β	λ		Z	Q	N_1	I	log N	β	λ		Z	Q	N_1	I	log N
+35°	100°	s	47°	GE	47	2	1.95	+25°	110°	s	40°	G	29	5	1.77
	110	s	43	G	35	3	1.86		120	s	40	G	14	2	1.46
	120	s	29	FG	31	4	1.85		130	s	26	G	31	7	1.74
	130	s	26	FG	45	3	2.01		140	s	11	G	37	10	1.83
	140	s	33	GE	56	7	1.98		150	h	27	G	52	2	1.84
	150	s	33	GE	82	26	2.14		160	s	23	G	47	10	1.94
	160	s*	9	GE	60	7	2.38		170	s	16	GE	46	9	1.87
	170	s	39	GE	52	6	1.97		180	h	30	FG	44	6	1.85
	180	s	21	E	61	11	1.96		190	h	42	FG	49	8	1.93
	190	s*	28	E	18	2	1.84		200	h	46	GE	76	6	2.00
	200	s	39	GE	22	3	1.59		210	h	43	FG	45	7	1.89
	210	s*	41	GE	19	4	1.94		220	h	56	G	45	7	1.89
	220	h*	46	GE	21	1	1.84		230	h	59	G	25	5	1.67
	230	s	51	G	30	3	1.84		240	h	64	F	31	5	2.00
	240	h*	55	FG	17	3	1.94								
	250	h*	59	F	18	3	2.11		300	h	64	G	14	3	1.48
	260	h*	62	F	7	0	1.73		310	h	59	GE	11	1	1.25
	270	h*	62	F	8	1	1.78		320	h	55	G	12	0	1.31
	280	h*	62	F	31	0	2.37		330	h	48	G	9	1	1.14
	290	h*	60	FG	44	4	2.40		340	s	42	FG	6	0	1.18
	300	h	56	P	6	1	1.62		350	s	43	G	10	1	1.32
	310	s	51	G	39	4	1.95								
	320	s	46	G	8	0	1.24	20	0	h	25	G	14	1	1.27
	330	s	42	FG	16	5	1.60		10	h	25	G	32	2	1.63
	340	s	35	GE	37	3	1.81		20	s	8	GE	21	4	1.52
	350	s	28	G	30	6	1.76		30	s	31	G	27	4	1.72
									40	s	35	F	19	3	1.76
30	0	h	40	F	32	5	1.84		50	s	23	GE	22	7	1.55
	10	h	42	F	19	1	1.62		60	s	29	GE	22	4	1.56
	20	h	41	G	40	6	1.76		70	s	40	GE	0	....	.....
	30	s	21	FG	17	3	1.58		80	s	46	G	0	....	.....
	40	s	32	G	26	2	1.70		90	s	52	FG	7	2	1.30
	50	s	25	GE	40	15	1.82		100	s	44	G	8	2	1.23
	60	s	36	GE	17	1	1.47		110	s	38	FG	23	5	1.75
	70	s	47	GE	15	1	1.46		120	s	30	G	12	4	1.37
	80	s	54	FG	11	3	1.50		130	s	38	F	16	1	1.69
	90	s	53	GE	17	2	1.55		140	s	27	FP	15	2	1.81
	100	s	48	F	26	3	1.94		150	h	10	GE	150	14	2.22
	110	s	46	G	32	3	1.85		160	h	22	G	49	5	1.80
	120	s	36	GE	48	9	1.92		170	s	26	G	51	4	1.99
	130	s	31	GE	64	11	2.04		180	s	25	G	32	3	1.79
	140	h	41	F	44	7	1.98		190	s	44	G	30	7	1.81
	150	s	14	G	35	3	1.80		200	h	44	G	36	7	1.73
	160	h	5	FG	32	4	1.69		210	h	49	F	27	2	1.80
	170	s	33	G	118	16	2.36		220	h	56	F	41	3	2.03
	180	h	30	F	33	5	1.83		230	h	63	FG	24	1	1.77
	190	s	29	FG	32	4	1.87								
	200	g	48	G	45	4	1.84		320	h	56	F	0	....	.....
	210	h	43	FG	56	9	1.99		330	h	50	F	0	....	.....
	220	h	49	G	39	7	1.78		340	s	44	FG	0	....	.....
	230	h	55	FG	24	0	1.69		350	s	43	G	0	....	.....
	240	h	60	G	16	2	1.48								
	250	h	63	F	22	2	1.83	+15	0	h	29	FG	30	3	1.68
									10	h	33	FG	14	2	1.36
	290	h	64	FP	38	2	2.26		20	s	19	G	18	3	1.53
	300	h	60	F	33	2	1.98		30	h	19	G	30	5	1.69
	310	h	55	FG	16	3	1.51		40	s	30	FG	6	0	1.15
	320	h	50	FG	18	5	1.54		50	s	44	F	18	3	1.77
	330	h	46	F	15	1	1.54		60	s	28	G	13	4	1.39
	340	h	38	FG	18	2	1.49		70	s	38	F	0	....	.....
	350	h	38	F	20	4	1.63		80	s	43	FG	1	0	0.40
									90	s	47	FG	0	....	.....
+25	0	h	27	FG	24	3	1.58		100	s	40	F	4	0	1.09
	10	h	30	FG	53	4	1.93		110	s	33	G	9	4	1.24
	20	h	35	FG	29	5	1.68		120	s	26	F	4	2	1.06
	30	h	47	G	25	2	1.58		130	s	31	FG	9	2	1.32
	40	s	28	F	18	3	1.72		140	s	19	F	10	1	1.45
	50	s	38	G	27	9	1.74		150	h	12	G	40	10	1.70
	60	s	31	FG	23	5	1.73		160	h	12	G	43	5	1.73
	70	s	41	G	20	4	1.62		170	h	36	F	12	1	1.40
	80	s	49	G	22	2	1.69		180	h	27	F	30	5	1.78
	90	s	53	G	10	1	1.38		190	h	38	G	79	13	2.05
	100	s	46	FG	18	1	1.68		200	h	45	G	48	3	1.86

TABLE I—*Continued*

β	λ		Z	Q	N_1	I	log N	β	λ		Z	Q	N_1	I	log N
+15°	210°	h	53°	F	11	1	1.44	− 5°	90°	s	23°	G	0	....	.....
	220	h	59	F	7	1	1.30		100	s	22	G	2	0	0.57
									110	s	24	FG	1	0	0.36
	320	h	60	FG	0	....	.....		120	s	37	G	0	....	.....
	330	h	58	F	0	....	.....		130	s	6	G	0	....	.....
	340	h	47	F	0	....	.....		140	h	27	F	0	....	.....
	350	h	37	FG	0	....	.....		150	h	23	G	0	....	.....
									160	h	50	FG	11	2	1.32
10	0	h	36	F	0	....	.....		170	h	28	G	7	0	0.97
	10	s	25	G	2	1	0.58		180	h	50	FP	0	....	.....
	20	h	15	G	7	1	0.95		190	h	46	GE	0	....	.....
	30	h	21	FG	1	0	0.19		200	h	55	F	0	....	.....
	40	h	15	G	44	10	1.74		210	h	63	F	2	0	0.79
	50	s	14	G	22	4	1.60								
	60	s	22	G	0	....	.....		330	h	64	G	0	....	.....
	70	s	34	FG	0	....	.....		340	h	60	G	0	....	.....
	80	s	40	FG	0	....	.....		350	s	46	F	0	....	.....
	90	s	45	G	0	....	.....								
	100	s	39	G	0	....	.....	10	0	h	39	F	0	....	.....
	110	s	38	GE	0	....	.....		10	s	35	G	0	....	.....
	120	s	26	G	0	....	.....		20	h	25	G	9	1	1.07
	130	s	41	F	3	1	0.98		30	h	14	G	4	0	0.70
	140	s	25	G	7	0	1.13		40	s	31	G	2	0	0.59
	150	s	34	FG	2	0	0.68		50	h	45	FG	11	0	1.29
	160	h	27	G	7	2	0.97		60	s	21	G	7	1	1.12
	170	h	27	G	10	1	1.12		70	s	26	G	12	4	1.36
	180	h	50	F	3	1	0.86		80	s	28	G	23	4	1.64
	190	h	40	FP	10	0	1.50		90	s	25	FG	0	....	.....
	200	h	47	G	25	8	1.58		100	s	20	G	9	1	1.22
	210	h	55	F	21	3	1.73		110	s	37	G	17	5	1.53
	220	h	63	FG	3	2	0.87		120	h	50	FG	6	1	1.06
									130	h	38	F	0	....	.....
	320	h	65	G	0	....	.....		140	h	45	F	0	....	.....
	330	h	55	F	0	....	.....		150	h	23	F	7	1	1.14
	340	h	47	G	0	....	.....		160	h	26	G	0	....	.....
	350	h	44	G	0	....	.....		170	h	33	G	0	....	.....
									180	s	41	G	0	....	.....
+ 5	0	h	36	FP	0	....	.....		190	h	48	FG	0	....	.....
	10	h	24	F	4	2	0.90		200	h	57	FP	4	1	1.20
	20	s	23	G	0	....	.....		210	h	65	FP	4	0	1.29
	30	s	18	G	1	0	0.27								
	40	h	6	FG	2	0	0.48		340	s	56	FG	0	....	.....
	50	s	30	G	0	....	.....		350	s	46	G	0	....	.....
	60	s	24	FG	0	....	.....								
	70	s	44	F	0	....	.....	15	0	h	47	FP	16	1	1.73
	80	s	43	F	0	....	.....		10	h	39	F	22	3	1.67
	90	s	37	G	0	....	.....		20	h	38	F	10	1	1.33
	100	s	33	G	0	....	.....		30	s	26	G	10	1	1.28
	110	s	32	G	0	....	.....		40	s	17	G	9	1	1.22
	120	s	38	FG	0	....	.....		50	s	38	F	4	1	1.09
	130	s	14	G	0	....	.....		60	h	32	G	39	3	1.72
	140	s	16	G	0	....	.....		70	s	35	GE	12	0	1.32
	150	h	32	G	3	0	0.61		80	s	18	G	22	3	1.61
	160	h	38	F	0	....	.....		90	h	48	F	22	1	1.71
	170	h	24	G	2	0	0.42		100	s	19	FG	13	1	1.46
	180	s	32	F	2	0	0.59		110	h	45	FG	74	11	2.12
	190	h	44	G	0	....	.....		120	h	40	FP	5	0	1.20
	200	h	49	F	0	....	.....		130	h	31	G	11	1	1.17
	210	h	52	F	7	0	1.24		140	h	14	P	3	0	1.18
									150	h	18	F	0	....	.....
	330	h	63	FG	0	....	.....		160	h	29	G	21	4	1.44
	340	s	50	F	0	....	.....		170	h	43	G	23	2	1.52
	350	s	42	G	0	....	.....		180	h	44	G	3	1	0.65
									190	h	50	FP	14	0	1.70
− 5	0	h	37	FG	0	....	.....		200	h	62	FG	44	4	2.02
	10	h	28	G	0	....	.....								
	20	h	19	G	0	....	.....		340	h	59	F	0	....	.....
	30	h	27	FG	0	....	.....		350	s	52	F	1	0	0.55
	40	h	25	FG	0	....	.....								
	50	h	30	G	0	....	.....	−20	0	h	43	G	16	1	1.36
	60	s	12	G	0	....	.....		10	h	38	G	20	1	1.45
	70	s	23	FG	7	1	1.20		20	h	50	FG	14	0	1.43
	80	s	41	F	0	....	.....		30	s	39	FG	13	2	1.50

TABLE I—*Continued*

β	λ		Z	Q	N_1	I	log N	β	λ		Z	Q	N_1	I	log N
−20°	40°	h	33°	GE	13	1	1.18	−35°	30°	h	43°	GE	27	2	1.53
	50	h	6	FG	12	1	1.26		40	s	25	F	12	0	1.54
	60	h	31	GE	12	0	1.15		50	s	41	G	27	5	1.75
	70	h	26	F	11	2	1.34		60	s	27	GE	42	4	1.84
	80	h	43	F	30	7	1.82		70	h	34	GE	125	11	2.18
	90	s	16	F	14	3	1.60		80	h	34	GE	52	6	1.80
	100	h	28	F	45	5	1.95		90	s	14	GE	33	3	1.72
	110	h	26	FG	36	5	1.76		100	h	45	E	69	5	1.91
	120	h	25	G	37	7	1.69		110	h	39	GE	29	1	1.55
	130	h	25	F	9	0	1.25		120	h	33	E	48	4	1.71
	140	h	19	FG	4	0	0.79		130	h	50	G	40	1	1.80
	150	h	23	F	1	0	0.29		140	s	39	GE	2	0	0.55
	160	h	27	G	36	3	1.68		150	h	50	GE	17	3	1.37
	170	s	41	G	40	5	1.92		160	h	52	GE	39	2	1.74
	180	h	43	FP	14	3	1.66		170	h	45	F	21	3	1.67
	190	h	50	FG	75	17	2.16		180	s	49	G	16	2	1.55
	200	h	61	G	41	6	1.90		190	h	58	FP	18	4	1.87
	340	h	60	G	6	2	1.06		350	h	57	FG	27	2	1.76
	350	s	53	GE	9	1	1.26								
								40	0	s	52	GE	42	11	1.93
25	0	s	46	GE	18	0	1.54		10	s	45	G	29	5	1.79
	10	s	42	GE	20	2	1.56		20	s	38	E	64	13	2.02
	20	s	43	GE	20	1	1.56		30	s	32	GE	35	8	1.77
	30	s	46	GE	44	6	1.92		40	s	29	E	48	8	1.86
	40	s	21	FG	12	3	1.43		50	s	22	GE	42	8	1.83
	50	s	45	E	33	5	1.75		60	s	23	E	47	3	1.84
	60	s	38	G	17	8	1.54		70	s	17	G	55	6	2.01
	70	s	27	GE	41	3	1.83		80	s	20	E	61	5	1.96
	80	s	32	GE	22	2	1.57		90	s	15	FG	27	4	1.77
	90	s	36	GE	62	5	2.03		100	s	22	E	75	14	2.05
	100	s	29	E	56	14	1.93		110	s	18	G	35	6	1.81
	110	h	27	F	25	4	1.72		120	s	27	E	45	5	1.83
	120	h	20	GE	51	10	1.76		130	s	26	GE	66	5	2.04
	130	s	50	F	20	3	1.84		140	h	27	FG	6	0	0.98
	140	s	32	FG	6	1	1.15		150	h	57	G	24	2	1.63
	150	h	26	FP	0	....	.....		160	h	52	G	25	2	1.61
	160	h	41	FG	12	2	1.32		170	h	46	GE	70	9	1.97
	170	h	46	FP	20	1	1.83		180	h	54	G	27	3	1.65
	180	h	46	FG	32	2	1.77		190	h	59	G	51	5	1.98
	190	h	50	FG	42	7	1.90								
									350	h	59	F	20	1	1.75
	340	h	63	G	13	4	1.42								
	350	s	55	E	12	3	1.37	45	0	h	54	GE	56	6	1.91
									10	h*	47	G	14	1	1.73
30	0	s	48	GE	25	1	1.69		20	h*	41	GE	50	5	2.20
	10	s	42	GE	25	4	1.66		30	h*	35	GE	16	1	1.68
	20	s	43	E	16	1	1.42		40	h*	32	E	15	2	1.61
	30	s	37	E	28	2	1.65		50	h*	35	E	23	2	1.80
	40	s	38	GE	28	2	1.70		60	h*	30	E	34	8	1.96
	50	s	20	GE	17	4	1.44		70	h*	21	E	52	5	2.13
	60	s	10	E	25	2	1.56		80	h	45	G	46	7	1.83
	70	s	31	GE	31	6	1.72		90	h	36	E	56	3	1.79
	80	s	14	G	66	5	2.08		100	h	43	E	74	9	1.93
	90	s	24	G	48	8	1.96		110	h	33	GE	54	5	1.80
	100	s	15	E	89	11	2.11		120	h	42	G	30	3	1.64
	110	s	22	G	53	6	1.99		130	h	35	E	67	7	1.87
	120	s	30	GE	55	19	1.97		140	h	37	G	21	1	1.46
	130	s	39	FG	24	5	1.77		150	h	49	E	61	9	1.88
	140	s	51	F	34	5	2.07		160	h	44	F	67	5	2.18
	150	h	34	F	21	3	1.64		170	s	48	E	45	6	1.90
	160	s	38	G	28	6	1.76		180	h	53	F	36	5	1.96
	170	h	41	FP	16	3	1.71								
	180	h	51	FG	29	2	1.74		350	h	60	GE	45	6	1.87
	190	h	56	F	37	2	1.99								
	200	h	64	GE	41	2	1.88	−50	0	h	56	GE	77	9	2.07
									10	h	51	FG	43	4	1.91
	340	h	64	G	13	4	1.44		20	s	43	F	35	4	2.04
	350	h	57	FP	12	0	1.68		30	h	39	FG	39	4	1.82
									40	s	40	F	28	4	1.94
−35	0	h	53	FG	21	3	1.62		50	h	33	F	49	7	2.00
	10	s	50	FG	25	2	1.84		60	s	40	F	28	6	1.94
	20	h	47	F	22	4	1.70		70	h	43	F	61	5	2.13

TABLE I—*Continued*

β	λ		Z	Q	N_1	I	log N	β	λ		Z	Q	N_1	I	log N
−50°	80°	h	34°	F	25	2	1.72	−60°	190°	h	64°	GE	38	8	1.85
	90	h	33	FG	21	3	1.53								
	100	h	37	F	26	2	1.73		350	h	64	G	25	4	1.73
	110	h	46	FP	22	1	1.87								
	120	s	44	GE	65	19	2.08	65	0	h	60	GE	43	3	1.85
	130	s	35	F	25	5	1.88		10	h	56	GE	43	1	1.81
	140	s	45	FG	39	5	2.00		20	s	51	GE	37	5	1.87
	150	h	42	F	51	4	2.05		30	s	45	E	49	5	1.92
	160	h	44	FP	24	3	1.90		40	s	51	GE	36	4	1.86
	170	h	51	GE	57	10	1.90		50	s	43	GE	33	3	1.78
	180	h	56	G	81	6	2.15		60	s	40	E	58	10	1.97
	190	h	62	G	29	3	1.76		70	h	46	FG	34	4	1.79
									80	s*	39	E	21	3	1.93
	350	h	62	GE	45	2	1.89		90	h*	40	FG	39	3	2.22
									100	s	39	FG	65	6	2.20
55	0	h	59	GE	70	7	2.06		110	h	38	G	32	2	1.66
	10	s	51	GE	47	7	1.97		120	s	41	E	52	2	1.94
	20	h*	41	G	21	1	1.88		130	s	45	GE	30	2	1.75
	30	h*	44	G	34	1	2.10		140	s	40	E	31	5	1.70
	40	h*	40	G	16	1	1.75		150	s	48	E	39	6	1.84
	50	s	34	GE	40	1	1.84		160	s	52	GE	40	7	1.91
	60	s*	36	E	14	0	1.75		170	h	56	E	33	4	1.66
	70	s	42	GE	43	7	1.89		180	h	60	F	23	1	1.82
	80	s	36	FG	34	6	1.91								
	90	h*	34	FG	23	2	1.98	70	0	h	61	FG	47	4	2.04
	100	h*	28	F	14	1	1.85		20	h	58	G	83	7	2.18
	110	s	30	E	48	4	1.87		40	h	48	F	26	1	1.78
	120	s	33	E	47	7	1.86		60	h	45	F	43	6	1.98
	130	s	39	E	42	6	1.83		80	h	43	G	61	7	1.95
	140	s	42	E	54	6	1.95		100	h	43	G	68	6	1.99
	150	s	43	GE	32	7	1.77		120	h	45	F	43	2	1.98
	160	s	46	E	45	9	1.89		140	h	51	G	62	8	1.99
	170	s	52	FG	20	0	1.75		160	h	54	FG	33	2	1.82
	180	h	57	FG	28	3	1.78		180	h	60	FG	48	8	2.04
	350	h	63	FG	25	2	1.79	75	0	h	61	GE	32	5	1.74
									30	s	54	G	34	7	1.91
−60	0	h	59	FG	52	11	2.07		60	s	49	GE	29	3	1.75
	10	h	53	G	45	5	1.87		90	s	48	G	23	5	1.71
	20	h	49	G	63	8	1.99		120	s	49	E	111	9	2.30
	30	h	45	GE	98	13	2.10		150	h	54	F	27	2	1.83
	40	h	43	E	34	8	1.59		180	h	63	GE	64	3	2.06
	50	s	43	G	32	2	1.83								
	60	h	41	F	30	4	1.82	80	0	h	62	F	45	3	2.13
	70	s	44	GE	76	11	2.15		30	h	58	GE	61	8	1.99
	80	h	34	FP	23	1	1.85		60	h	53	G	43	3	1.85
	90	s	49	GE	51	9	2.00		90	h	53	G	109	7	2.26
	100	h	37	F	44	4	1.96		120	h	53	G	63	1	2.02
	110	h	44	F	46	3	2.01		150	h	58	GE	148	20	2.37
	120	s	42	GE	27	4	1.69		180	h	62	FG	58	7	2.14
	130	h	51	FP	25	2	1.95								
	140	h	42	FP	28	2	1.96	85	30	h	60	FG	41	8	1.97
	150	h	46	F	42	2	1.98		90	h	57	FG	35	1	1.87
	160	h	50	FP	24	3	1.93		150	h	59	F	28	2	1.90
	170	h	55	G	40	3	1.83								
	180	h	60	G	43	4	1.91	−90	.....	h	62	GE	49	2	1.93

tually counted) and ΔZ, ΔQ, and ΔE as derived from Tables VI, VII, and IX, respectively. The first entry ($\beta = +90°$), for instance, represents an hour's exposure with the 100-inch of excellent quality at $Z = 39°$, on which 71 nebulae were counted. Log N_1 is 1.85, ΔZ is 0.05, ΔQ and ΔE are both zero, hence log N, the sum of these quantities, is 1.90.

Tables II*a*, *b*, and *c* give the extra-survey plates conforming to the

standard conditions and centered on co-ordinates, stars, or small planetaries. The arrangement is similar to that in Table I, with the addition of E, the exposure time in minutes. The 27 plates with twenty-minute exposures in Table IIc were included as bearing on the relation between log N and log E.

TABLE IIc*

100-INCH; EXTRA-SURVEY FIELDS

β	λ	E	Q	Z	N_1	I	log N	β	λ	E	Q	Z	N_1	I	log N
+85°	168°	60	GE	42°	130	6	2.21	− 9°	42°	130	FG	38°	10	3	0.78
84	208	60	FG	46	64	6	2.07	9	119	60	G	10	5	1	0.80
81	231	60	FG	35	95	9	2.20	9	119	110	G	25	42	1	1.39
78	242	60	FG	23	54	5	1.92	12	78	60	FG	51	15	1	1.46
75	243	45	GE	24	43	3	1.86	14	133	100	FG	9	6	2	0.67
75	262	60	E	21	150	18	2.19	15	355	60	GE	46	9	1	1.07
74	249	60	F	21	83	5	2.21	16	10	60	G	41	27	3	1.59
74	262	60	E	23	120	13	2.09	16	158	50	G	28	12	2	1.31
74	276	60	E	28	127	27	2.12	21	90	60	FG	13	87	5	2.12
73	250	60	E	29	132	16	2.14	22	89	60	G	14	71	12	1.95
73	250	60	FG	30	68	2	2.04	22	90	60	G	6	92	13	2.06
73	288	60	E	25	138	8	2.16	25	139	50	FG	32	33	3	1.84
72	237	60	G	31	58	11	1.89	27	191	60	GE	56	65	7	1.99
72	300	60	GE	32	138	13	2.21	37	22	40	G	45	14	0	1.55
70	229	60	G	22	252	22	2.51	37	93	60	GE	37	62	9	1.87
70	253	60	G	43	71	4	2.01	40	145	60	GE	35	29	2	1.54
70	310	60	GE	28	196	30	2.35	40	155	60	G	48	36	4	1.75
67	221	60	G	27	84	4	2.04	42	104	30	E	15	42	6	2.02
66	255	60	FG	41	80	10	2.14	52	87	60	GE	28	41	1	1.67
65	323	60	GE	37	152	15	2.26	53	187	60	FG	60	48	7	2.04
63	0	150	GE	40	363	41	2.12	54	22	30	G	46	23	1	1.94
63	257	60	FG	36	100	16	2.22	56	100	30	F	28	24	2	2.08
59	259	60	G	37	101	9	2.14	60	107	40	FG	45	41	4	2.09
58	318	30	FG	18	20	2	1.89	71	37	85	G	50	123	13	2.09
56	200	60	F	23	96	10	2.27	−72	40	135	GE	51	301	36	2.15
40	325	60	GE	46	41	0	1.73								
40	335	60	E	39	44	3	1.69								
34	232	60	FG	52	45	4	1.94								
28	39	60	GE	19	93	11	2.02								
+11	191	60	FG	46	16	2	1.46								

* E = exposure time in minutes. Two fields at $\beta = +73°$, $\lambda = 250°$ overlap about 10 per cent; two at $\beta = -9°$, $\lambda = 119°$ overlap about 5 per cent; two, $\beta = +75°$, $\lambda = 243°$ and $\beta = +28°$, $\lambda = 39°$, are also included in Table IIb.

Tables IIIa and b list plates conforming to the standard conditions but centered on selected nebulae. Reduction to the homogeneous system requires elimination of the central nebulae and correction for the areas they cover, the corrected counts being designated by N_1'. For this purpose the products of the two diameters in minutes of arc, ab, are listed, from which, on the assumption that the images approximate ellipses, the fraction of the inner circles, I, can readily be estimated. Since very large nebulae are not included in

the table, N_1' differs but little from N_1, and, in general, $N_1' = N_1 - 1$ within the uncertainty of the counts; but for deriving distance cor-

TABLE II*b*

60-INCH; EXTRA-SURVEY FIELDS

β	λ	E	Q	Z	N_1	I	log N	β	λ	E	Q	Z	N_1	I	log N
+87°	28°	90	G	33°	64	8	1.87	+28	39	60	GE	18°	54	9	1.94
85	13	90	G	36	124	21	2.16	23	187	60	G	30	67	2	2.12
80	163	60	E	12	85	6	2.09	15	25	60	G	5	22	6	1.60
78	172	90	G	9	100	26	2.03	+13	19	60	G	14	14	1	1.41
75	243	60	GE	21	79	11	2.11	−12	119	60	FG	47	26	1	1.83
70	161	60	G	10	49	7	1.95	13	118	60	FG	11	48	3	2.02
69	228	60	FG	26	60	5	2.14	19	19	60	G	31	9	0	1.24
67	220	60	GE	37	91	10	2.20	25	15	60	GE	42	24	4	1.64
61	209	60	G	45	45	1	1.98	25	35	60	GE	26	18	2	1.48
60	158	60	G	33	23	3	1.65	26	95	60	G	8	67	8	2.09
60	291	60	GE	49	36	11	1.85	35	145	60	E	27	13	2	1.29
58	114	100	GE	27	176	15	2.18	36	60	60	G	19	75	5	2.15
58	299	60	GE	40	39	5	1.84	49	38	60	E	51	46	7	1.92
55	224	60	GE	51	44	6	1.94	−51	101	60	FG	32	17	3	1.60
54	201	60	G	28	133	13	2.41								
44	1	60	G	51	32	8	1.87								
41	206	60	GE	35	77	20	2.13								
40	59	60	GE	37	21	3	1.56								
35	112	60	GE	39	56	10	2.00								
+30	180	45	FG	21	23	2	1.88								

TABLE II*c**

60-INCH; EXTRA-SURVEY FIELDS; 20-MINUTE EXPOSURES

β	λ	Z	Q	N_1	I	log N_2	β	λ	Z	Q	N_1	I	log N_2
+75°	320°	32°	E	18	4	1.45	−45	109	33°	E	17	1	1.42
74	315	28	GE	10	0	1.22	53	52	32	E	19	1	1.47
73	313	25	E	18	2	1.44	54	36	42	GE	11	0	1.30
63	323	24	GE	24	2	1.60	54	51	34	E	13	1	1.31
63	325	24	E	15	1	1.36	55	35	45	E	13	3	1.34
62	338	28	GE	23	5	1.58	55	50	37	E	26	4	1.61
62	340	33	E	16	3	1.39	63	99	36	E	20	1	1.50
60	20	31	E	10	2	1.19	63	118	41	E	22	3	1.56
59	24	30	E	21	4	1.51	64	100	36	E	33	4	1.72
59	28	37	E	21	6	1.52	64	119	41	E	18	3	1.48
58	34	42	GE	6	1	1.04	65	100	38	E	34	4	1.74
58	36	31	GE	13	0	1.34	−65	120	40	E	21	3	1.53
58	40	38	GE	5	1	0.95							
53	294	42	GE	17	0	1.49							
+51	247	43	GE	10	0	1.26							

* N_2 = corrected number of nebulae for a 20^m exposure. To obtain log N, corresponding to the standard one-hour exposure, add $\Delta E = +0.63$.

rections or "coma factors," by which the counts are eventually reduced to uniform definition over the entire plates equal to that in the central circles, the procedure is essential.

TABLE III*a**

100-INCH; FIELDS CENTERED ON NEBULAE

NGC	β	λ	E	Q	Z	N_1	I	ab	N_1'	log N
4459	+87°	160°	60	GE	6°	66	5	60	71	1.89
4725	87	303	120	G	10	108	1	100	120	1.78
4008	79	169	60	FG	47	54	4	0.7	53	1.98
4293	79	230	60	G	29	72	14	27	76	2.00
			30	FP	39	12	2	27	11	1.94
4651	78	269	60	*F*	32	35	2	9	34	1.84
4192	75	240	40	E	25	77	1	100	84	2.17
4762	73	276	135	FG	29	157	21	8	156	1.92
4178	72	245	60	G	43	68	5	9.5	66	1.98
4124	71	242	60	GE	24	81	8	48	86	1.99
4535	70	261	60	F	31	53	1	100	56	2.06
4612	70	266	60	F	29	43	5	1.6	41	1.91
4532	68	262	60	FG	27	97	17	4.8	95	2.18
4215	67	250	40	G	37	40	6	0.3	39	1.96
3430	65	162	60	F	31	46	5	6.2	45	1.96
3489	63	203	60	G	26	75	8	2.1	74	1.99
5363	62	310	45	E	30	38	4	2.6	37	1.77
3412	60	202	45	F	35	20	1	2.5	19	1.77
5829	59	0	80	G	14	187	35	3.2	187	2.20
4593	57	268	60	G	39	78	5	12	78	2.04
3521	53	223	60	G	34	55	1	100	61	1.93
4742	52	272	90	F	46	38	6	.....	37	1.70
5713	51	320	40	GE	47	50	8	4	49	2.04
2859	47	159	135	FG	20	146	11	19	147	1.89
2830	46	159	60	E	14	83	14	.....	82	1.91
5850	46	329	110	G	45	140	15	19	142	1.97
5964	44	340	60	G	29	37	4	28	37	1.69
2712	43	144	45	FG	12	55	3	1.6	54	2.08
2693	42	135	20	F	20	10	2	0.3	9	1.87
5812	42	318	45	G	42	19	4	1	18	1.59
5990	41	337	60	G	32	35	7	1.4	34	1.66
6014	40	344	60	FG	32	47	4	0.8	46	1.87
2639	39	135	45	FG	22	28	8	0.3	27	1.79
6070	34	340	60	G	45	51	10	5.8	51	1.88
6080	34	342	60	GE	41	67	15	0.5	66	1.92
2545	28	169	60	GE	40	54	11	2.2	53	1.81
2855	27	212	45	F	50	20	1	2.3	19	1.83
6280	26	354	60	G	27	23	5	0.1	22	1.46
2642	23	198	60	F	51	13	1	13	12	1.46
6296	+23	352	60	GE	29	27	4	1	26	1.47

* N_1' is derived from N_1 by rejecting the central nebula and correcting for the area which it covers. If the product of the two diameters, ab in the ninth column, is not listed, the nebula falls outside the central circle, I, and, while the nebula is omitted in deriving N_1, the correction for the area covered is negligible. The four cases for which $ab = 100$ refer to central nebulae so large that the entire central circles are omitted.

Duplicate plates are included for NGC 4293 and 524.

The two nebulae, $\beta = -47°$, $\lambda = 61°$, and $\beta = -51°$, $\lambda = 54°$, are uncatalogued.

Plates in the Virgo cluster with the numbers of nebulae omitted in the reductions as presumably members of the cluster are:

NGC 4293	1 neb.	NGC 4124	2 neb.
4651	1	4535	3
4192	2	4612	2
4762	3	4532	3
4178	2	4215	1

The following fields are in both Tables III*a* and III*b*:

FIELD	LOG N	
	60-In.	100-In.
NGC 4762	1.87	1.92
4535	2.06	2.06
2859	2.03	1.89
4454	2.03	1.93

TABLE III*a*—*Continued*

NGC	β	λ	E	Q	Z	N_1	I	ab	N_1'	log N
6384	+20°	358°	50	FG	29°	13	2	14	12	1.39
6610	13	10	60	G	20	14	2	0.1	13	1.22
6661	13	19	60	G	16	33	6	1.5	32	1.62
6674	13	22	70	FG	10	11	1	6.7	10	1.09
6710	+11	25	60	FG	21	20	3	1	19	1.47
6921	− 9	35	75	G	17	10	5	0.2	9	0.93
2325	10	208	45	F	63	7	3	0.3	6	1.44
147	14	87	90	GE	23	38	8	32	40	1.42
185	14	89	75	G	14	33	8	12	33	1.49
IC 5180	15	60	60	GE	13	53	9	1.1	52	1.76
6814	17	357	60	G	45	6	1	6.7	5	0.87
IC 5000	18	18	60	FG	37	24	3	.....	23	1.58
6906	19	18	60	FG	31	13	4	2.1	12	1.29
6928	19	22	60	GE	24	50	11	2	49	1.75
6944	21	20	60	FG	27	25	4	0.1	24	1.58
7363	22	63	40	GE	24	49	6	0.8	48	1.97
6969	23	22	60	FG	33	18	2	0.5	17	1.44
7033	23	32	60	G	20	51	14	0.1	50	1.81
6915	24	9	75	GE	44	56	8	0.5	55	1.72
6954	24	18	60	G	37	9	4	0.4	8	1.04
6962	27	15	60	FG	34	40	6	6.5	39	1.81
7040	27	27	60	G	27	21	4	0.6	20	1.42
1156	28	125	45	FG	10	39	2	7.5	38	1.93
7177	30	43	90	G	35	82	9	6.3	82	1.82
7046	31	22	60	E	35	95	9	.....	94	2.01
IC 1380	34	24	60	GE	42	63	13	.....	62	1.89
7102	34	30	60	FG	32	44	10	2.2	43	1.84
1507	35	161	60	E	37	49	6	2.8	48	1.72
160	39	87	60	E	31	215	18	4	215	2.36
169	39	87	75	E	11	76	5	0.4	75	1.75
7454	40	57	120	G	34	157	16	0.4	156	1.93
1453	41	161	80	FP	47	36	4	0.6	35	1.90
877	43	121	60	E	19	61	8	.....	60	1.79
.....	47	61	40	E	23	31	6	0.2	30	1.72
.....	51	54	30	E	29	22	3	0.1	21	1.74
524	52	106	60	GE	41	54	6	4.4	53	1.82
			150	FG	28	134	17	4.4	134	1.80
741	53	120	60	G	32	96	13	0.6	95	2.11
7393	55	34	110	GE	41	132	12	2.2	131	1.87
7785	55	66	60	FG	40	51	7	1	50	1.93
718	55	118	60	E	30	76	6	5.7	75	1.91
1084	55	151	60	G	43	44	5	6.7	43	1.79
488	56	106	90	FG	30	134	15	18	136	2.11
1042	56	151	60	GE	43	55	7	16	55	1.84
7716	58	57	60	FG	34	62	5	4.3	61	2.01
200	59	87	60	E	44	200	16	2.6	199	2.37
521	60	111	60	FG	42	109	6	9	108	2.27
533	60	111	45	E	33	135	15	.....	134	2.33
IC 48	70	89	90	G	43	142	12	1	141	2.08
210	76	85	60	GE	50	82	6	21	82	2.05
578	78	157	90	G	58	120	10	10	120	2.11
134	83	296	60	FG	69	23	3	8.7	22	1.84
289	−85	245	60	G	66	67	2	40	67	2.19

TABLE III*b**

60-INCH; FIELDS CENTERED ON NEBULAE

NGC	β	λ	E	Q	Z	N_1	I	ab	N_1'	log N
4251	+84°	165°	60	GE	24°	93	10	1.8	92	2.18
4203	82	139	50	G	4	41	8	6.6	40	1.97
5127	81	28	50	G	33	38	4	0.6	37	1.97
4450	80	249	45	E	25	57	5	10	54	2.08
3900	77	180	60	GE	34	58	8	2.4	57	2.00
4421	77	250	50	G	44	20	1	1	17	1.67
3941	76	138	45	G	24	33	6	2.8	32	1.96
4267	75	247	45	F	28	49	7	5.5	45	2.28
4377	75	250	50	GE	30	61	13	1	57	2.10
4406	75	251	60	GE	40	80	9	5.5	70	2.10
4552	75	261	80	G	22	55	8	2.6	50	1.80
3813	74	144	60	FP	15	31	1	2.1	30	2.09
4138	73	110	50	G	34	37	4	1.3	36	1.97
4111	73	113	50	FG	11	86	13	4	85	2.38
4452	73	253	60	GE	23	119	15	0.5	116	2.27
4596	73	266	40	G	54	17	1	3.2	15	1.79
4762	73	276	60	FG	39	32	7	8	30	1.87
4451	71	257	50	GE	35	50	8	0.4	46	2.01
4698	71	272	40	G	38	24	3	3.8	23	1.90
5297	70	57	50	G	12	44	5	8	43	2.00
4535	70	261	40	G	40	36	3	36	33	2.06
3949	68	113	40	GE	37	19	7	3.1	18	1.73
3655	68	206	50	G	39	43	6	1	42	2.04
3893	67	113	50	G	36	41	8	12.3	41	2.02
3877	67	115	60	FG	19	46	3	3.1	45	2.00
3605	67	198	60	G	27	46	6	.....	45	1.93
3607	67	198	90	G	34	59	6	1.5	58	1.83
4586	67	266	60	G	35	46	4	4.1	44	1.94
4157	66	104	60	GE	17	53	5	7.2	52	1.93
4088	65	105	45	F	30	24	3	9.5	23	2.00
3953	65	108	60	G	37	53	5	15	52	2.02
3432	65	154	50	FG	46	41	4	6.2	40	2.13
3628	65	210	60	E	24	85	7	2	84	2.10
5250	64	71	50	FG	47	23	3	0.2	22	1.87
4102	64	103	60	G	24	82	7	5.4	81	2.19
3414	64	170	60	GE	37	74	7	.....	73	2.10
3437	64	185	60	G	17	63	7	1.8	62	2.06
4179	63	253	35	FG	57	8	1	1.1	6	1.58
5772	61	35	60	GE	31	46	9	2	45	1.88
5689	60	52	80	FP	49	20	2	1	19	1.81
3631	60	115	70	FG	29	56	7	16	56	2.02
5473	59	66	45	G	35	33	5	1	32	1.98
5485	59	66	45	G	30	51	8	1	50	2.16
4814	59	87	60	G	26	67	9	.....	66	2.10
4500	59	93	50	G	24	40	7	2.3	39	1.98
5204	58	80	45	GE	33	33	6	10.4	32	1.91
3549	58	117	50	FG	41	24	3	3	23	1.87
5585	57	65	40	GE	38	39	5	24	39	2.07
3945	57	101	45	FG	29	30	2	2.1	29	1.99
3895	+57	103	50	E	26	46	7	0.8	45	1.94

* Plates in the Virgo cluster with the numbers of nebulae omitted in the reductions as presumably members of the cluster are:

NGC 4450	3 neb.	NGC 4596	2 neb.
4421	3	4762	3
4267	4	4451	4
4377	4	4698	1
4406	10	4535	3
4552	5	4586	2
4452	3	4179	2

TABLE III*b*—*Continued*

NGC	β	λ	E	Q	Z	N_1	I	ab	N_1'	log N
5576	+57°	317°	40	FG	38°	26	5	0.8	25	2.02
5631	56	65	60	GE	31	74	6	1	73	2.09
5379	56	74	40	GE	36	25	2	.....	24	1.85
3642	56	108	60	G	29	81	9	17.5	81	2.19
3610	56	110	45	GE	25	50	7	1	49	2.08
3189	56	180	45	E	12	36	5	3.6	35	1.87
5322	55	76	90	G	36	78	8	2	77	1.96
3488	55	114	50	F	38	58	8	1.8	57	2.36
3458	55	115	120	FG	31	92	3	3	91	1.93
4995	55	281	40	G	57	26	6	6.3	25	2.04
5820	54	56	60	GE	24	71	20	0.3	70	2.07
5216	54	81	45	FG	33	46	5	0.3	45	2.19
4699	54	272	50	G	42	51	7	8.5	50	2.13
4958	54	280	50	G	43	66	9	4	65	2.24
4125	52	96	45	FG	36	18	5	2	17	1.78
3021	52	160	50	F	39	32	2	1.5	31	2.09
3206	51	121	45	E	19	41	6	5.6	40	1.94
2971	51	155	60	F	15	36	4	0.6	35	1.98
3182	50	119	45	E	29	33	6	0.5	32	1.86
3682	49	102	60	GE	34	62	13	0.7	61	2.03
4250	47	93	60	FP	35	11	1	3	10	1.65
2859	47	159	45	E	27	49	5	12	48	2.03
5846	47	328	60	GE	40	45	8	1	44	1.89
2950	46	122	45	GE	38	32	4	1.1	31	1.91
5984	46	351	60	GE	32	58	6	2.2	57	1.99
2841	45	135	80	G	24	87	5	36	87	2.05
2782	45	150	45	FP	21	20	2	3.6	19	2.07
5044	45	280	40	GE	55	50	7	0.5	49	2.25
5970	45	346	45	GE	27	61	11	4.3	60	2.17
2770	44	159	60	FG	20	46	7	4.4	45	2.00
3516	43	100	60	FG	42	43	5	1.6	42	2.02
6143	42	52	60	GE	26	57	12	0.8	56	1.97
5832	42	76	45	GE	45	24	2	5	23	1.80
3348	42	102	50	E	41	49	7	0.6	48	2.01
3034	42	108	90	F	37	29	2	40	28	1.70
2742	41	122	45	G	26	13	2	4.8	12	1.53
3147	40	103	45	F	40	11	3	3.6	10	1.66
2787	39	111	45	F	41	22	5	2.8	21	1.99
3063	38	347	60	G	34	26	3	2	25	1.70
2608	37	162	40	FG	36	16	2	2	15	1.79
2650	36	111	45	E	42	36	6	1.2	35	1.93
2974	36	208	45	G	44	34	10	0.4	33	2.02
2748	35	103	45	GE	23	16	1	0.8	15	1.56
2633	35	106	60	G	48	41	4	4.9	40	1.95
2775	35	193	50	G	40	79	7	9	78	2.31
6359	34	58	35	G	30	9	3	1	8	1.50
6217	34	78	30	F	44	12	3	3.8	11	1.95
2732	34	100	45	G	46	30	6	0.5	29	1.97
2715	34	102	45	F	44	12	2	6.8	11	1.72
2655	33	102	60	FG	48	32	6	30	32	1.94
2543	33	153	45	G	33	44	5	.....	43	2.09
6690	27	68	60	FG	43	49	4	.....	48	2.08
2424	27	149	60	F	20	29	3	2	28	1.90
6240	26	348	60	GE	38	23	9	1.4	22	1.79
2781	24	212	50	FG	53	27	2	1	26	1.98
2389	23	153	60	FG	15	45	7	3.4	44	1.98
2811	23	215	60	G	50	15	1	1.2	14	1.51
6732	20	50	60	FP	19	17	7	1	16	1.82
1530	18	103	90	FG	42	17	1	20	16	1.37
6824	+15	55	60	GE	22	24	10	1.2	23	1.57

On plates in the Virgo cluster all nebulae brighter than about the fifteenth magnitude have been omitted as presumably members of the cluster—perhaps an unnecessary refinement, but consistent with the general principle of omitting the great isolated clusters in discussing the general distribution of the background on which they

TABLE III*b*—*Continued*

NGC	β	λ	E	Q	Z	N_1	I	ab	N_1'	log N
6570	+14°	9°	60	G	21°	12	4	1.4	11	1.31
6615	12	9	60	G	27	9	2	0.3	8	1.18
IC 1303	+ 7	37	55	FG	16	19	2	1	18	1.66
1233	−15	119	60	FP	5	7	1	1.5	6	1.39
1003	17	112	60	G	22	55	10	5.3	54	2.00
7640	19	73	45	G	20	24	8	.....	23	1.80
IC 1320	21	15	60	GE	35	19	3	0.3	18	1.50
925	24	113	60	F	10	16	2	96	16	1.64
753†	25	105	60	G	10	35	4	7.8	34	1.79
			45	GE	15	45	5	7.8	44	2.00
1620	28	164	50	FP	35	21	5	2.4	20	2.06
1588	29	162	60	FG	33	38	6	.....	37	1.94
IC 1377	32	25	60	GE	36	42	3	0.4	41	1.85
IC 1401	38	27	60	GE	33	29	5	1.6	28	1.68
7448	40	56	60	GE	27	56	4	.....	55	1.96
7454	40	57	45	G	25	39	7	0.5	38	2.03
7374	42	49	60	E	24	54	11	0.4	53	1.90
7385	42	51	60	GE	28	120	23	0.3	119	2.30
IC 1437	44	33	50	G	43	24	5	0.5	23	1.79
7469	46	52	60	G	31	63	8	2.2	62	2.08
660	47	111	60	FG	28	60	9	31	61	2.15
IC 5241	48	40	60	GE	44	40	7	0.4	39	1.86
IC 1460	49	47	60	GE	33	63	9	0.1	62	2.02
7743	50	66	60	E	26	78	18	2.2	77	2.07
1073	50	139	60	G	34	45	4	20	44	1.94
7541	51	52	60	GE	31	35	4	3.3	34	1.76
95	52	81	60	GE	25	55	10	2.3	54	1.95
936	54	136	75	G	36	96	23	11.2	96	2.15
193	59	87	60	G	38	58	7	.....	57	2.07
196	62	87	60	FG	38	77	12	0.6	76	2.27
779	62	132	100	F	41	73	10	4	72	2.07
596	−66	121	40	G	42	27	2	.....	26	1.96

† A duplicate plate of NGC 753 is included which gives the maximum difference in log N derived from an examination of about forty pairs of duplicates. This difference of 0.21 corresponds to a difference in limiting magnitude of the order of 0.35, which must be accounted for by variations in sky transparency, emulsion, definition, and development.

are spotted. The list of omissions, given in footnotes to Tables III*a* and *b*, indicates their small or negligible effect on the general statistical results.

Table IV*a* gives 139 extra-survey plates on which no nebulae were found. These, together with 75 such fields in the survey, determine the zone of avoidance. Table IV*b* lists 28 plates bordering the zone of avoidance, on which a few nebulae were found. These plates do

not conform to the survey conditions but are useful in defining the borders of the zone. Positions alone are listed in Tables IV, but in all cases the exposures are equivalent to at least an hour on fast plates with the 60-inch reflector.

TABLE IV*a*

FIELDS WITH NO NEBULAE

β	λ	β	λ	β	λ	β	λ	β	λ
+35°	334°	+ 6°	330°	+ 2°	336°	− 1°	319°	− 4°	355°
20	75	5	21	+ 1	28		345	5	4
20	85		34		29	2	35		28
20	323		35		36		53	6	14
18	350		61		55		56		62
16	321		199		159		334		91
15	346		347		179		335		353
14	71		349		195	2	343	7	133
	320	4	22		30	2	346	8	22
	321		35	0	34		348		356
	344		106		37		349	9	164
13	337		124		46		354	10	181
12	0		156		73		355		182
	74		162		78	3	26	12	142
	330		350		80		198	13	173
	340	3	8		110		199	14	136
	350		45		188		333		137
10	73	3	46		317		334	15	174
	335	3	87		321		339		175
9	6		106		335		353	17	128
	68		171	− 1	1		354	18	176
8	10	+ 2	43		27	− 4	10	19	125
	333		48		52		37		126
7	112		105		54		152	20	126
	329		142		91		205		144
	336		169		140		330	21	126
+ 6	14		170		193		335	−23	171
	65		171		205		336		

TABLE IV*b*

SUPPLEMENTARY LIST OF FIELDS WITH VERY FEW NEBULAE

β	λ		β	λ		β	λ	
+30°	335°	Field	+12°	108°	IC 342	−10°	99°	Field
25	325	Field	11	29	Field	12	43	NGC 7013
20	65	Field		63	NGC 6946	13	52	IC 1392
19	309	NGC 5968		213	2613	16	0	NGC 6821
18	321	6093	10	312	IC 4597		172	IC 423
14	106	IC 356	+ 9	333	NGC 6333	22	134	Pleiades
	165	NGC 2339	− 7	161	Field	25	355	Field
13	0	6509	9	34	Field	−35	135	Field
+12	11	6627		40	Field			
	55	Field	−10	43	Field			

The complete data, including about 1283 independent samples covering a total area of about 650 square degrees, or a trifle more than 2 per cent of the three-quarters of the sky included in the survey, are summarized in Table V. They comprise fairly comparable

groups representing the two telescopes and the survey and extra-survey fields. The groups for the two hemispheres are roughly in

TABLE V

SUMMARY OF OBSERVATIONAL DATA

	100-INCH		60-INCH		TOTAL	
	Fields	Neb.	Fields	Neb.	Fields	Neb.
Survey, Table I	387	13,130	378	11,515	765	24,645
Extra-survey, Tables II	55	4,412	61	2,331	116	6,743
Extra-survey, Tables III	93	5,685	142	6,128	235	11,813
Total	535	23,227	581	19,974	1,116	43,201

Extra-survey blank fields, Table IV*a*	139
Supplementary, Table IV*b*	28
Total fields	1,283

Polar Caps

	NORTH		SOUTH		TOTAL	
	Fields	Neb.	Fields	Neb.	Fields	Neb.
Survey	247	10,693	150	6,461	397	17,154
Extra-survey	179	10,666	65	4,363	244	15,029
Total	426	21,359	215	10,824	641	32,183

Galactic Belt

	Fields	Neb.	Fields	Neb.	Fields	Neb.
Survey	207	4,409	161	3,082	368	7,491
Extra-survey	129	1,459	145	2,068	274	3,527
Total	336	5,868	306	5,150	642	11,018

proportion to the relative areas over which they are distributed. The various groups have been analyzed separately and collectively, but

the only striking differences are the systematically larger values of log N for the extra-survey plates in high latitudes as compared with those for the survey. The excess amounts to approximately 0.10 in log N or about 25 per cent in the numbers. Various possible explanations were considered, but eventually the two groups were simply combined for evaluating the final results. The discussion, however, should be followed with this discrepancy in mind.

REDUCTION TO A HOMOGENEOUS SYSTEM

The data were reduced to a homogeneous system by applying the corrections ΔZ, ΔQ, and ΔE as already mentioned, and thus corrected were used to investigate the distribution over the sphere to a uniform but undetermined limiting magnitude. The results are independent of the second part of the investigation, in which the data are reduced to numbers of nebulae per unit area to definite limiting magnitudes. The final reductions are the culmination of a series of successive approximations of which only the later stages will be presented in detail. Preliminary analysis led to the following general conclusions, which are merely more precise formulations of previous indications:[16]

1. No nebulae are found along the heart of the Milky Way. The zone of avoidance is irregular and unsymmetrical, the width varying from 10° to 40°.

2. Nebulae are scarce along the borders of the zone and in certain regions the scarcity can be followed out to latitude 40°.

3. In the higher latitudes the nebular distribution, to a first rough approximation, is random, with occasional clusters superposed.

4. In the higher latitudes the numbers of nebulae increase with limiting magnitudes (or exposure times) at a rate which indicates a fair approximation to uniform distribution in depth, i.e., $\log N_m = 0.6m + C$.

On the basis of these results, the sphere was divided into the galactic belt ($\beta = -40°$ to $+40°$) and the polar caps ($\beta = 40°$ to $90°$). Data in the polar caps were assumed to represent nebular distribution alone; those in the galactic belt, a combination of nebular distribution and local galactic obscuration. Since the preliminary results in-

[16] *Publications of the Astronomical Society of the Pacific*, **43**, 282, 1931.

dicated an approximately uniform or random distribution in the polar caps, the corrections ΔQ and ΔE, for quality of images and exposure times, were derived from those regions alone.

ATMOSPHERIC EXTINCTION

As a first step the counts were corrected for atmospheric extinction by adding to log N_1 or log N_1' the factor

$$\Delta Z = 0.6\ \Delta m\ ,$$

where Δm is the extinction in photographic magnitudes at zenith distance Z, taken from the table in current use at Mount Wilson.[17] The coefficient 0.6 follows from No. 4 of the preliminary results. Since the relation

$$\log N_m = 0.6m + C$$

holds approximately over a considerable range in m, the assumption that it holds precisely over the limited range in atmospheric extinction covered by the observations will not introduce serious errors.

The corrections are listed in Table VI as a function of Z. Up to $Z = 60^\circ$ the values were interpolated from a smooth curve constructed from the extinction tables. Beyond 60° they are extrapolations following the theoretical trend of extinction-curves; but since very few plates were exposed at low altitudes, the uncertainties are not important. The values of ΔZ in Tables I–III range up to 0.32, but only 18 exceed 0.20 and the mean is about 0.053.

The corrections might be applied to exposures rather than to the counts, thus avoiding the assumption of uniform distribution. This procedure, however, would introduce an assumption concerning the relation between limiting magnitude and exposure time which is probably as uncertain as that concerning distribution, and hence offers little advantage over the convenient method actually adopted.

CORRECTION FOR QUALITY OF IMAGES

The quality factor, ΔQ, is perhaps the most important and at the same time the most arbitrary factor in the entire investigation.

[17] F. H. Seares *et al.*, *Carnegie Institution of Washington Publication*, No. 402; *Papers of the Mount Wilson Observatory*, **4**, Introd., p. 36, 1930.

It measures the effect of definition on the threshold of identification or the ability to distinguish between nebulae and stars. The plates were rated on an arbitrary scale as "Excellent," "Good," "Fair," and "Poor," with the intermediate steps "GE," "FG," and "FP," according to the sharpness of the star images. For one-hour exposures in the polar caps, mean values of $\log N_1 + \Delta Z$ were then derived

TABLE VI

CORRECTIONS TO LOG N DEPENDING ON ZENITH DISTANCE

Z	Δm_{pg}	ΔZ^*	Z	Δm_{pg}	ΔZ^*	Z	Δm_{pg}	ΔZ^*
10°	0.004	0.00	43°	.....	0.06	57°	.....	0.15
16	.....	.01	44	.....	.07	58	.....	.16
20	.019	.01	45	0.122	.07	59	.....	.17
23	.....	.01	46	.....	.08	60	0.295	.18
24	.....	.02	47	.....	.08	61	.....	(.19)
29	.....	.02	48	.....	.09	62	.....	(.20)
30	.046	.03	49	.....	.09	63	.....	(.21)
33	.....	.03	50	.164	.10	64	.....	(.23)
34	.....	.04	51	.....	.10	65	(.40)	(.24)
35	.065	.04	52	.....	.11	66	.....	(.26)
37	.....	.04	53	.....	.12	69	.....	(.32)
38	.....	.05	54	.....	.12	70	(0.59)	(0.35)
40	0.090	.05	55	0.219	.13			
41	.....	0.06	56	.....	0.14			

* $\Delta Z = 0.6 \Delta m_{pg}$.

for each quality class.[18] These values are listed in Table VII for each telescope and for survey and extra-survey groups, both separately and combined, together with the number of plates, n, and the mean latitude corresponding to each value. The latitudes are included because a correlation was found later between $\log N$ and β which, although of little importance in the higher latitudes, might possibly influence the derivation of the quality factors. Rereductions which take into account the latitude effect indicate, however, no very significant revisions of the factors actually adopted.

The data are presented graphically in Figure 1, where values of $\log N$ are plotted against quality classes, both for the survey alone and for the totals. The quality classes are arbitrarily separated by

[18] Four fields were omitted as obviously affected by local obscuration. These are $\beta = +40$, $\lambda = 330°$ and 340°; $\lambda = 140°$, $\beta = -40°$ and $-45°$. One field ($\beta = +55°$, $\lambda = 10°$) was omitted because it includes a conspicuous cluster.

equal intervals along the horizontal axis. The curves for the two telescopes are approximately parallel, with a displacement of the

TABLE VII

QUALITY FACTORS

Q	Survey			Extra-survey			Total		
	n	log N	β	n	log N	β	n	log N	β
	100-Inch								
E	17	1.838	66°.2	9	2.076	63°.6	26	1.920	65°.3
GE	32	1.877	61.1	12	1.923	63.9	44	1.890	61.8
G	34	1.775	60.0	16	1.883	61.3	50	1.809	60.4
FG	38	1.720	57.0	14	1.870	67.2	52	1.761	59.7
F	35	1.633	55.3	6	1.761	68.8	41	1.652	57.3
FP	15	1.447	53.7	.....	.....	.....	15	1.447	53.7
Total	171	1.730	58.6	57	1.906	64.2	228	1.774	60.1
	60-Inch								
E	39	1.758	58.2	5	1.856	57.2	44	1.770	58.1
GE	56	1.696	54.1	26	1.799	56.6	82	1.729	55.1
G	33	1.627	56.5	15	1.765	59.1	48	1.670	57.3
FG	15	1.544	54.7	8	1.667	59.0	23	1.587	55.5
F	13	1.438	55.0	1	1.540	51.0	14	1.446	54.7
FP	1	1.340	40.0	2	1.260	60.5	3	1.287	53.7
Total	157	1.659	55.7	57	1.753	57.4	214	1.680	56.1

Q	100-Inch		60-Inch		Mean log N	ΔQ	Adopted ΔQ	
	n	log N	n	log N + 0.16			100-Inch	60-Inch
E	26	1.920	44	1.930	1.926	0.000	0.00	0.16
GE	44	1.890	82	1.889	1.889	.037	.04	.20
G	50	1.809	48	1.830	1.820	.106	.10	.26
FG	52	1.761	23	1.747	1.756	.170	.18	.34
F	41	1.652	14	1.606	1.640	.286	.28	.44
FP	15	1.447	3	1.447	1.447	0.479	0.45*	0.61

* The value 0.45 is adopted on the basis of results from 18 rejected FP plates.

order of 0.16 in log N. This quantity was accordingly added to log N for the 60-inch, and mean values were then derived from the data

for the two telescopes combined. Figure 1 indicates the fairly satisfactory manner in which the data are represented by smooth curves adjusted to the mean values.

More detailed information is furnished in Table VII. The outstanding residual in the curve representing all data combined (upper curve in Fig. 1) is the 60-inch point for quality F, which depends upon only 14 plates. Of the two large residuals for the survey alone

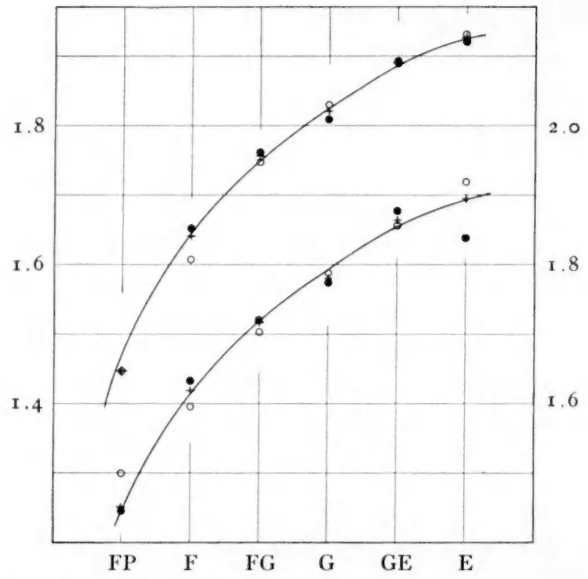

FIG. 1.—Quality factors. Mean log N for one-hour exposures, $\beta \gtrless 40°$, plotted against quality classes. The lower curve represents the survey alone; the upper curve, all the data combined. Disks indicate data with the 100-inch; circles, with the 60-inch but with log N increased by 0.16; crosses, means for both telescopes, weighted according to the relative numbers of plates. Data from Table VII.

(lower curve) the 100-inch point for quality E depends upon 17 plates; the 60-inch point for FP on a single plate. Plates of quality P were in general discarded as unreliable, and the relatively few of quality FP that are included were retained for the sake of completeness when efforts at replacement had not succeeded. Examination of discarded plates suggested a slight revision of the quality factor for FP, indicated by the data in Table VII, and a tentative factor

of 0.70 for the two 100-inch P plates,[19] which were retained for completeness. The adopted quality factors, ΔQ, listed at the end of Table VII, are slightly smoothed in order to represent a uniform progression, but, except for the FP factor already mentioned, the revisions do not exceed 0.01. The systematic term, 0.16, added to the factors for the 100-inch, gives factors for the 60-inch which reduce the counts to the standard conditions of excellent plates with the 100-inch.

The factors were derived from one-hour exposures alone and are assumed to apply over the entire range of exposures (20–150 min.). The data are too restricted for conclusive evidence on this point, but they are not inconsistent with the assumption. The quality scale is arbitrary, the smooth progression of the factors being more or less accidental. Each class covers a considerable range in the scale and this circumstance introduces an artificial scatter into the corrected counts. The procedure, in fact, represents a much-simplified statistical approximation, but it is doubtful whether the nature of the data justifies more refined methods.[20]

CORRECTION FOR EXPOSURE TIME

Preliminary examination suggested that, as a first approximation, tripling the exposure quadruples the numbers of nebulae. Tripling the exposure was supposed to extend the limit by 1 mag. (the usual assumption in photographic photometry with fast plates); hence quadrupling the nebulae suggested uniform distribution in depth. The relation is

$$\log N = \frac{0.602}{0.477} \log E + C ,$$

$$= 1.26 \log E + C .$$

This relation ignores the effect of red shifts in diminishing apparent luminosities and assumes a deviation from the photographic reciprocity law represented by a value of about 0.84, for the Schwarzschild exponent p.

[19] These are survey fields at $\beta = +35°$, $\lambda = 300°$ and $\beta = -15°$, $\lambda = 140°$. The data are uncertain but do not affect the general results.

[20] Since the number of FP plates is small, the greatest scatter should be in class F where, as indicated in Fig. 1, log N ranges from about 1.57 to 1.70. These plates were

Detailed analysis of the present data indicates, however, a coefficient for log E in the preceding relation definitely greater than 1.26; and interpretation of this result introduces problems of far wider significance than the immediate purpose, which is merely the reduction of the counts to a uniform exposure of one hour. Further discussion of these problems will be deferred, but it may be mentioned that the present results appear to represent the combination of a close approach to the reciprocity law[21] under the particular observing conditions (small surface images at the threshold of Eastman 40 plates), which increases the coefficient, and the effect of the red shift, which diminishes the coefficient. This interpretation is sufficiently probable to justify the retention of the provisional assumption that the nebulae are distributed uniformly in depth.

In Figure 2, log N (representing the counts reduced to quality E with the 100-inch at the zenith) is plotted against log E (exposure time in minutes) for 636 fields in the polar caps (omitting the 5 fields not used in deriving the quality factors). A casual inspection indicates an approximately linear correlation in which the coefficient of log E is of the order of 1.3. The data are grouped according to a small number of values of log E and in each group of any considerable size the frequency distribution of log N approximates an error-curve more or less symmetrical about the mean value. The diagram is dominated by the excessively large group of one-hour exposures in which the range in log N, as expected from the form of the frequency distribution, is disproportionately large. This restricts the significance of a correlation ratio and limits the analysis to the regression-curve of log N on log E, or to the usual least-squares solution with the data grouped according to log E. A direct solution

re-examined and divided into three groups, F+, F, and F−. Log N then fell in the same order, but the results did not appear to justify the general application of the refinement.

[21] Some observations bearing on the reciprocity law are mentioned later in connection with the determination of limiting magnitudes corresponding to particular exposure times. These data are more or less consistent with various recent investigations which tend to reduce the failure of the reciprocity law, at least for low intensities and fast plates, as compared with the results found in earlier investigations. See, for instance, Jones and Huse (*Journal of the Optical Society of America*, **11**, 338, 1925) for data on the fast Seed 30 plate and Twyman and Harvey (*Transactions of the Optical Society*, **33**, 1, 1931) for tests of the Schwarzschild relation at the threshold.

of this nature, with equal weights for all fields, leads to the relation

$$\log N = 1.290 \log E - 0.362 , \qquad (1)$$

which is indicated by a full line in the figure.

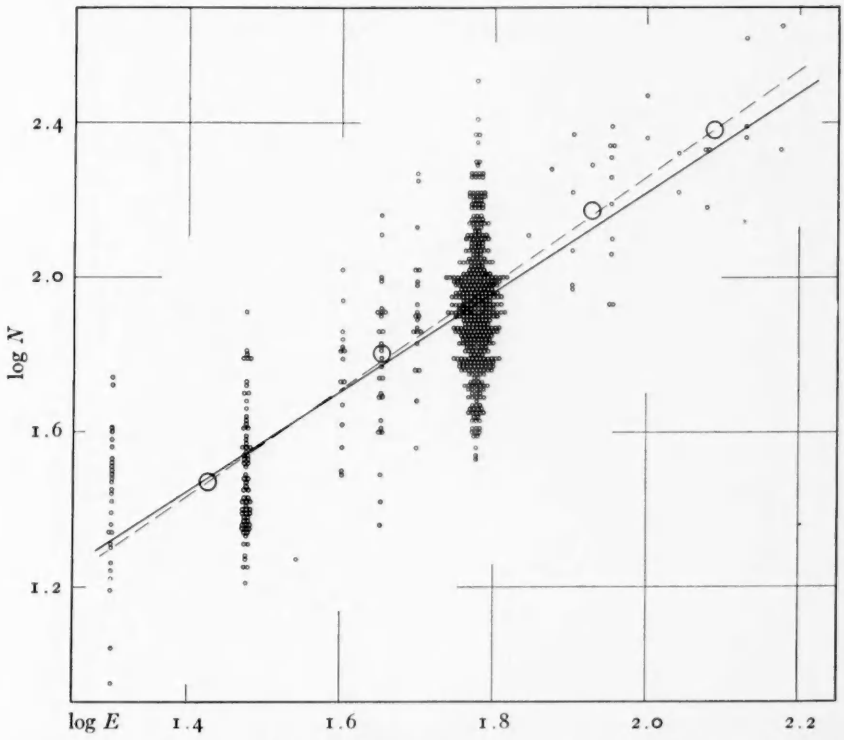

FIG. 2.—Log N as a function of exposure time. Log N, corrected for quality and atmospheric extinction, plotted against log E (exposure time in minutes) for all plates with $\beta \gtrless 40°$. The five large circles are mean points from Table VIII, from which is derived the correlation indicated by the dash line (log $N = 1.376$ log $E - 0.493$). The full line is the relation, log $N = 1.290$ log $E - 0.362$, derived from a least-squares solution for a grouping according to log E with equal weights for all plates.

The assignment of equal weights, however, is open to criticism. If the nebulae are distributed approximately at random, the volume of space explored, and hence the number of nebulae recorded per plate, should increase with exposure and, of course, the errors of sampling should decrease as the size of the samples increases. The

weights, therefore, should increase with the exposure, and hence in Figure 2 the systematic departures of the longer exposures from the foregoing relation cannot be entirely ignored, notwithstanding the relatively small numbers of plates involved. The 30 plates with exposures longer than an hour represent about 5400 nebulae, as compared with about 6600 nebulae found on the 164 plates with exposures shorter than an hour. The relative weights of the two groups as derived from plates and from nebulae are about 1 to 5.5 and 1 to 1.2, respectively.

The effect of weighting according to numbers of nebulae can be partially ascertained by grouping the data for exposures other than one hour into mean points representing comparable numbers of nebulae and including the mean for the hour exposures with the same weight. The necessary data are found in Table VIII, which gives, both for plates centered on selected nebulae and for plates centered without reference to nebulae, the mean log N for each exposure time and for various groupings of the exposures. For the immediate purpose the significant data are the 3-groups and the 5-groups for all fields combined. These mean points lead to coefficients of log E equal to 1.364 and 1.376, respectively. The latter relation is indicated in Figure 2 by a dash line, and the 5-points from which it is derived are represented by large open circles.

Other methods of grouping the data lead to values of the coefficient of log E which, in general, lie between the extremes already mentioned, namely, 1.29 and 1.37. Largely for this reason, and without further discussion of the relative merits of weighting by plates or by counts, a value of 1.33 has been adopted for the reductions as a compromise. This arbitrary procedure is admittedly a makeshift to serve the immediate purpose. It has little justification beyond the fact that the corresponding corrections to log N differ from those derived from either extreme value by more than 0.01 only for the twenty-minute exposures and the four longest exposures for which the difference is 0.02. These quantities are well within the uncertainties of the counts. The corrections for each exposure time which reduce the values of log N to the standard exposure of one hour are given in Table IX.

APPARENT DISTRIBUTION OF NEBULAE

The general features of the apparent nebular distribution are indicated in Figure 3 where the fields are plotted by galactic co-ordinates on Aitoff's equal-area projection of the sphere. The term "nor-

TABLE VIII

RELATION BETWEEN LOG N AND EXPOSURE TIME

Exposure	Survey and Extra-survey Fields			Fields Centered on Nebulae		
	n	$\overline{\log N}$	$\overline{\log E}$	n	$\overline{\log N}$	$\overline{\log E}$
20^m	27	1.419	1.301	1	1.240	1.301
30	68	1.495	1.477	2	1.440	1.477
35	.....	.....	.....	1	1.270	1.544
40	1	1.860	1.602	14	1.739	1.602
45	2	1.590	1.653	27	1.783	1.653
50	.....	.....	.....	21	1.916	1.699
60	371	1.912	1.778	71	1.997	1.778
70	.....	.....	.....	1	2.110	1.845
75	.....	.....	.....	1	2.280	1.875
80	.....	.....	.....	5	2.122	1.903
85	1	2.290	1.929	.....	.....	.....
90	3	2.250	1.954	7	2.157	1.954
100	1	2.470	2.000	1	2.360	2.000
110	.....	.....	.....	2	2.270	2.041
120	.....	.....	.....	3	2.280	2.079
135	1	2.620	2.130	2	2.375	2.130
150	1	2.650	2.176	1	2.330	2.176
Total	476	1.830	1.711	160	1.942	1.754
3-Groups						
20–50	98	1.480	1.435	66	1.789	1.646
60	371	1.912	1.778	71	1.997	1.778
70–150	7	2.397	2.014	23	2.214	1.986

ALL FIELDS

5-Groups				3-Groups			
20– 30	98	1.471	1.427	20– 50	164	1.604	1.518
35– 50	66	1.803	1.654	60	442	1.925	1.778
60	442	1.925	1.778	70–150	30	2.257	1.992
70– 90	18	2.174	1.928				
100–150	12	2.380	2.088				

mal distribution" is here applied to fields in which the numbers of nebulae lie between about one-half and twice the mean for fields within the polar caps; more precisely, log $N = 1.63-2.22$. About 93 per cent of the fields in the polar caps fall within the definition and are unobtrusively represented by small dots. Excesses and deficiencies are indicated by black disks and open circles, respectively, and crosses are superposed where the deviations from the mean exceed 0.60 in log N. Clusters, other than those appearing on survey plates, are omitted, and hence the crosses, with one exception,[22] are confined

TABLE IX

CORRECTIONS WHICH REDUCE LOG N_1 TO EXPOSURES OF ONE HOUR

E	ΔE*	E	ΔE*	E	ΔE*
20^m	+0.63	60^m	0.00	100^m	−0.29
30	.40	70	− .09	110	.35
35	.31	75	.13	120	.40
40	.23	80	.17	130	.45
45	.17	85	.20	135	.47
50	+0.10	90	−0.23	150	−0.53

* $\Delta E = 1.33 \log E$.

to deficiencies referring to galactic obscuration. Fields with no nebulae are indicated by dashes and, with one exception,[23] fall within the zone of avoidance along the Milky Way. The large-scale features are as follows: An irregular zone of avoidance runs along the Milky Way and is bordered by partial obscuration which fades away into the general field of normal distribution. The influence of the Milky Way is most conspicuous in the direction of the center of the galactic system ($\lambda = 325° \pm$), where it extends more than 30° on either side of the galactic plane. In the opposite direction ($\lambda = 145° \pm$) there is extensive obscuration to the south (Taurus region), but on the northern side the normal distribution sweeps down to latitude 15° or less.

THE ZONE OF AVOIDANCE

The zone of avoidance was outlined from the distribution of dashes alone, although the inclusion of crossed circles might have

[22] The cluster in Corona Borealis, falling in the survey field ($\beta = +55°$, $\lambda = 10°$).

[23] The small detached obscuring cloud near $\beta = +35°$, $\lambda = 335°$, marked *A*.

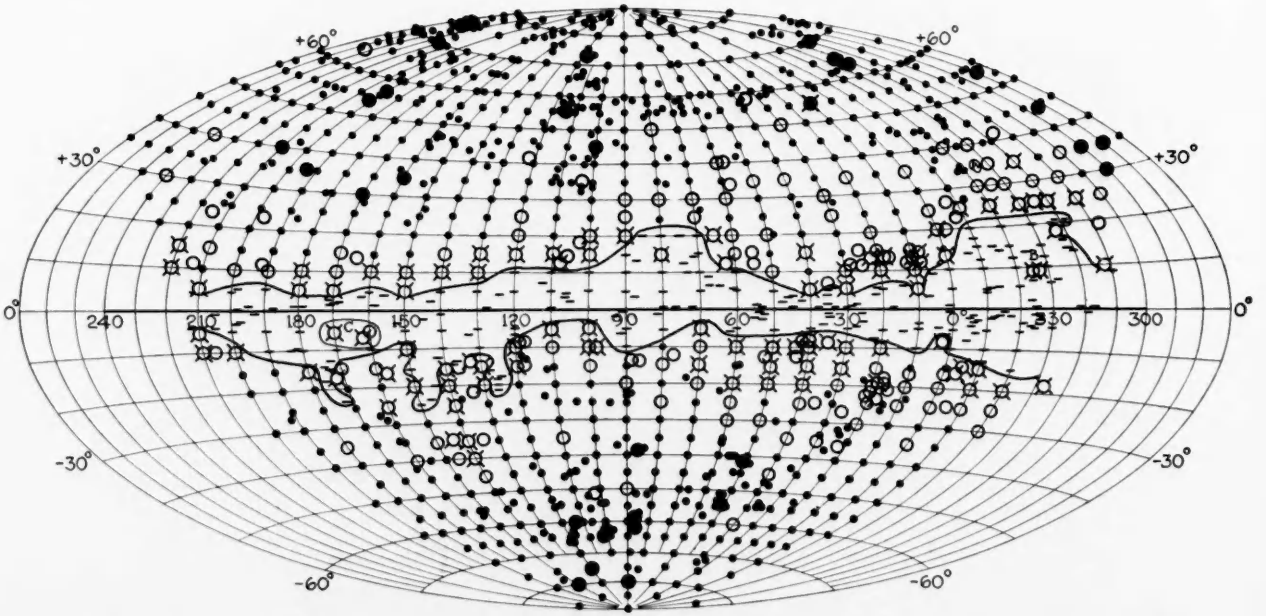

FIG. 3.—Distribution of extra-galactic nebulae. Small dots represent normal distribution (log $N = 1.63$–2.22); large disks and circles represent excesses (log $N = 2.23$–2.52) and deficiencies (log $N = 1.33$–1.62); crosses are added where log $N > 2.52$ or < 1.33; dashes represent fields with no nebulae.

enhanced its significance. Either method leads to the same general picture—a continuous irregular belt along the Milky Way with two small and significantly located exterior patches. The general pattern follows the distribution of known obscuring clouds, and the zone is presumed to represent analogous phenomena. The irregularity is strong evidence that the obscuration is due largely to isolated clouds rather than to a uniform layer of diffuse material.

The zone appears to consist of a narrow belt from 10° to 20° wide, centered approximately on the galactic plane, from which several great flares extend out into the higher latitudes. The two flares which extend to the highest latitudes coincide with the tips of the inclined belt of helium stars and diffuse nebulosity where it reaches its greatest departures from the galactic plane. These regions are the well-known areas in Ophiuchus and in Taurus, in the directions of the galactic center and anticenter respectively, the former representing the northern and the latter the southern reaches of the inclined belt. Beyond either tip are found the small detached outliers already mentioned[24]—one patch of obscuration near $\lambda = 335°$, $\beta = +35°$, the other near $\lambda = 145°$, $\beta = -35°$. The regions covered by these flares are so well known from the many published reproductions of camera plates that further description is unnecessary. The narrow winding flare leading up to the Orion nebula may perhaps be regarded as a detached outlier from the Taurus flare.

The Cepheus flare, north of the galactic plane and between longitudes 60° and 100°, is perhaps less familiar, although camera plates indicate that the entire region is affected by considerable obscuration. The flare extends out to latitude 20° or more, and the partial obscuration along its borders includes the position of the celestial pole ($\lambda = 90°$, $\beta = +28°$). The partial obscuration accounts for the

[24] The northern field, marked *A* in Fig. 3, is in the vicinity of R.A. $= 15^h46^m \pm$ Dec. $-3°.5 \pm$ 1900 (BD $-2°.4064$ falls near the preceding edge of the north-following extension). It has long been known at Mount Wilson and parts were photographed with the 100-inch as early as 1923. The edge of the cloud is a striking object visually, and suggests the region south of ζ Orionis without the luminous background or the nebulous stars. The field was included by Lundmark and Melotte in their catalogue of dark markings found on the Franklin-Adams charts, but is about the only obscuring cloud catalogued in high latitudes whose nature is not questioned. The southern region, on the other hand, appears as an extensive area of partial obscuration with no conspicuous opaque clouds.

scarcity of nebulae in the immediate vicinity of the pole and probably affects some of the stars in the Polar Sequence. Fortunately, there is no reason to assume that the absorption is selective to any considerable degree, hence it may not seriously influence the relation between color index and spectral type as derived from the precise data of the sequence.

Within the zone as outlined by the dashes, five fields (two in the Ophiuchus flare marked *B*, two in the Taurus flare marked *C*, and one in the Cepheus flare) are included, in which occasional nebulae are recorded. Reference to camera plates indicates that these fields are relatively rich in stars and may represent thin spots in obscuring clouds. Those in Ophiuchus[25] are at $\beta = +9^\circ$, in the star clouds near the base of the dark lanes leading out to ρ Ophiuchi, and appear to be veiled by the flare rather than by the narrow belt along the galactic plane. At any rate, nebulae are consistently found at $\beta = +10^\circ$, some 35° away in longitude. It seems plausible to assume that the chances for thin spots are greater in the isolated flares than in the galactic belt where clouds may be scattered one behind the other to very great depths. The same supposition applies to the field in the Cepheus flare at $\beta = +15^\circ$ and perhaps to the Taurus flare as well, where, although the nebular fields are at $\beta = -5^\circ$, the galactic belt appears to be relatively narrow and where, moreover, the distribution of clouds in depth should be much less, since the direction is nearly opposite to that of the galactic center.

From $\lambda = 340^\circ$, where the survey begins, to about $\lambda = 70^\circ$ the southern hemisphere is affected by irregularly distributed partial obscuration reaching out in places to $\beta = -30^\circ$ and more, although the zone of avoidance, as arbitrarily defined, extends to less than 10°. The region might be described as a flare consisting of semi-transparent clouds. North of the galactic plane and in the same latitudes, i.e., between the Cepheus and the Ophiuchus flares, large open circles are mingled among dots in a manner which suggests isolated patches of obscuration in this region as well. Here also nebulae can be fol-

[25] Curtis found two nebulae in the field of NGC 6333, near this region, and also four in the adjacent Selected Area No. 133. Nebulae are found in both fields on the Mount Wilson plates, but others mentioned by Curtis in the zone of avoidance have not been confirmed.

lowed down close to the galactic plane. Three of the survey fields at $\beta = +5^\circ$ record nebulae, and a group of spirals (IC 1303, etc.) is found at $\beta = +7^\circ$.

REGION OF NORMAL DISTRIBUTION

Between the southern region of partial obscuration and the Taurus flare, the field of normal distribution sweeps up toward the galactic plane and reaches $\beta < 15^\circ$ in the vicinity of $\lambda = 110^\circ$. M 31, at $\beta = -22^\circ$, falls in this region, and also Wolf's cluster of nebulae in Perseus at $\beta = -12^\circ$. In the northern hemisphere, to the east of the Cepheus flare ($\lambda < 105^\circ$), the region of normal distribution again sweeps down to latitude 15° and is uninterrupted out to the limits of the survey, i.e., $\lambda = 210^\circ \pm$, where nebulae on opposite sides of the galactic plane are recorded only 10° apart. This latter region, just south of Sirius, represents the narrowest and least conspicuous portion of the Milky Way that falls within the survey.

The conspicuous effects of local obscuration are so extensive that they seriously limit the regions in which the real distribution of nebulae can be investigated with confidence. Irregular limits might be estimated from the manner in which the partial obscuration fades into normal distribution, but it seems less arbitrary to restrict the provisional investigation to the two polar caps. Analysis of the distribution in the polar caps leads to the following results:

1. There is no conspicuous systematic variation in longitude.

2. There is a definite variation in latitude closely approximating a cosecant law.

3. The frequency distribution of log N approximates a Gaussian error-curve.

4. The two caps, northern and southern, are similar, and the distributions agree within the uncertainties of the data.

DISTRIBUTION IN LONGITUDE

This feature was provisionally investigated along successive narrow zones of latitude in order to avoid the possibility of latitude effects, but no conspicuous harmonics were found. Similar investigations in the galactic belt, dodging the flares in the zone of avoidance, emphasized the contrast between the directions of the galactic

center (log N minimum) and the anticenter (log N maximum). Later, when the latitude effect was established and tentative cor-

TABLE X

LONGITUDE EFFECT IN LOG N

λ	$\beta = 20°$–$30°$				$\beta = 40°$–$50°$			
	North		South		North		South	
	n	log N	n	log N	n	log N	n	log N
0°	2	1.885	2	1.790	4	2.080	3	2.033
10	3	1.940	7	1.836	3	1.953	3	1.873
20	3	1.867	5	1.774	3	2.010	3	2.150
30	3	1.840	6	1.838	3	1.873	4	1.830
40	4	1.992	3	1.817	3	1.907	5	1.896
50	4	1.965	2	1.770	4	2.055	7	2.053
60	2	1.890	3	1.883	4	1.765	7	1.981
70	2	2.040	3	1.843	3	1.880	4	2.145
80	1	1.890	3	2.037	4	1.807	3	1.900
90	.....	.....	7	2.201	4	1.920	3	1.760
100	2	1.895	5	2.164	7	1.839	4	1.972
110	3	2.005	4	1.992	4	1.887	5	1.998
120	3	1.797	4	2.040	6	1.897	4	1.900
130	3	2.037	2	1.980	5	2.070	3	1.993
140	3	2.087	2	2.130	4	1.970	4	1.887
150	4	2.070	.....	.....	4	1.992	4	1.895
160	3	2.023	4	2.052	7	2.016	4	1.965
170	3	2.110	3	2.033	3	1.970	3	1.987
180	4	2.035	3	1.937	3	1.910	3	1.983
190	4	2.150	4	2.215	3	1.860	3	1.950
200	4	1.975	2	2.110	3	1.920	.....	.....
210	6	2.045	.....	.....	4	2.275	.....	.....
220	3	2.113	.....	.....	3	1.997	.....	.....
230	3	1.923	.....	.....	3	1.907	.....	.....
240	2	1.915	.....	.....	3	1.833	.....	.....
250	1	1.980	.....	.....	3	1.830	.....	.....
260	.....	.....	.....	.....	3	1.813	.....	.....
270	.....	.....	.....	.....	3	2.073	.....	.....
280	.....	.....	.....	.....	4	1.945	.....	.....
290	1	(2.410)*	.....	.....	3	2.033	.....	.....
300	2	1.905	.....	.....	3	1.960	.....	.....
310	.....	.....	.....	.....	3	1.827	.....	.....
320	.....	.....	.....	.....	6	1.895	.....	.....
330	.....	.....	.....	.....	6	1.882	.....	.....
340	.....	.....	.....	.....	5	1.900	.....	.....
350	3	1.820	1	1.830	5	2.022	3	1.900

* Quality FP, hence log N is uncertain and the corresponding point is omitted from Fig. 4.

rections could be applied, the distribution in longitude was re-examined on the basis of wider zones and the provisional results con-

firmed. The nature of the data and the results for two zones are indicated in Table X and in Figure 4. One zone, $\beta = 20°$ to $30°$, is in the galactic belt; the other, $\beta = 40°$ to $50°$, is the lowest zone in the polar caps.

Values of mean log N reduced to the galactic pole, together with the numbers of fields represented by the means, are tabulated for intervals of 10° in longitude. Omissions in the zone $\beta = 20°$ to $30°$

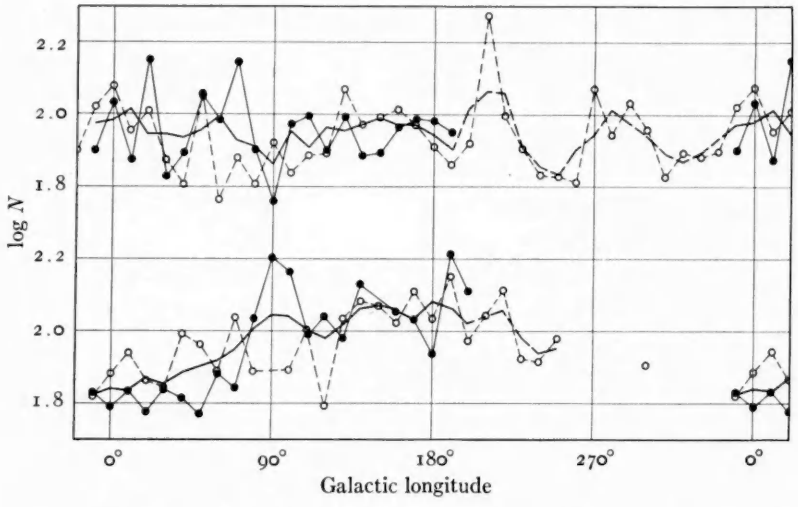

FIG. 4.—Log N as a function of longitude. The upper diagram represents the distribution in zone $\beta = 40°$ to $50°$; the lower, in zone $\beta = 20°$ to $30°$. Circles indicate northern latitudes; and disks, southern latitudes. The heavy line represents overlapping means of three successive intervals of longitude. Data from Table X; all values of log N reduced to the galactic poles by the corrections in Table XII.

refer to flares from the zone of avoidance with their bordering obscuration or to regions beyond the limits of the survey. A single FP plate for a southern field, $\lambda = 290°$, with an abnormal log N, is omitted as uncertain.

The heavy lines in Figure 4 represent overlapping means of three successive values, derived from the combined data for the two hemispheres (full lines) when both are available, and otherwise, for the northern hemisphere alone (dash lines). The zones $\beta = 40°$ to $50°$ show no conspicuous systematic variations. Certain residual effects might suggest galactic obscuration, but apparent abnormalities do

not in general survive a comparison of similar diagrams for zones 35° to 45° and 45° to 55°.

Zones 20° to 30° exhibit the conspicuous excess in log N in the direction of the galactic anticenter over those in the direction of the center typical of the galactic belt. Qualitatively the data suggest appreciably greater obscuration in the direction of the center, and, quantitatively, an overcorrection for the latitude effect.

DISTRIBUTION IN LATITUDE

Since longitude effects are not conspicuous in the polar caps, variation with latitude can there be investigated simply by plotting the mean log N for various latitude zones against the latitudes. A preliminary analysis indicated a definite correlation following the trend of a cosecant law. Attempts were then made to extend the investigation into the low latitudes of the galactic belt. Contours were drawn beyond the borders of the zone of avoidance, purporting to avoid the fringe of local partial obscuration without prejudice to obscuration which might arise from a pervading medium. All fields outside the contours were then used in deriving values of mean log N for latitude zones within the galactic belt itself. The procedure is admittedly arbitrary and, in fact, selective effects actually appear in the final results. Nevertheless, large areas in the lower latitudes were added in which the trend of the correlation could be examined with some confidence.

The data for both polar caps and galactic belt are listed in Table XI, where log N is given for successive 10° zones (the two extreme zones range from 0° to 7° and from 78° to 90°). Survey and extra-survey and northern and southern fields are listed both separately and combined. All fields in Tables II and III were used without exception, but numerous survey fields were omitted as indicated in the footnotes. The latitude effect is apparent in both survey and extra-survey fields, but it is more conspicuous in the latter. It seems probable, however, that the most reliable representation is given by the two groups combined.

Figure 5 exhibits all the data for the two hemispheres, separately and combined. The curves for the two hemispheres are in good agreement; they cross and recross, and the greatest differences are at the

extremities where the data are few. The southern point nearest the pole, for instance, depends upon only 14 plates, while the points

TABLE XI*

LOG N AS A FUNCTION OF GALACTIC LATITUDE

β	Extra-survey			Survey			Total			
	n	$\overline{\log N}$	$\bar{\beta}$	n	$\overline{\log N}$	$\bar{\beta}$	n	$\log N$	β	O−C†
	Northern Hemisphere									
78°–90°	18	2.010	81°.9	19	1.889	82°.1	37	1.948	82°.0	−0.016
68 –77	45	2.049	72.6	30	1.887	72.0	75	1.984	72.4	+ .026
58 –67	53	1.988	62.2	54	1.881	61.7	107	1.934	61.9	− .011
48 –57	32	2.032	54.1	71	1.892	52.5	103	1.935	53.0	+ .008
38 –47	34	1.873	43.0	72	1.894	42.5	106	1.887	42.7	− .007
28 –37	20	1.906	33.3	58	1.848	32.9	78	1.863	33.0	+ .023
18 –27	14	1.726	23.6	38	1.766	22.8	52	1.755	23.0	+ .024
8 –17	10	1.393	13.0	18	1.611	13.6	28	1.533	13.4	+ .065
0 – 7	1	1.660	7.0	1	1.240	5.0	2	1.450	6.0	+0.770
90 – 0	227	1.940	54.5	361	1.854	46.7	588	1.887	49.7	.....
	Southern Hemisphere									
78 –90	3	2.047	82.0	11	2.039	82.3	14	2.041	82.2	+0.077
68 –77	4	2.092	72.2	17	1.944	72.1	21	1.972	72.1	+ .015
58 –67	15	2.183	62.1	40	1.889	62.4	55	1.969	62.3	+ .023
48 –57	28	1.932	52.9	41	1.897	52.4	69	1.911	52.6	− .015
38 –47	18	1.928	41.9	39	1.868	42.4	57	1.887	42.3	− .005
28 –37	13	1.840	32.8	40	1.766	32.4	53	1.784	32.5	− .052
18 –27	25	1.702	22.7	31	1.721	22.7	56	1.712	22.8	− .016
8 –17	18	1.346	13.1	18	1.570	13.3	36	1.458	13.2	.000
0 – 7	.....	.....	.....	4	1.070	5.0	4	1.070	5.0	+0.675
90 – 0	124	1.829	39.8	241	1.818	44.4	365	1.822	42.8	.....

* The following survey fields in the galactic belt ($\beta < 40°$) are omitted (in zones 25°, 30°, and 35°) as seriously affected by partial obscuration bordering the zone of avoidance, or used (in the lower zones) as probably free from such obscuration:

$\beta = +35°$, omit	$\lambda = 320°$–$300°$	$\beta = -35°$, omit	$\lambda = 140°$–$150°$
30 , omit	60–90, 310–340	30 , omit	150, 340
25 , omit	60–90, 300–350	25 , omit	140–160, 340–350
20 , use	10–50, 110–230	20 , use	10–30, 70–120, 160–200
15 , use	20–50, 140–220	15 , use	0–10, 60–110, 160–170, 190–200
10 , use	30–40, 190–210	10 , use	70–80, 100–110, 200–210
+ 5 , use	210	− 5 , use	70, 160–170, 210

The two cluster fields at $\beta = +20°$, $\lambda = 150°$ and $\beta = +30°$, $\lambda = 170°$ are also omitted.

† The calculated values are derived from the equation, $\log N = 2.115 - 0.15 \operatorname{cosec} \beta$.

nearest the galactic plane represent only 2 and 4 plates in the northern and southern hemispheres, respectively.

TABLE XI—*Continued*

β	Extra-Survey			Survey			Total			
	n	$\overline{\log N}$	$\bar{\beta}$	n	$\overline{\log N}$	$\bar{\beta}$	n	$\overline{\log N}$	$\bar{\beta}$	O−C†
	Combined									
78°–90°	21	2.015	81.9	30	1.944	82.2	51	1.973	82.1	+0.009
68 –77	49	2.053	72.6	47	1.908	72.0	96	1.982	72.3	+ .024
58 –67	68	2.031	62.2	94	1.884	62.0	162	1.946	62.1	+ .001
48 –57	60	1.986	53.5	112	1.894	52.5	172	1.926	52.8	− .001
38 –47	52	1.856	42.6	111	1.885	42.5	163	1.887	42.5	− .006
28 –37	33	1.880	33.1	98	1.814	32.7	131	1.831	32.8	− .007
18 –27	39	1.711	23.2	69	1.746	22.8	108	1.733	22.9	+ .003
8 –17	28	1.362	13.1	36	1.591	13.5	64	1.491	13.3	+ .028
0 – 7	1	1.660	7.0	5	1.104	5.0	6	1.197	5.3	+0.706
90 – 0	351	1.901	49.3	602	1.840	45.6	953	1.862	47.4	.....

The means for the two hemispheres combined (the crosses) are represented with remarkable fidelity from 90° down to about 15° by the smooth curve

$$\log N = 2.115 - 0.15 \operatorname{cosec} \beta . \qquad (2)$$

Below 15°, the crosses fall above the curve, a result either of selection or of a failure of the cosecant law. Some further information is furnished by the two triangles at $\beta = 10^{\circ}.1$ and $14^{\circ}.9$, which represent means for all plates in the zones 8° to 12° and 13° to 17° on which any nebulae at all could be found, i.e., only the zone of avoidance itself has been excluded, while the fringe of presumably partial obscuration is included in the data.[26] Effects of selection should force the triangles below the true relation while possibly forcing the crosses above. It is uncertain how much significance may be attached to

[26] The results for all plates on which any nebulae are found for $\beta < 22°$ are as follows:

Interval	n	$\overline{\log N}$	$\bar{\beta}$	O−C	
				$\log N$	β
18°–22°	59	1.593	20.0	−0.083	−3°.3
13 –17	60	1.425	14.9	− .107	−2.4
8 –12	38	1.169	10.1	− .091	−1.0
0 – 7	14	0.813	5.1	+0.385	+1.5

the fact that the cosecant curve does fall between the crosses and the triangles.

The deviations from the cosecant law, equation (2), given in Table XI, include only one significant residual for the two hemispheres combined exceeding 0.01, namely, +0.024 for the zone 68° to 77°.

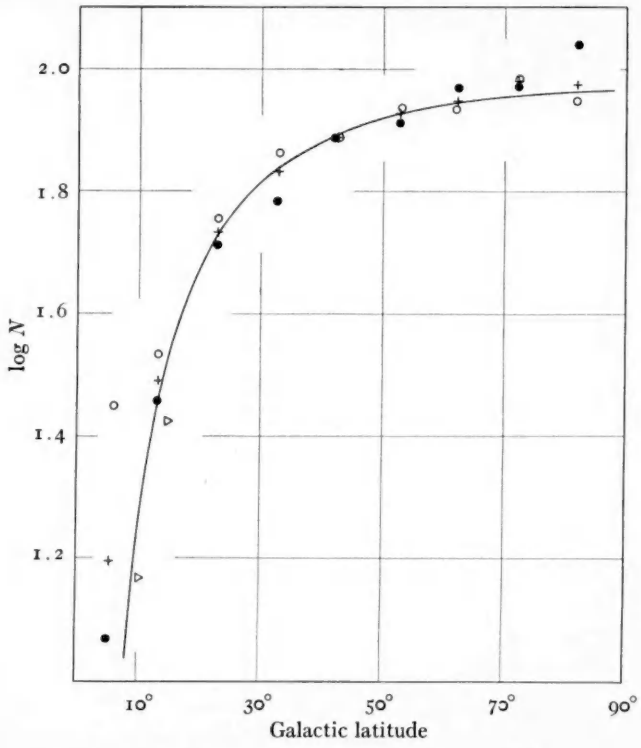

FIG. 5.—Log N as a function of latitude. Data from Table XI. Circles represent northern latitudes; disks, southern latitudes; and crosses, the means. The two triangles indicate supplementary data in low latitudes as described in the text. The curve is the cosecant relation $\log N = 2.115 - 0.15 \operatorname{cosec} \beta$.

Moreover, when the two lowest zones are omitted as uncertain, the systematic deviations of the northern and southern hemispheres from the cosecant law are +0.006 and −0.007, respectively. The systematic difference between the two hemispheres, 0.013, is within the uncertainties of the data. The similarity in the distribution for the two hemispheres is in sharp contrast to previous results. The greatest un-

certainty probably arises from incompleteness in the southern hemisphere, although it may be emphasized that 60 per cent of the southern polar cap and a larger fraction of the galactic belt are included in the survey.

On the assumption of uniform distribution (effects of red shift being ignored), the coefficient in the cosecant law indicates a differential obscuration between 30° and the pole, and hence a total obscuration at the pole, of

$$0.15 \div 0.6 = 0.25 \text{ pg mag.}$$

The optical thickness of the obscuring medium, from pole to pole, is therefore 0.5 mag., with an estimated uncertainty of the order of 0.1 mag. In view of the close agreement between the two hemispheres, the sun is presumed to be near the median plane of the obscuring medium.

Two other recent investigations of the latitude effect lead to results of the same general nature. In 1931, E. F. Carpenter[27] reported that the nebulae "show, with some scatter, essentially uniform surface brightness approximately down to latitude 30° or 40°, where a diminution sets in which at 20° amounts to nearly half a magnitude." Actually, the cosecant law indicates differential obscuration at 20° of about 0.48 mag., and in the high latitudes the obscuration is so inconspicuous that Carpenter's results cannot be considered as inconsistent.

In 1932, P. van de Kamp[28] fitted cosecant relations to the distribution in latitude of the Harvard survey of bright nebulae and of Fath's counts in Selected Areas. The optical thickness, from pole to pole, was found to be of the order of 0.8 mag. from the former and 1.4 mag. from the latter, as compared to 0.5 mag. from the present data. His analysis indicated, however, conspicuously greater obscuration in the southern hemisphere, and accordingly he located the

[27] *Publications of the American Astronomical Society*, **7**, 25, 1931. The results are reported in an abstract and are not given in detail, hence they cannot be compared with Wirtz's earlier investigation (*Meddelanden från Lunds Astron. Observatorium*, Ser. II, No. 29, 1923) which indicated no conspicuous correlation between surface brightness and latitude. J. Dufay (*Comptus rendus*, **196**, 101, 1933) has also discussed the material, finding a positive effect but of a smaller amount.

[28] *Astronomical Journal*, **42**, 97, 1932.

sun well to the north of the median plane of the obscuring medium, in marked contrast to the present results, which indicate no appreciable difference.

The obscuration for the most part is general rather than selective, since no conspicuous relation has been detected between latitude and color excess of nebulae. For instance, the group of spirals including IC 1303, at $\beta = +7^\circ$, has been investigated by the method of exposure-ratios and, although the data are by no means precise, it seems probable that the color excess, if present, does not differ by more than 0.2 mag. from that exhibited by nebulae in high latitudes. The cosecant law indicates a differential absorption of the order of 1.8 pg mag. between the field and the pole, and hence color excess of any amount might be expected up to the maximum of 0.9 mag. corresponding to Rayleigh scattering.

The large color excesses of globular clusters measured by Stebbins[29] refer for the most part to objects actually within the zone of avoidance and presumably affected by the isolated clouds which define the zone. This, together with results from nebular distribution, suggests that the cosecant law in equation (2) may refer to material other than that concentrated in the great clouds. A strict interpretation of the cosecant law leads, of course, to a widely extended uniform layer of diffuse matter such as Eddington and others have discussed at length. The law was derived from mean points representing all available fields in each latitude zone. In the polar caps this appears to be unobjectionable, but in the low latitudes of the galactic belt the systematic effect in longitude (Fig. 4) must be taken into account. Since the mean points fall close to the curve while the residuals are distributed harmonically, the excess of obscuration in the direction of the galactic center more or less balances the deficiency in the opposite direction. This fact invites speculation and suggests the possibility of an extensive flattened cloud of thinly distributed material, oriented on the galactic plane, in which the sun is located near the median plane but between the center and the outer rim. Similar clouds are actually seen as dim lens-shaped silhouettes ex-

[29] *Proceedings of the National Academy of Sciences*, **19**, 222, 1933. Stebbins' results, if referred to a uniform layer of diffuse material, would give a color excess at $\beta = 7^\circ$ of about 0.65 mag. for distances corresponding to those of the globular clusters.

tending for many degrees along the Milky Way. Such speculations will have no significance, however, until the very complex data on local obscuration in low latitudes are more carefully explored and untangled. They are mentioned merely to emphasize the fact that, while a uniformly diffused medium may be postulated for statistical purposes, the present data on nebular distribution cannot be considered as inconsistent with the assumption that the major part of

TABLE XII

LATITUDE CORRECTIONS, REDUCING LOG N TO THE GALACTIC POLE

β	$\Delta\beta$*	β	$\Delta\beta$*	β	$\Delta\beta$*
76°–90°	0.00	31°	0.14	17°	0.36
66 –90	.01	30	.15	16	.39
59 –65	.02	29	.16	15	.43
55 –58	.03	28	.17	14	.47
51 –54	.04	27	.18	13	.52
48 –50	.05	26	.19	12	.57
45 –47	.06	25	.20	11	.64
42 –44	.07	24	.22	10	.71
40 –41	.08	23	.23	9	.81
38 –39	.09	22	.25	8	0.93
37	.10	21	.27	7	1.08
35 –36	.11	20	.29	6	1.28
34	.12	19	.31	5	1.57
32 –33	0.13	18	0.34		

* $\Delta\beta = 0.15$ (cosec $\beta - 1$).

galactic obscuration arises from isolated clouds rather than from a uniform medium.

Latitude corrections, $\Delta\beta$, derived from the cosecant law, are listed in Table XII. When added to log N, they reduce the counts to the galactic poles. The equivalent obscuration in photographic magnitudes is $\Delta\beta/0.6$. For statistical purposes the corrections are probably significant down to 15°, but below 40° the longitude effect introduces an artificial scatter which should be considered in interpreting results.

The latitude effect necessitates a revision of the reductions and analyses—the last step in the series of approximations. The correction for atmospheric extinction is not affected. The corrections for quality and exposure time have been redetermined, but since the revisions are of minor significance and do not materially affect the

final results, they will not be considered in detail. The application of the latitude corrections to the analysis of distribution in longitude has been anticipated, and there remains only the effect on the general distribution. The corrected distribution is shown in Figure 6, which is similar to Figure 3, but with log N reduced to the poles and the irregularities exhibited in greater detail.

The range in log N formerly defined as normal distribution is divided into a central range only half as large (maximum numbers about twice the minimum), bordered by moderate excesses and deficiencies. The mean log N for the polar caps is 1.965, and normal distribution, indicated by small crosses, is now defined log $N = 1.82$–2.11. Moderate deviations are represented by small disks for excesses (log $N = 2.12$–2.26) and small circles for deficiencies (log $N = 1.67$–1.81). The remaining symbols, for large deviations, are the same in both maps and have the same significance. In Figure 6, however, the blank fields in the zone of avoidance are omitted.

The large circles emphasize the effects of local obscuration and the map represents a second approximation to their delineation. The failure of the cosecant law, i.e., the longitude effect in the galactic belt, is indicated by the frequency of large excesses in the low latitudes opposite the galactic center. Normal distribution, even when so narrowly defined, still dominates the polar caps and sweeps down to the Milky Way between the great flares in the zone of avoidance. Nearly 65 per cent of the fields in the polar caps are normal, and the others are about equally divided between excesses and deficiencies.

FREQUENCY DISTRIBUTION OF LOG N

The significance of normal distribution is emphasized by the frequency distribution of log N. This has been investigated in two steps. In the first, only fields in the polar caps were used, uncorrected for latitude; in the second, latitude corrections were applied, and all fields down to and including 15° were used, excepting those obviously affected by obscuration bordering the flares in the zone of avoidance. The data[30] are given in Tables XIII and XIV, where numbers of sur-

[30] Two fields only were omitted in the polar caps (Table XIII), the cluster field $\beta = +55°$, $\lambda = 10°$, and the heavily obscured survey field $\beta = -40°$, $\lambda = 140°$. The fields in Table XIV are essentially those used in Table XI for $\beta \geqq 15°$.

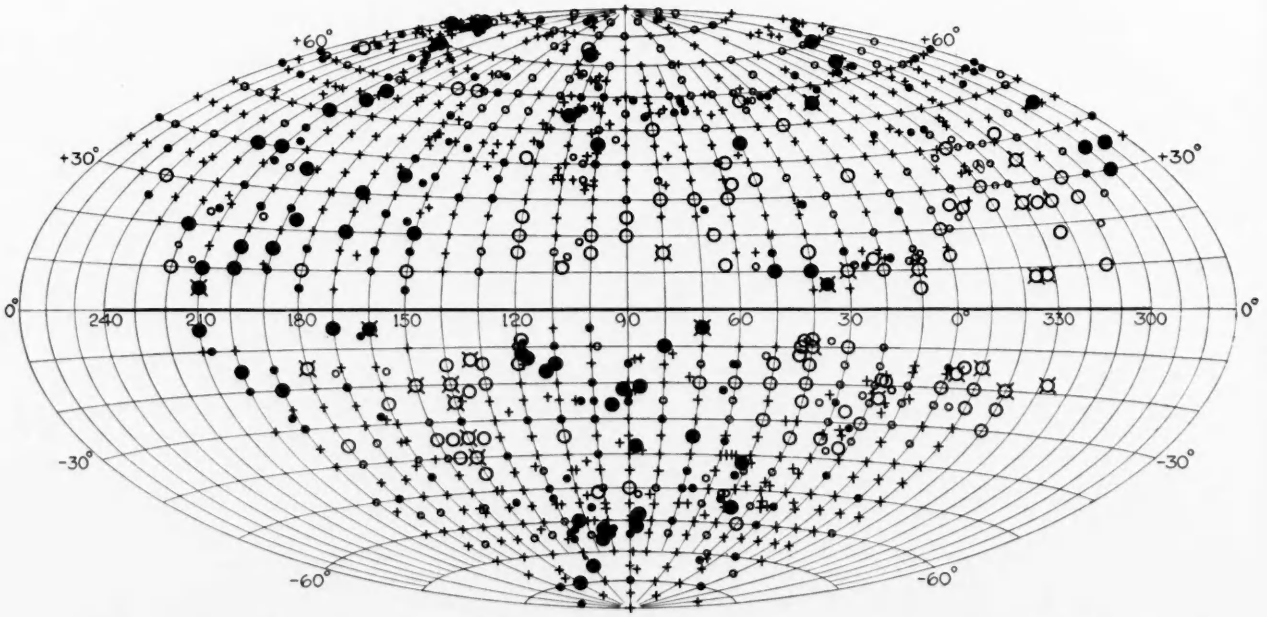

FIG. 6.—Distribution of extra-galactic nebulae when observed data are corrected for the latitude effect. Small crosses represent normal distribution (log $N = 1.82–2.11$); small disks and circles, moderate excesses (log $N = 2.12–2.26$) and deficiencies (log $N = 1.67–1.81$); large disks and circles, considerable excesses (log $N = 2.27–2.56$) and deficiencies (log $N = 1.37–1.66$), with crosses added for log $N > 2.56$ and log $N < 1.37$. Fields with no nebulae are omitted.

vey and extra-survey fields are listed both separately and combined for successive intervals of 0.05 in log N. Fields falling on divisions are equally divided between the adjacent intervals. The last three columns in each table represent smoothed frequencies derived from overlapping means of three successive counts.

TABLE XIII

FREQUENCY DISTRIBUTION OF LOG N
($\beta \geqq 40°$)

log N	Counts			Overlapping Means of Three		
	Survey	Extra-survey	Total	Survey	Extra-survey	Total
1.40–1.45	.....	.....	.....	0.3	.....	0.3
.45– .50	1	.....	1	1	0.7	1.7
.50– .55	2	2	4	2.2	2.2	4.3
.55– .60	3.5	4.5	8	6.2	2.7	8.8
.60– .65	13	1.5	14.5	10.8	5	15.8
.65– .70	16	9	25	18.3	5.3	23.7
.70– .75	26	5.5	31.5	32.7	8.5	41.2
.75– .80	56	11	67	41.2	9.2	50.3
.80– .85	41.5	11	52.5	47.8	14.7	62.5
.85– .90	46	22	68	46.4	19.5	65.8
.90–1.95	51.5	25.5	77	50.8	25.2	76
1.95–2.00	55	28	83	45	27	72
2.00– .05	28.5	27.5	56	32.7	28.3	61
.05– .10	14.5	29.5	44	20.3	26.3	46.7
.10– .15	18	22	40	14	23.3	37.3
.15– .20	9.5	18.5	28	11.8	16.8	28.7
.20– .25	8	10	18	6.7	11.8	18.5
.25– .30	2.5	7	9.5	4	6.5	10.5
.30– .35	1.5	2.5	4	1.7	4.8	6.5
.35– .40	1	5	6	0.8	2.8	3.7
.40– .45	.....	1	1	0.3	2	2.3
.45– .50	.....	.....	.....	.....	0.7	0.7
.50– .55	.....	1	1	.....	0.3	0.3
2.55–2.60	.....	.....	.....	.....	0.3	0.3
Total	395	244	639	394.9	243.9	638.9

The data are exhibited graphically in Figure 7 (for the polar cap alone) and in Figure 8 (for the longer list in Table XIV). Figure 7 is included to emphasize the fact that the complication of latitude corrections in Figure 8 does not affect the general order of the results, while the additional data appreciably smooth the shapes of the curves.

The outstanding feature in Figure 7 is the displacement of the

extra-survey group with respect to the survey, which was mentioned earlier in the discussion. The discrepancy is slightly reduced in Figure 8, but remains conspicuous.

TABLE XIV

FREQUENCY DISTRIBUTION OF LOG N CORRECTED FOR LATITUDE EFFECT

LOG N	COUNTS			OVERLAPPING MEANS OF THREE		
	Survey	Extra-survey	Total	Survey	Extra-survey	Total
1.15–1.20	.....	.....	.....	.....	0.3	0.3
.20– .25	.....	1	1	.....	0.7	0.7
.25– .30	.....	1	1	.....	0.7	0.7
.30– .35	.....	.....	.....	.....	0.5	0.5
.35– .40	.....	0.5	0.5	0.3	0.3	0.7
.40– .45	1	0.5	1.5	0.3	0.5	0.8
.45– .50	.....	0.5	0.5	0.7	0.7	1.3
.50– .55	1	1	2	2	1.2	3.2
.55– .60	5	2	7	5.3	3.8	9.2
.60– .65	10	8.5	18.5	12.3	7	19.3
.65– .70	22	10.5	32.5	21.8	9.5	31.3
.70– .75	33.5	9.5	43	33.7	10.7	44.3
.75– .80	45.5	12	57.5	45.2	13	58.2
.80– .85	56.5	17.5	74	57.2	16.5	73.7
.85– .90	69.5	20	89.5	64.2	19.7	83.8
.90–1.95	66.5	21.5	88	69.8	28.2	98
1.95–2.00	73.5	43	116.5	67.2	33.2	100.3
2.00– .05	61.5	35	96.5	58.2	38	96.2
.05– .10	39.5	36	75.5	47.8	35.5	83.3
.10– .15	42.5	35.5	78	33	32.2	65.2
.15– .20	17	25	42	26.2	27.5	53.7
.20– .25	19	22	41	15.3	19.3	34.7
.25– .30	10	11	21	10.5	12.2	22.7
.30– .35	2.5	3.5	6	5.2	8.2	13.3
.35– .40	3	10	13	2.4	5.2	7.7
.40– .45	2	2	4	3	4.3	7.3
.45– .50	4	1	5	2.5	1.3	3.8
.50– .55	1.5	1	2.5	2	0.7	2.7
.55– .60	0.5	.....	0.5	0.7	0.3	1.0
2.60–2.65	.....	.....	.....	0.2	.....	0.2
Total	587	331	918	587.0	331.2	918.1

The curve for the survey fields in Figure 8 is fairly symmetrical about the most frequent value log $N = 1.925$, while that for the extra-survey fields exhibits an appreciable skewness with the peak about log $N = 2.03$. The skewness suggests effects of selection which, since it is shared by fields centered both on co-ordinates and on nebulae, must be referred to abnormal distribution rather than to the sup-

position, once current, that small nebulae tend to cluster around large nebulae. Minor selective effects are clearly evident and most of the skewness can be traced to about fifty apparently abnormal

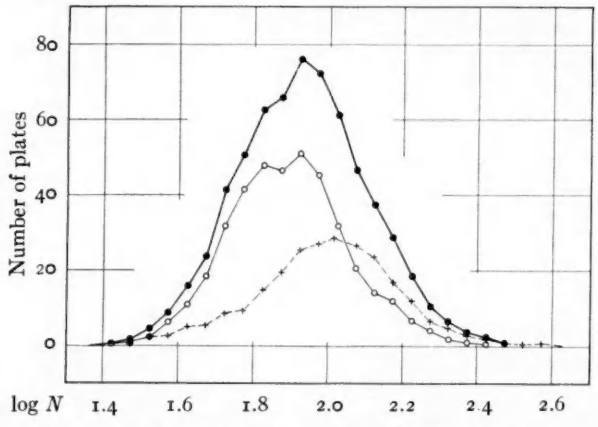

FIG. 7.—Frequency distribution of log N for fields in the polar caps with no correction for latitude effect. Data from Table XIII. Circles represent the 395 survey fields; crosses, the 244 extra-survey fields; disks, the combined data, 639 fields.

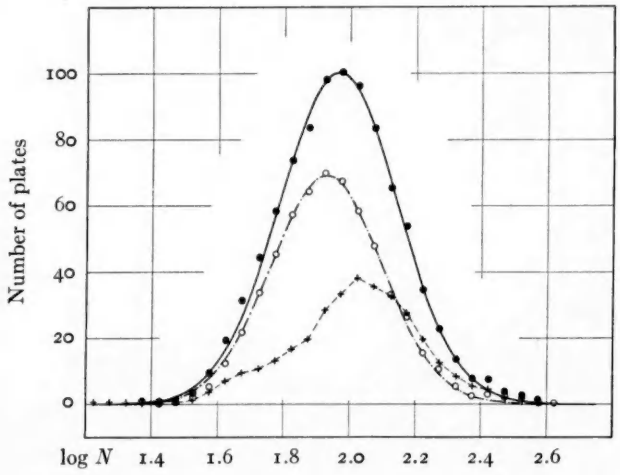

FIG. 8.—Frequency distribution of log N reduced to the galactic poles. Data from Table XIV. Crosses represent the 331 extra-survey fields; circles, the 587 survey fields; disks, the combined data, 918 fields. The smooth curves through the survey fields and the combined data (the two upper curves) are normal error-curves adjusted to the points.

fields. Attempts to improve the data involve rather arbitrary methods and criteria, however, and eventually the two groups, survey and extra-survey, were simply combined. This procedure gives the broad features of the frequency distribution as indicated by the sum total of the data without prejudice to the minor deviations which more detailed analysis may ultimately disentangle.

The curve represents a random distribution of log N—the percentage deviations from the geometrical mean of the counts are distributed according to the normal error-curve. This probably corresponds to what may be termed a normal distribution of the counts themselves, which, since they range upward from a finite lower limit, may be expected to exhibit a positive skewness in their frequency distribution. The transformation to logarithms, which range in theory from minus to plus infinity, offers a possibility of representation by the Gaussian curve which is actually realized by the data to a very close approximation. This feature characterizes all the data from the regions of normal distribution, including the original uncorrected counts as well as those reduced to the standard conditions, and in addition the counts by Curtis and the Harvard survey of the brighter nebulae. The approximately Gaussian distribution of log N may therefore be considered an observed characteristic of nebular distribution except in so far as modified by local galactic obscuration.

A detailed analysis of the curves, including the influence of reductions, the calculation of numerical characteristics, possible interpretations, etc., is reserved for a more extended discussion. Meanwhile, it may be mentioned that the upper curve in Figure 8, representing the most extensive list of data, has a range in log N of the order of 1.0 (1.5–2.5 when seven fields are omitted from the total of 918) and a "probable error" of the order of 0.12 for a single field, including errors of observation and of reduction. The mode and mean are about equal at log $N = 1.965$ (92 nebulae), and the standard samples are derived from counts averaging about fifty nebulae per field in the polar caps. The dispersion in any other random collection of homogeneous samples should be comparable with these results when adjusted for relative richness of the samples. Moreover, since the average richness depends upon volumes of space and not upon angu-

lar areas represented by samples, the statement may be expected to apply to counts of bright nebulae over large areas as well as counts of faint nebulae over small areas.

The Harvard survey, for instance, includes about 738 nebulae in the polar caps brighter than 13.0 pg mag. The caps can each be very simply divided into say 40 equal areas by dividing each 10° zone, e.g., 40°–50°, 50°–60°, etc., into the appropriate number of blocks and combining the odd bits left over. In an actual trial, 8 of the 80 fields were blank, and in general the frequency of the fields diminished as the number of nebulae increased. Nevertheless, when logarithms were used, a fairly symmetrical distribution was suggested with a peak at about 0.90 and a probable error of the order of ± 0.28. When adjacent pairs of areas were combined and only 40 areas were used for the distribution, no field was blank and the approximation to a Gaussian curve was much improved. The most frequent log N was then about 1.10 and the probable error about $\times 0.24$.

Curtis' counts, including 177 fields in the polar caps, 1 of which is blank, show the same features—a conspicuous positive skewness in the distribution of numbers but an approximately Gaussian distribution of logarithms with the peak at about log $N = 1.30$ and a probable error of the order of ± 0.20. The approximation is closer when Curtis' counts are corrected for varying quality and exposure times—a conclusion derived from an examination of the plates made possible through the courtesy of the Director of the Lick Observatory. The most frequent log N is then about 1.40 and the probable error of the order of ± 0.18.

Fath's counts in Selected Areas include 55 fields in the polar caps, 2 of which are blank. They do not conform so well, but the failure can be attributed to the wide range in the limiting magnitudes of the plates. A forced representation of the data suggests a most frequent log N of about 0.95 with a probable error of the order of 0.30.

CLUSTERS OF NEBULAE

The great clusters, recognized as such from casual inspection, have not been included in the discussions. They are relatively rare; perhaps twenty are recognized at the present time, and most of them have been photographed at Mount Wilson. If included in Figure 8

they would in general fall beyond log $N = 2.40$ and increase the slight excess over the error-curve which is already apparent. The excess may indicate unrecognized clusters, but at least part of it refers to the artificial scatter introduced by the reductions.

The usage of the term "cluster" is quite arbitrary, ranging from the conservative practice which applies the name only to the great conspicuous examples to the other extreme in which almost any grouping is glorified by the title. The writer is obviously a conservative, and the following remarks apply only to the great aggregations of several hundred members each. Three such clusters in the northern sky—those in Virgo and Coma, both well known, and the new cluster in Corona Borealis found on the survey plate at $\beta = +55°$, $\lambda = 10°$—are especially important, since they are extraordinarily rich and at widely different distances. For these reasons they afford excellent opportunities for statistical investigations of characteristics which vary with distance. Each contains between five hundred and one thousand members of various types, and their distances are of the order of 2, 14, and 40 million parsecs, respectively.

Clusters were found in only two other survey fields, namely, $\beta = +20°$, $\lambda = 150°$ (Gemini) and $\beta = +30°$, $\lambda = 170°$ (Cancer). Thus, from the survey fields, the frequency is uncertainly estimated as of the order of 3 clusters per 590 fields, or 1 per 100 square degrees. Mayall and the writer found two faint clusters in a survey covering 50 square degrees in the Virgo cluster, and Baade reports two typical clusters and one doubtful case from a survey of 103 square degrees in Ursa Major made with the 1-m reflector at Hamburg. These scanty data suggest a frequency of the order of perhaps 1 cluster per 50 square degrees.[31] On the assumption of an average population of four to

[31] Results of neither survey are published. Baade's data were communicated privately to the writer with permission to mention them. The clusters in Gemini and in Cancer (the latter found independently by Carpenter at the Steward Observatory) and one of the clusters in Ursa Major (found independently at Mount Wilson) are described in *Mt. Wilson Contr.*, No. 427; *Astrophysical Journal*, **74**, 43, 1931.

The Harvard survey of the Virgo cluster (*Harvard Bulletin*, No. 865, 1929) calls attention to five independent groups in the area of about 125 square degrees covered by the survey. None of these is within the smaller area of the Mount Wilson survey, and only two, Harvard groups *c* and *d*, approach the dignity of clusters as the term is here used. On plates with the 60-inch reflector at Mount Wilson, these fields lead to log $N = 2.31$ and 2.37, respectively, and hence are borderline cases.

five hundred nebulae per cluster, about 10 per square degree may be assigned to the great clusters recognized as such with large reflectors,[32] or about 1 per cent of all nebulae to the limits involved. When groups are included, the clustering tendency becomes more appreciable and significant, especially when considered in connection with the systematic advance in average type from the dense clusters to the random nebulae.

On the grand scale, however, the tendency to cluster averages out. The counts with large reflectors conform rather closely with the theory of sampling for a homogeneous population. Statistically uniform distribution of nebulae appears to be a general characteristic of the observable region as a whole.

PART II. NUMERICAL CALIBRATION OF THE COUNTS

The discussion thus far has been concerned with relative numbers of nebulae per field. The reduction of the numbers per unit area to a definite limiting magnitude requires a correction for distance from the optical axis, here called the "coma factor," and the determination of the limiting magnitude for a particular exposure time.

COMA FACTOR

Distortions of stellar images, the coma effect in particular, increase rapidly with distance from the optical axes of short-focus reflectors. This circumstance enhances the difficulties of distinguishing nebulae from stars and renders the threshold of identification a function of distance from the axis, the counts of nebulae tending to thin out toward the edges of the plates. The effect can be determined by combining a sufficient number of fields to smooth out accidental irregularities in distribution and plotting numbers of nebulae in concentric rings against the radii of the rings.

For the immediate purpose, however, an even simpler procedure is sufficient. In addition to counts over the entire plates, Tables I–III list, in the columns headed *I*, the numbers of nebulae in central cir-

[32] Clusters on plates other than systematic surveys cannot be used with the same confidence since they represent a certain degree of deliberate selection. It may be significant, however, that 10 additional clusters appear on such Mount Wilson plates whose combined areas total about 400 square degrees in the regions free from the more conspicuous effects of local obscuration.

cles with radii of 18.75 mm = 5′ for the 5×7-inch plates with the 100-inch and 15.25 mm = 6′.9 for the 4×5-inch plates with the 60-inch. If the definition were uniform, the ratio of the number of nebulae on the entire plate to the number in the inner circle should be the same as the ratio of the areas. Actually the former ratio is the larger, since the numbers fall off in the outer regions; and in order to equalize them the counts for the entire plate must be multiplied by a factor which is the quotient of the two ratios. In this manner the counts may be reduced to a uniform definition over the entire plate equal to the average definition within the central circle. The coma factor, of course, must be derived for each telescope separately. The procedure assumes that the relative numbers of bright and faint nebulae are statistically uniform; but it amounts to something more than merely deriving the numbers per unit area from the inner circles alone, since all plates[33] with six or more nebulae are included, whether in the polar caps or the galactic belt.

The essential data are summarized in Table XV, which includes both the coma factor adopted for each telescope and the area factor. The area factors are merely the reciprocals of the effective areas of the plates expressed in square degrees, by means of which the numbers of nebulae per plate are reduced to numbers per square degree. In deriving the coma factors, outer circles with radii double those of the inner were used as controls. The corresponding counts are omitted from Tables I–III, but the sums are given in Table XV where n refers to the number of fields, N_1 to the sums of the counts over the entire plate, I to the counts in the inner circle, II to those in the larger circle less the inner circle, $I+II$ to the counts in the larger circle complete. The data from Tables I, II, and III are tabulated both separately and combined. Ratios were first calculated for each quality class in order to examine the possibility of systematic variations with quality, but differences were not conspicuous (except for the class FP where the data are too meager for reliable results) and were ignored in the final determinations.

The fields in Table III, centered on selected nebulae, required special treatment, since it was necessary to eliminate the central nebulae and correct for the areas they covered. This was accomplished with

[33] Except the cluster fields.

the aid of the quantities *ab*, the products of the two diameters of the nebulae, listed in the table, by means of which the areas were estimated as fractions of the inner circles. The values of *ab* are not precise and are often unduly large in order to avoid uncertainties which might arise from small detached outliers of the later-type spirals.

TABLE XV

COMA FACTOR

	n	N_1	I	II	N_1/I	N_1/II	$N_1/I+II$
	100-Inch						
Survey	340	12,761	1379	3411	9.254	3.741	2.664
Fields	55	4,412	464	1179	9.509	3.711	2.669
Nebulae	93	5,671	658	1516	8.619	3.741	2.609
Total	488	22,844	2501	6116	9.134	3.735	2.651
	60-Inch						
Survey	332	11,051	1547	3152	7.144	3.506	2.352
Fields	34	1,857	244	500	7.611	3.714	2.496
Nebulae	142	6,017	752	1708	8.001	3.523	2.446
Total	508	18,925	2543	5360	7.442	3.531	2.395

	100-Inch	60-Inch
Adopted value of N_1/I	9.15	7.40
Ratio of areas	17.71	14.56
Coma factor	1.936	1.968
Area factor	2.590	1.647

Ratios for the plates centered on nebulae are more uncertain than the others, but it is interesting to note that the values from the two telescopes are one above and one below the mean ratios from the other plates. For the two telescopes combined, the ratio from the plates centered on nebulae is very closely the same as that from plates centered without reference to nebulae. This appears to dispose of the

opinion, once current, that small nebulae tend to cluster around large nebulae.

NEBULAR MAGNITUDES AT THE THRESHOLD OF IDENTIFICATION FOR HOUR EXPOSURES

Limiting photographic magnitudes on the international scale of nebulae at the threshold of identification for hour exposures with each telescope are given in Table XVI. The internal agreement is good, since each value represents the mean of several selected plates for a field rich in nebulae. The more important systematic scale error, however, is less certain. Only two standard sequences, the Pole and S.A. 57, were used for the comparisons, and only the latter

TABLE XVI

THRESHOLD MAGNITUDES OF NEBULAE FOR ONE-HOUR EXPOSURES

60-INCH			100-INCH		
Field	m(thres.)	Plates	Field	m(thres.)	Plates
Ursa Major.....	19.3	6	Coma.....	20.05	5
Perseus.....	19.5	2	Perseus.....	20.1	3
Cor. Borealis.....	19.4	3	Cor. Borealis....	19.9	4
Virgo Field.....	19.5	4	Gemini.....	20.0	2
Mean.....	19.4	.....	Mean.....	20.0	.....

was available for direct use with the 100-inch. The two standard sequences were compared directly down to about 19.0 by the writer with the 60-inch. The scale in S.A. 57 was extended to 19.5 and fainter with the 100-inch by Baade, who has very kindly permitted the use of his unpublished results.

With the aid of these standards, sequences of stellar magnitudes were established in each field listed in Table XVI which were considered reliable to 19.0 or 19.5 and could be extrapolated with reasonable confidence to 20.0 or thereabouts. Magnitudes of small faint nebulae were then derived from long-exposure schraffierkassette plates taken with the 100-inch, with images about 1 mm square, which to limits ranging from 19.0 to 19.3 are considered to be of the same order of accuracy as the stellar magnitudes. These values are the standard nebular magnitudes upon which the results in Table

XVI are ultimately based, although the latter in general depend upon extrapolations.

With the 60-inch, standard magnitudes were available for threshold images on direct exposures ranging up to about forty-five minutes and, with slight extrapolations, up to the full hour. With the 100-inch, however, even thirty minutes' direct exposure generally involved some extrapolation, and estimates of threshold magnitudes for hour exposures depended upon the relation between limiting magnitude and exposure time for the particular observing conditions. The latter relation assumes such importance that an extensive collection of data was assembled from plates by several different observers, using different telescopes and observing conditions. These data all led to the same conclusion, namely, that for small surface images at the threshold of fully developed Eastman 40 plates, exposed from about ten minutes to two hours, the simple reciprocity law very closely represents the observations.[34] The Schwarzschild exponent is not less than unity and occasionally, possibly under optical conditions of sky fog, may be greater than unity. The reciprocity law in its appropriate form,

$$\text{Threshold mag.} = 2.5 \log E + C ,$$

was therefore used to extrapolate the observed threshold magnitudes on direct exposures from fifteen to forty-five minutes to corresponding magnitudes for one-hour exposures.

Another and independent approach to the subject is offered by a relation previously derived[35] between surface brightness and diam-

[34] The data were derived from plates under the following conditions: (*a*) 100-inch with schraffierkassette, images 2 mm and 1 mm square, exposures 6–180 minutes, magnitudes from Selected Area No. 57. Plates by the writer. (*b*) 10-inch Cooke refractor with schraffierkassette, images 2 mm and 1 mm square, exposures 4–110 minutes, magnitudes from N.P.S. Plates by Willis and by Christie. (*c*) 5-inch Ross camera extra-focal, with excellent uniform images 1.1 mm and 0.45 mm in diameter, exposure 10–120 minutes, magnitudes from N.P.S. Plates by Willis.

The investigation consisted in identifying the faintest star images seen with certainty and comparing the known magnitudes with the logarithms of the exposure times. Each group, representing a particular size of image with a particular instrument, was examined separately and no group suggested a Schwarzschild exponent less than unity. A detailed discussion of the investigation will be given later.

[35] *Mt. Wilson Contr.*, No. 453; *Astrophysical Journal*, **76**, 106, 1932.

eters of threshold images on Eastman 40 plates. For very small images the total magnitude is independent of the size; for very large images the surface brightness is independent of the size. The observed relation is a smooth transition between these limiting conditions and was determined numerically for the express purpose of deriving statistical values for limiting magnitudes of nebulae in the present investigation.

The data for large images were derived from extra-focal exposures ranging from one to ninety minutes and were originally reduced to a uniform exposure time by means of the assumption that tripling the exposure increases the limit of the plate by 1 mag. This assumption is now believed to be wrong for surface images, and, in fact, an inspection of residuals in the previous discussion indicates some systematic deviations in the direction anticipated. The data have been reduced on the assumption of a strict reciprocity law, and new curves derived accordingly. The major features are unaffected, although the numerical values are slightly modified and the former systematic discrepancy between the two reflectors appreciably reduced. Systematic deviations related to exposure times are still apparent but opposite in direction to those found on the assumption previously used. It appears, therefore, that the particular data are best represented by an intermediate form of the law of blackening and that mean values from the two curves will not be greatly in error.

This conclusion was confirmed by an inspection of a large number of plates of qualities E and GE, which indicated that the average diameters of threshold images of the nebulae actually identified are of the order of $4''$ and $5''$ for the 100-inch and 60-inch, respectively. The corresponding total magnitudes for hour exposures, as derived from the curves of surface brightness revised by the reciprocity law, are 20.06 and 19.50, and 19.72 and 19.30 from the curves as originally published. The differences for the two instruments are only 0.34 and 0.2 mag., respectively. The mean values, 19.89 and 19.40, should be of the proper order at least, and are in fact in fair agreement with the values in Table XVI. Another way of stating the agreement is that the mean values correspond to diameters of $4''.25$ and $5''.5$ from the reciprocity-curve and of $3''$ and $4''.5$ from the original curve for the two reflectors, respectively, and that these values are all of the gen-

eral order of the limiting diameters of nebulae actually identified. In view of the uncertainties in estimating diameters of threshold images, the agreement is all that can be expected, and the values in Table XVI are used in the discussions which follow.

The fact that the adopted values are a half-magnitude and more brighter than the limiting magnitudes for star images on good plates suggests that many nebulae below the threshold of identification are recorded on the plates and that their numbers may be comparable with those of the nebulae actually identified. A comparison of eight

TABLE XVII

NUMBERS OF NEBULAE PER SQUARE DEGREE TO DEFINITE LIMITING MAGNITUDE

	100-Inch	60-Inch
log N	1.965	1.805
log Coma factor	0.287	0.294
log Area factor	0.413	0.217
log N (sq. deg.)	2.665	2.316
m (threshold)	20.0	19.4

two-hour exposures with the 100-inch with one-hour exposures of the same fields with the 60-inch amply confirmed this expectation, indicating about 300 unrecognizable nebulae on the 60-inch plates in addition to 395 which had previously been identified. The available data are insufficient for a comprehensive discussion of the subthreshold images, but for the immediate purpose such a discussion is unnecessary, provided a definite threshold is consistently maintained and the corresponding limiting magnitude fairly established. The data emphasize, however, the importance of personal equations and their calibration.

NUMBERS OF NEBULAE PER SQUARE DEGREE TO DEFINITE LIMITING MAGNITUDES

The counts can now be reduced to numbers of nebulae per square degree. The mean log N for the 100-inch, from the upper curve in Figure 8, is 1.965, and for the 60-inch is 0.16 less, or 1.805. When the logarithms of the coma and area factors (Table XV) are added, the results are as shown in Table XVII.

Assuming uniform distribution and ignoring effects of red shifts, we have from these results the relation

$$\log N_m = 0.6m - 9.335 \quad \text{(100-in.)}$$
$$9.324 \quad \text{(60-in.)}$$
$$\overline{9.33} \quad \text{(mean)}$$

EFFECT OF THE RED SHIFT

Regardless of the unit of distance, the red shift is approximately indicated by the relation[36]

$$\log v = 0.2m + 0.5 ,$$

where v is the red shift expressed as a velocity in km/sec. and m the photographic magnitude corrected for the effect of the shift. At $m = 20$, the velocity is of the order of 30,000 km/sec. and $d\lambda/\lambda$ about 10 per cent. Some simple approximations already published[36] indicate that the effect on the photographic magnitudes at such distances is very appreciable and cannot be ignored.[37]

The approximations were based on two assumptions. The first, that $d\lambda/\lambda$ is constant throughout the spectrum, is established within the uncertainties over an observed range between the emission lines normally at 5007 and 3727 A and is generally accepted by those who interpret the shifts as Doppler effects. The second assumption is that nebular luminosity approximates black-body radiation, with effective spectral type, G3d, temperature, and color (for nebulae showing small shifts) similar to those of the sun. The normal observed spectra are similar to the solar spectrum as far as the small scale permits comparison, and for the brightest nebulae, the greater the scale the closer the analogy, except for the widened lines in the nebular spectra. It is possible that the mixture of stars supposed to exist in nebulae may seriously affect the assumed distribution of

[36] *Mt. Wilson Contr.*, No. 427; *Astrophysical Journal*, **74**, 43, 1931. For the present purpose, the significant quantity is $d\lambda/\lambda$. From the relation above, $\log d\lambda/\lambda = 0.2m - 5$ approximately.

[37] J. Stobbe (*Astronomische Nachrichten*, **243**, 53, 1931) has constructed intensity-curves for black-body radiation at various temperatures, as affected by red shifts of various amounts. These indicate the effect on the bolometric intensity at any wavelength and furnish data for following the effect up to the photographic magnitudes.

energy, and there are some reasons for believing that even the nearer nebulae in high latitudes exhibit an appreciable color excess. For the present, however, we may use the assumption as a first approximation.

On these two assumptions red shifts produce redistributions of intensity which can be represented by new black-body curves corresponding to lower temperatures, and hence to later spectral types. The decrease in ν introduces an increment to the bolometric magnitude that can be followed in a purely empirical manner up to the photographic magnitude, which it enters in a magnified form. De-

TABLE XVIII

OBSERVED PHOTOGRAPHIC MAGNITUDES OF NEBULAE CORRECTED FOR EFFECT OF RED SHIFT

Obs.	Corr.	Obs.	Corr.	Obs.	Corr.
22.0	21.15	19.5	19.22	17.0	16.90
21.5	20.83	19.0	18.78	16.0	15.94
21.0	20.45	18.5	18.32	15.0	14.96
20.5	20.05	18.0	17.85	14.0	13.97
20.0	19.65	17.5	17.38		

tails will be found in the previous publication,[38] where Δm_{pg} are tabulated for various values of $d\lambda/\lambda$.

Table XVIII, giving corrected photographic magnitudes corresponding to various observed magnitudes, is derived from these data. The corrected limiting magnitudes for one-hour exposures with the 100-inch and 60-inch reflectors are 19.6 and 19.1, respectively. The revised relation between numbers of nebulae and limiting magnitude is

$$\log N_m = 0.6m - 9.095 \quad (100\text{-in.})$$
$$9.140 \quad (60\text{-in.})$$
$$\overline{9.12} \quad (\text{mean})$$

where m now refers to the corrected apparent magnitude. Unless the estimated effects of red shifts are greatly in error, the relation may be expected to hold generally.

[38] *Mt. Wilson Contr.*, No. 427; *Astrophysical Journal*, **74**, 43, 1931.

The Harvard survey of brighter nebulae leads to a fairly symmetrical frequency distribution of log N in the polar caps around a mode at about log $N = -1.46$ per square degree.[39] The corresponding limit of survey is $(9.12 - 1.46) \div 0.6 = 12.8$, which is very close to the limit assigned by the authors of the survey.

The Harvard counts of fainter nebulae have not been sufficiently calibrated for a comparison to indicate more than the general order of the agreement. The most extensive data[40] are given in the form of mean values, log N per square degree, reduced to a uniform limiting stellar magnitude of 18.2, for successive zones of latitude 10° wide. One hundred and forty-five fields in the polar caps are included, each representing 9 square degrees. The mean log N for this extensive material is 1.26, or 1.30 if the latitude corrections for the middle of each zone are added. The latter value corresponds to a corrected limiting magnitude of 17.4, or an observed magnitude of about 17.5, which is of the general order to be expected for a limiting stellar magnitude of 18.2.

Other fragmentary data are fairly consistent, although no great weight can be assigned to the results. For instance, unpublished counts of about two thousand nebulae in twenty fields with the 10-inch Cooke refractor at Mount Wilson indicate an average of about three nebulae per square degree to a limiting magnitude of about 16.0. These are round numbers, but the calculated limit is 16.0, plus a correction of less than 0.1 mag., which indicates the order of the agreement.

Seares's[41] analysis of Fath's counts in Selected Areas indicates an average of about 14 nebulae per square degree over the polar caps—55 fields are in these regions—representing a calculated observed limit of about 17.2 as compared with Seares's estimates of 18.6 for the average stellar limiting magnitude. The apparent discrepancy is due largely to the personal equation in the counts since an inspec-

[39] A mean value can be used if proper allowance is made for the Virgo cluster. Thus, about 625 nebulae are scattered over the 14,600 square degrees in the polar caps (less the area of the Virgo cluster), or approximately 1 nebula per 23.5 square degrees. Log N is thus of the order of -1.37 and the resulting m of the order of $(9.12 - 1.37) \div 0.6 = 12.9$.

[40] *Proceedings of the National Academy of Sciences*, **19**, 389, 1933.

[41] *Mt. Wilson Contr.*, No. 297; *Astrophysical Journal*, **62**, 168, 1925.

tion of the plates clearly indicates the very conservative criteria used in the identification of nebulae.

Curtis' counts can be used with confidence only when fully calibrated, but a preliminary comparison of fields included in the Mount Wilson collection suggests an agreement in the general order of the results which detailed investigation may be expected to confirm.

The nebulae increase with limiting magnitude at such a rate that near the galactic poles they equal the stars in number[42] at about 21.25 mag. Since this limit represents rather closely the threshold of identification that can be reached with long exposures under good conditions with the 100-inch, the equality offers an interesting measure of the greatest penetrating power available at the present time. Log N at the limit is about 3.25, corresponding to about 1780 nebulae per square degree, or 75,000,000 over the sphere. The number actually observable is reduced by local obscuration, but the reduction is more than compensated by the numbers registered below the threshold of identification. It is interesting also that the number is only a fraction, possibly one-third, of the number that would be expected in the absence of fading due to red shifts over and above the fading due to distance alone.

DENSITY OF NEBULAR DISTRIBUTION

Since the density of nebulae in space is merely the numbers divided by the volume,

$$\log \rho = \log N - \log V ;$$

and since for the entire sphere, in nebulae per cubic parsec,

$$\begin{aligned} \log N &= 0.6m - 9.12 + 4.62 , \\ &= 0.6m - 4.50 ; \end{aligned}$$

and

$$\begin{aligned} \log V &= \log \frac{4}{3}\pi + 3\left(\frac{m-M+5}{5}\right) , \\ &= 0.6m - 0.6M + 3.62 , \end{aligned}$$

[42] *Mt. Wilson Contr.*, No. 301; *Astrophysical Journal*, **62**, 320, 1925.

it follows that

$$\log \rho = 0.6M - 8.12 ,$$

where M is the mean absolute photographic magnitude of nebulae.

The density is expressed in this form because M is still uncertain, owing largely to uncertainties in the scale of apparent magnitudes. The value[43] $M = -13.8$, derived from Holetschek's visual magnitudes corrected by a color index, gives $\log \rho = -16.40$. Another value, $M = 14.5$, giving $\log \rho = -16.82$, was derived for isolated nebulae by H. Knox-Shaw[44] and has since been used by Shapley.[45] The latter value was based upon the Harvard magnitudes of bright nebulae, which were derived from direct comparisons with star images on focal exposures, and hence are subject to possible scale errors of the kind exhibited in an exaggerated form by the Harvard magnitudes of globular clusters. Discrepancies of this order will continue to be current until a reliable system of photographic magnitudes is available, derived from large uniform images comparable for both stars and nebulae. Such a program is under way at Mount Wilson, involving extra-focal exposures and the schraffierkassette with various telescopes, and until the necessary data are available, either here or elsewhere, there is little point in enlarging the discussion.

MASSES OF NEBULAE

A revision of the data on the masses of nebulae is possible and may have some significance since the derivation of the density of matter in space is only slightly affected by uncertainties in the absolute magnitudes. The most hopeful present prospect of deriving masses appears to be Öpik's assumption that, on the average, the mass is a constant multiple of the luminosity,

$$\text{Mass} = b \times \text{Luminosity}.$$

The factor b can be evaluated from masses of particular nebulae as indicated by spectrographic rotation, and then applied to the mean

[43] *Mt. Wilson Contr.*, No. 427; *Astrophysical Journal*, **74**, 43, 1931.

[44] *Monthly Notices of the Royal Astronomical Society*, **93**, 304, 1933.

[45] *Proceedings of the National Academy of Sciences*, **19**, 591, 1933.

luminosity of nebulae in general. Reliable data on rotations share with the magnitude scale the distinction of being the most pressing immediate need in the general field of nebular investigations. Such data are restricted at present to the three nebulae M 31, M 33, and NGC 4594, in addition to the galactic system itself; and in each case the evaluation of the factor b is subject to uncertainties from other sources. Two of the three nebulae are among the brightest known, and hence a simple mean of the masses cannot represent the nebulae in general. The factor b, or some equivalent, must be introduced, and hence it is important to estimate the order of the factor. The uncertainties are so great, however, that the discussion will be restricted to simple estimates of the general order, with no claim to precision.

Messier 31.—No revision of the mass-luminosity relation is available for this spiral, although it is hoped that continued spectrographic observations of the clusters scattered throughout the nebula may contribute information concerning the outer regions which can be added to the rotational data already available for the nuclear region. The greatest uncertainty in the factor b arises from the necessity of extrapolating the mass from the nuclear region actually observed to the entire nebula, together with uncertainties in the magnitudes. The difficulties are discussed in a former publication[46] where a tentative value of the factor, 5.5, is estimated for mass and luminosity expressed in terms of the sun as the unit.

Messier 33.—The distance and the luminosity are fairly well known, as is also the radial velocity of NGC 604, a bright patch of emission nebulosity near the major axis and about 700″ from the nucleus. The bright lines in NGC 604 have been measured with moderately large dispersion, and the velocity, −270 km/sec., is probably certain within 10 km/sec. A new value for the velocity of the nucleus has been derived by Humason from several plates, one with relatively large dispersion. This value,[47] −320 km/sec., is probably correct within 20 km/sec., and agrees with those for M 31 and its

[46] *Mt. Wilson Contr.*, No. 376; *Astrophysical Journal*, **69**, 103, 1929.

[47] This represents a revision, based upon new data, of the value −330, given in the catalogue of velocities (*Publications of the Lick Observatory*, **18**, 1932). The unpublished results were privately communicated to the writer with permission to use them.

companions in reflecting the rotation of the sun around the galactic center.

The differential velocity of NGC 604, 50 km/sec., when corrected for tilt of the plane of the spiral, gives a rotational velocity of 67 km/sec., which is uncertain by perhaps half its value. Nevertheless it represents a decided improvement on the former value[48] and indicates a revised mass of the order of $9\times10^{8}\odot$, which is more consistent with the other nebulae. The photographic absolute magnitude is of the order of -13.9, hence the luminosity is about $7\times10^{7}\odot$, and the factor b, about 13.

NGC 4594.—The distance as indicated by the red shift is of the order of 2,000,000 parsecs, subject to uncertainties arising from the unknown peculiar motion. The rotation is measured out to about two minutes of arc from the nucleus, where it reaches 330 km/sec., and hence the contribution of the luminosity from the outer unobserved regions is unimportant. The mass is estimated as of the order of $3\times10^{10}\odot$, although some questionable assumptions are introduced concerning the nature of the rotation. The apparent photographic magnitude is given in the Harvard survey as 8.0, but extra-focal and schraffierkassette plates with the 5-inch and 10-inch cameras indicate that it is probably a magnitude fainter,[49] and hence that the absolute luminosity is about $2\times10^{9}\odot$. The factor b is then about 15.

The three values of b—5, 13, and 15—suggest a factor of the order of 10 for nebulae in general. The mean mass is then of the order of 6×10^{8} or $10^{9}\odot$, depending on the adoption of -13.8 or -14.5 as the mean absolute magnitude.

DENSITY OF MATTER IN SPACE

The mean mass of nebulae, in terms of the sun as the unit, is

$$\log \text{Mass} = \log b + 0.4(5.7 - M) .$$

[48] The mass of M 33 was formerly estimated on the basis of a nuclear velocity of -70 km/sec., a value recognized as very uncertain since it was derived from a single plate of very low dispersion.

[49] The precise value is uncertain owing to uncertainties in the comparison stars. If the *HD* magnitudes are used the nebula is about 9.8, nearly the same magnitude as that of the star BD$-11^{\circ}3342$, listed in the *HD* as Go, 9.3 visual and 9.9 photographic.

Hence, from the previous expression for the density of nebular distribution,

$$\log \rho = 0.2M + \log b - 5.84 ,$$

where the density is expressed in suns per cubic parsec. In grams per cubic centimeter,

$$\log \rho = 0.2M + \log b - 28.02 .$$

Since $\log b$ is of the order of unity and M is variously estimated as -13.8 to -14.5,

$$\log \rho = -29.8 \text{ or } -29.9 ,$$

with an uncertainty probably less than 0.5. The round number -30 is convenient and within the uncertainties. It has been widely used of late, although the justification has been largely convenience rather than quantitative investigation. The value is of the order of ten times greater than the first tentative estimate put forward in 1926, and it is believed that further significant revisions of the order of the density must await more extensive investigations of spectrographic rotations.

The discussion, of course, ignores the existence of internebular matter, the density of which, even in an optimal form, might be several thousand times greater without introducing appreciable absorption. Since absorption depends upon the state of the material (the density for large meteorites, for instance, might surpass that of the galactic system without introducing appreciable obscuration), upper limits can be assigned to the density of internebular space only from dynamical considerations.

CARNEGIE INSTITUTION OF WASHINGTON
MOUNT WILSON OBSERVATORY
August 1933

THE RADIAL-VELOCITY VARIATIONS OF V URSAE MINORIS, R SAGITTAE, AND V VULPECULAE[1]

By ROSCOE F. SANFORD

ABSTRACT

The observations.—Table II gives the radial velocities for V Ursae Minoris, R Sagittae, and V Vulpeculae obtained at Mount Wilson, mostly with a dispersion of about 75 A per millimeter at $H\gamma$.

Velocity variation.—Plots in Figs. 1–3, respectively, by means of periods obtained from recent studies of extensive photometric data, fail to reveal any regularity in the velocity variations. These results are perhaps explicable on the assumption that the form of the velocity-curve changes markedly in the intervals over which the respective observations extend.

Spectral changes.—R Sagittae to some extent, and V Vulpeculae more definitely, undergo spectral changes and show the earliest type at maximum and the latest at minimum. The hydrogen-line absorption and the G band become progressively stronger from maximum to minimum light. In V Vulpeculae the bands of titanium oxide appear near one of the minima.

The variation of stars of the RV Tauri class is very imperfectly understood. Unquestioned light variation exists, but, unlike that of the Cepheids, is far from simple, for it does not repeat its form precisely over any considerable time.

A number of stars of this class are known to have variable radial velocities, but thus far only two have been so extensively observed with moderately high dispersion as to permit judgment of the nature of the variation. These two are AC Herculis[2] and U Monocerotis,[3] which give evidence of variation in a period the same as that of the light variation and probably with a double amplitude. The velocities scatter so about the mean results, however, that the variation itself must in some manner change. It is not surprising that fainter stars of this class have yielded even less positive results, since the radial velocities for the most part have been obtained with lower dispersion.

Several spectrograms have been obtained at Mount Wilson for each of the stars listed in Table I.

The radial velocities (Table II) are in each case well distributed in

[1] *Contributions from the Mount Wilson Observatory, Carnegie Institution of Washington*, No. 481.

[2] *Mt. Wilson Contr.*, No. 424; *Astrophysical Journal*, **73**, 364, 1931.

[3] *Mt. Wilson Contr.*, No. 465; *Astrophysical Journal*, **77**, 120, 1933.

phase, but conform so poorly to a mean curve that it is not thought worth while to continue the observations. The dispersion usually employed was about 75 A per millimeter at $H\gamma$. An asterisk following a plate number in Table II indicates a dispersion approximately double this value.

TABLE I

Variable	H.D.	B.D.	Sp.	Mag.	α(1900)	δ(1900)	Period
V U Min.....	119227	+75° 512	M4	7.1– 8.8	13^h36^m9	+74°49′	73^d34
R Sgte.....	192388	16 4197	cG7	8.6–10.4	20 9.5	16 25	70.88
V Vulp.....	.....	+26 3937	cG5p	8.2– 9.9	20 32.3	+26 16	75.678

V URSAE MINORIS

The sixteen radial velocities of this variable cover an interval of eight years. Their extreme range is 29 km/sec. (−150 to −179 km/sec.) and their mean −165 km/sec. The mean derived from twenty low-dispersion spectrograms by R. O. Redman[4] is also −165 km/sec., if the systematic correction[5] recommended by him is applied. The range for Redman's values is from −155 to −180, or 25 km/sec., during an interval of a little more than five months.

Certain observations of this star indicate the accuracy obtainable with the dispersion used for most of the spectrograms in Table II, provided the velocities do not change appreciably in an hour or two. Two values were obtained on J.D. 2426075, one at Victoria and one at Mount Wilson, and in five cases Redman obtained two spectrograms on the same night. The differences for these six pairs of values (Table III) indicate that the measured velocities are without doubt subject to errors as large as 5 km/sec.

The sixteen Mount Wilson and the twenty-two Victoria radial velocities with a range of 29 km/sec. have been plotted in Figure 1 with phases derived from[6]

$$\text{Max.} = \text{J.D. } 2418978.3 + 73^d34E - 0^d0055E^2 .$$

If the radial velocity undergoes the same change during each cycle, the general character of the change should be revealed by these ob-

[4] *Monthly Notices of the Royal Astronomical Society*, **92**, 109, 1931.

[5] *Ibid.*, p. 118.

[6] B. Gerasimovič, *Harvard Circular*, No. 388, 1929.

TABLE II

RADIAL VELOCITIES

Plate	Date	G.M.T.	Phase	Velocity	Qual.
	V Ursae Minoris				
				km/sec.	
γ 11676*	1923 March 27	21^h37^m	2^d	−175.2	P
11722*	April 24	23 26	30	−150.1	P
11775*	May 7	19 50	43	−160.7	F
11783*	23	19 25	59	−153.4	F
14857	1927 March 15	23 12	0	−163.3	F
16552	1929 April 27	17 45	50	−161.3	F
16602	May 23	18 41	4	−157.7	P
16633	June 16	18 28	28	−174.3	F
16679	26	17 17	38	−161.8	G
17371	1930 April 8	20 40	34	−156.0	G−
17429	May 9	20 36	65	−163.4	F+
17489	June 5	16 25	20	−161.2	F
17498	7	17 43	22	−174.4	G−
17557	July 5	17 27	51	−179.0	G
18055	1931 Feb. 1	23 02	44	−172.1	G
18079	May 1	21 38	61	−177.1	G
	R Sagittae				
γ 7233	1918 Aug. 21	20 44	14.8	− 8.2	G
8332	1919 July 4	22 47	48.3	+ 31.8	P
C 1909	1922 Sept. 30	15 33	27.2	+ 0.2	F
2382	1923 Aug. 18	20 12	65.9	+ 8.8	F
2450	Sept. 24	17 02	31.9	+ 22.4	F
2557	Nov. 25	15 55	23.0	+ 9.2	F
2928	1924 Aug. 12	19 25	0.6	− 1.0	G
3031	Oct. 7	17 58	56.6	+ 17.2	F
3412	1925 July 31	18 53	70.1	+ 10.8	G
3518	Sept. 24	19 35	54.3	+ 13.2	G
3961*	1926 Aug. 19	20 38	29.0	+ 22.0	F
3981	22	19 40	32.0	+ 21.3	G−
4027	Sept. 20	16 05	60.8	+ 25.2	G
4049	Oct. 19	15 30	18.9	+ 4.2	F
4095	Nov. 14	16 15	44.9	+ 22.2	F
4113	21	15 10	51.9	+ 20.6	G
4145	Dec. 17	15 5	7.0	+ 8.2	F+
4371	1927 July 17	22 10	6.7	+ 4.9	G
4434	Oct. 4	16 47	14.6	− 3.7	G
4461	10	17 36	20.7	− 10.1	F
4768	1928 April 25	23 45	6.3	− 1.8	G
4783	30	00 00	10.3	+ 4.5	G
4826	May 28	20 51	39.2	+ 6.3	G
4839	June 3	22 52	45.3	− 0.4	G
4844	12	22 30	54.2	− 7.6	P
4853	24	23 03	66.3	+ 5.0	G
4872	July 3	22 30	4.4	+ 7.4	G
4896	10	22 08	11.4	+ 6.3	G

TABLE II—*Continued*

Plate	Date	G.M.T.	Phase	Velocity	Qual.
	V Vulpeculae				
				km/sec.	
C 110*	1919 Oct. 11	15^h44^m	47^d8	+ 2.8	G
175*	Nov. 5	18 31	72.9	− 3.0	G
1763*	1922 July 3	23 10	60.3	−15.1	G
1806	Aug. 2	23 33	14.6	−16.0	F
1854*	Sept. 2	16 22	45.3	− 3.2	F
1910	30	16 47	73.3	−29.1	F
1980*	Oct. 31	16 55	28.7	−26.4	G
2324*	1923 June 26	20 35	39.8	− 4.6	P
2329*	27	20 45	40.8	−13.4	P
2385	Aug. 19	18 05	18.0	−26.2	P
2426*	Sept. 2	16 33	31.9	− 9.5	F
2433*	4	16 49	33.9	−19.8	G−
2454	26	16 20	55.9	− 7.2	G
2476	Oct. 3	15 42	62.9	−11.5	G
2485	20	16 20	4.3	−16.5	G
2491	21	15 42	5.3	− 8.0	G
2547	Nov. 22	15 50	37.3	− 9.0	P
2883	1924 July 17	20 38	48.4	+ 0.4	G
2907	22	22 55	53.5	− 6.0	F
2927	Aug. 12	18 10	74.3	− 9.5	G
2974	21	21 20	7.7	−25.5	G
2991	Sept. 8	19 00	25.6	−23.4	G
3003	13	19 00	30.6	−10.6	G
3024	18	15 35	35.4	+11.5	P
3055	Oct. 18	16 04	65.5	− 4.2	G
3311	1925 June 4	23 00	67.8	− 9.1	G
3369*	July 3	20 00	20.9	−30.2	G
3409	30	20 00	47.9	− 6.9	F
3450	Aug. 10	16 53	58.8	−15.6	G
4451	1927 Oct. 8	17 20	15.4	− 2.8	F

* A camera of 18-in. focal length was used for these spectrograms.

TABLE III

	Km/sec.	Km/sec.	Δ
J.D. 2426075	−156 (Mt. Wilson)	−166 (Victoria)	+10
5997	162 (Victoria)	167 (Victoria)	+ 5
6020	169 (Victoria)	165 (Victoria)	− 4
6064	166 (Victoria)	158 (Victoria)	− 8
6101	175 (Victoria)	157 (Victoria)	−18
6122	−165 (Victoria)	−169 (Victoria)	+ 5

servations. It is apparent, however, that the measures scatter indiscriminately about their mean value. Other periods were also tried with no results.

R SAGITTAE

The twenty-eight radial velocities given in Table II have a range of 42 km/sec., which, in spite of the large error of measurement, is good evidence of a variable velocity.

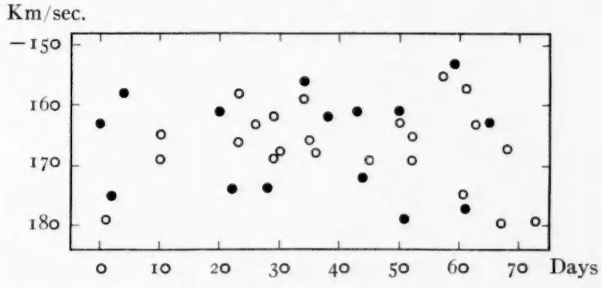

FIG. 1.—V Ursae Minoris. Circles represent Redman's Victoria observations; dots, Mount Wilson observations. Second Mount Wilson value inadvertently omitted from this figure.

Gerasimovič and Hufnagel[7] derived the formula

$$\text{Min.} = \text{J.D. } 2422025.8 + 70^{d}88E$$

to represent the considerable data with which they worked. The phases for the radial velocities were computed with this formula and used as abscissae for the plot in Figure 2, in which the vertical lines indicate the phases for the two light maxima and minima.[8] A velocity minimum possibly occurs at maximum II, and the principal light minimum perhaps precedes the maximum of the radial velocities; but the scatter in the velocities makes any conclusion as to a periodic change in velocity during the light cycle uncertain. From phase 33 to 54 days the location of the velocity-curve is quite uncertain.

Two spectral variations are of interest: The G band is most intense at the minima and least intense at the maxima; and the absorption at $H\gamma$ shows two maxima near the phases of light minima and two minima with phases at or slightly preceding the light maxima.

[7] *Op. cit.*, No. 340, p. 10, 1929.

[8] P. Ahnert, *Astronomische Nachrichten*, **239**, 75, 1930.

V VULPECULAE

The radial velocities have an extreme range of about 40 km/sec., much as for R Sagittae, which is here even stronger evidence of variability, since nearly the full amount of this range occurs among the several spectrograms obtained with the higher dispersion of the 18-inch camera.

Phases for the plot of velocities in Figure 3 were computed with Gerasimovič's[9] period ($75^{d}.678$; phases referred to minimum *A*). Ver-

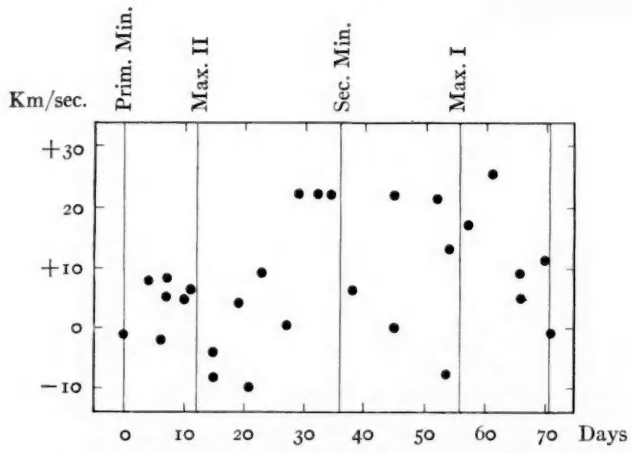

FIG. 2.—Radial-velocity plot for R Sagittae

tical lines in the figure show his determination of the phases of the maxima and minima of light.

The velocities clearly do not define any simple variation with the precision to be expected from their probable errors. A primary minimum is indicated, however, at phase 26 days, and a primary maximum at about phase 48 days; and there is some evidence, though weak, of a secondary maximum and minimum. These features are shown by the curve drawn (perhaps with some over-emphasis) through the observations. There is no correspondence of minimum velocity and maximum light or vice versa, but rather a tendency for the light maxima and minima to precede by a few days the velocity minima and maxima, respectively.

[9] *Op. cit.*, No. 321, 1927.

That the period used is correct is perhaps indicated by the fact that three plates showing the bands of titanium oxide all fall within the narrow phase range 35–40 days, which includes the light minimum, when presumably the temperature suffers a diminution along with the light. This minimum is perhaps the one from which phases should be reckoned.

None of these three variables displays with any certainty a velocity variation during the photometric cycle. The results are, however, about what would be expected if the form of the velocity-curve

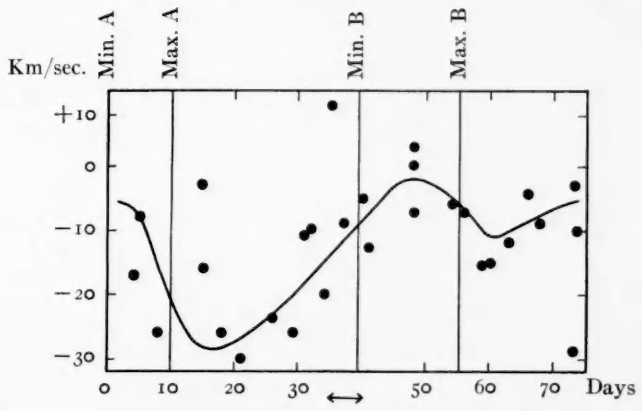

FIG. 3.—Radial-velocity plot for V Vulpeculae. Curve drawn arbitrarily free-hand. Arrow shows phase interval in which spectrum contained bands of titanium oxide.

changes from time to time or if there is a change in the velocity of the center of mass.

To obtain observations in sufficient number to define accurately the variation of velocity during a single cycle would be helpful. The length of period is, however, a serious obstacle, since at Mount Wilson the program for spectrographic observations covers alternate fortnights. On this account these stars will probably receive little further attention in the near future.

V Vulpeculae, like R Sagittae, undergoes spectral changes such that the earliest type is associated with light maxima and the latest with light minima.

CARNEGIE INSTITUTION OF WASHINGTON
MOUNT WILSON OBSERVATORY
June 1933

THE RADIAL-VELOCITY VARIATION OF UU CASSIOPEIAE[1]

By ROSCOE F. SANFORD

ABSTRACT

Light variation.—Periods of from 4 to 17 days have been assigned by different observers to the light variation of UU Cassiopeiae. The light-curves are in some cases, however, complicated by secondary maxima. Luizet classified this star as a Cepheid.

Spectrum and radial velocity.—Twenty-six spectrograms over an interval of five years show the spectral class to be B1. The star is therefore probably not a Cepheid. The radial velocity is variable.

Orbital elements and relation to light variation.—The radial velocities and the best two series of light observations can be harmonized with the relations for an eclipsing binary if one-half the 17-day period is used. The velocity-curve indicates circular motion with an orbital velocity of at least 161 km/sec. The total mass of the system must be at least thirty times that of the sun. The uncertainty in the light-curves is so large that it is impossible to derive the data which are normally furnished by a combination of photometric and spectroscopic elements.

The variability of UU Cassiopeiae[2] was discovered by Luizet[3] in 1913. From his own observations he concluded that this star is a Cepheid with a period of 4.314 days. Martin and Plummer[4] observed its brightness photographically from 1917 to 1921. Assembled according to phases computed by

$$\text{Maximum} = \text{J.D. } 2422745.09 + 4^{d}.31304E \text{ (G.M.T.)},$$

their observations gave a light-curve with a smoothly rising branch and a falling branch of much greater irregularity, which they represented by two secondary maxima. Luizet's observed maximum follows by half a day that computed from Martin and Plummer's formula.

Radial-velocity observations were begun at Mount Wilson in 1927 and continued as opportunity permitted until June, 1932. The twenty-six serviceable spectrograms are listed in Table I.

The star is so faint that all observations were obtained with one-prism spectrographs (C, 100-inch series; γ, 60-inch series) and short-

[1] *Contributions from the Mount Wilson Observatory, Carnegie Institution of Washington*, No. 482.

[2] BD+60°2629; (1900) α $23^{h}45^{m}.7$, δ +60°21′; BD mag. 9.3.

[3] *Astronomische Nachrichten*, **194**, 170, 1913.

[4] *Monthly Notices of the Royal Astronomical Society*, **81**, 464, 1921.

focus cameras such that the dispersion was about 75 A per millimeter at $H\gamma$.

The spectrum was found to be of class B1, in which the lines are very poorly defined. This fact, together with the low dispersion, explains the relatively large probable errors which these radial velocities undoubtedly have.

TABLE I

RADIAL-VELOCITY OBSERVATIONS OF UU CASSIOPEIAE

Plate	Date	G.M.T.	Phase	Velocity
				km/sec.
C 4437	1927 Oct. 4	21^h00^m	4^d32	−200
4970	1928 Sept. 3	21 45	7.04	− 13
4985	25	20 12	3.42	−172
4988	26	22 03	4.49	−225
5293	1929 Sept. 10	23 25	4.20	−199
5300	12	00 05	5.23	−176
γ 16905	12	22 25	6.16	− 72
C 5319	15	23 40	0.69	+ 94
5344	Oct. 19	21 18	0.51	+ 98
5349	20	21 4	1.50	− 30
γ 17025	21	20 6	2.46	−110
C 5519	1930 Aug. 13	23 35	0.38	+ 94
γ 17769	Sept. 11	22 57	3.79	−208
17775	12	22 58	4.79	−217
C 5605	Nov. 3	19 3	5.51	−174
5609	4	18 58	6.50	− 48
γ 17863	5	18 57	7.50	− 42
17867	6	19 13	8.51	+ 92
17894	12	18 56	5.98	−100
C 5767	1931 June 30	23 33	6.11	− 72
5771	July 1	23 15	7.10	+ 8
5774	2	21 20	8.02	+107
γ 18592	Nov. 30	18 02	5.51	−120
18595	Dec. 1	16 45	6.46	− 39
18605	19	16 15	7.40	+ 73
C 6071	1932 June 24	23 39	8.25	+ 92

It was soon evident, however, that the radial velocities could not be represented by a period of the order of four days. Moreover, the spectral class is most unusual for a Cepheid variable. A period twice as long was then tried and found not only to satisfy the radial velocities then available but also those obtained until June, 1932, when the observations were discontinued since all parts of the velocity-curve were then covered.

A search for later photometric measures revealed an extensive

series made by Seliwanow[5] in 1923, 1924, and 1925, from which he obtained a period of $17^{d}.041352$. Assemblage with this period gives a curve which shows four maxima and four minima. Seliwanow chose this period rather than one of one-half or one-quarter the length because it appeared to him that the first maximum was again duplicated only after three intervening maxima.

Three different periods in the ratio of 1:2:4 have therefore been associated with this star. The simplest conception is, of course, a single period which satisfies both light and velocity variations. Since the radial velocities appear to involve a period of about eight days, it seemed best to see whether the light-variation could not also be satisfied by such a period. Phases for both photometric observations and radial velocities were therefore computed with the expression

$$\text{Maximum} = \text{J.D. } 2423450.02 + 8^{d}.520676E \text{ (G.M.T.)},$$

in which the epoch is Seliwanow's principal maximum and the period one-half his value. His observations are sufficiently numerous to give normal places based on individual observations within phase intervals of $0^{d}.25$. Martin and Plummer's observations, which are much less numerous, were also formed into normal places, but with groupings that are less satisfactory. Separate plots for (*a*) radial velocities, (*b*) Seliwanow's normals, and (*c*) Martin and Plummer's normals are shown in Figure 1. The radial velocities are satisfactorily grouped, as was to be expected. With few exceptions Seliwanow's normals strongly suggest that the variability is caused by eclipse, a suggestion which is the more plausible because the two unequal minima are in the proper relation to the velocities of the primary star. The deeper minimum has the phase $2^{d}.59$, which is very nearly that of the zero value for the primary's velocity in changing from recession to approach, i.e., when the primary star is eclipsed by the secondary. Hence phases from principal eclipse may be computed with

$$\text{Primary min.} = \text{J.D. } 2423452.61 + 8^{d}.520676E \text{ (G.M.T.)}.$$

[5] *Verein von Freunden der Physik und Astronomie in Nishni-Novgorod, Veränderliche Sterne*, **3**, 151, 1931.

The spectroscopic orbital elements are necessarily uncertain by reason of the large probable error of the radial velocities. For this reason the observations were considered well enough represented by

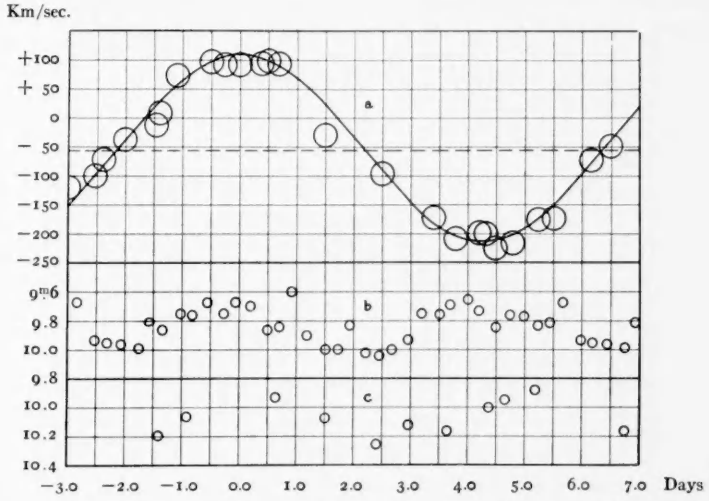

FIG. 1.—UU Cassiopeiae: (*a*) velocity-curve; (*b*) normals from Seliwanow's light observations; (*c*) normals from Martin and Plummer's photographic observations of light.

the following circular elements obtained by comparison with a set of standard curves.[6]

$$P = 8.520676$$

$$K = 161 \text{ km/sec.}$$

$$\gamma = -56 \text{ km/sec.}$$

T = J.D. 2423450.42 (G.M.T.), time of maximum positive velocity

$$a_1 \sin i = 18{,}863{,}000 \text{ km}$$

$$\frac{m_2^3 \sin^3 i}{(m_1+m_2)^2} = 3.693\odot$$

The large negative value of γ, the velocity of the center of mass, is noteworthy. The large value of K (the semi-amplitude of velocity variation), together with a period of more than eight days, is responsible for the large values of the two functions (mean distance and mass) following the elements. The magnitude of K is established

[6] *Harvard Annals*, **81**, 231, 1923.

by the radial velocities. The only escape from the eight-day period is the substitution of one very close to a day, a possibility not yet tested by two spectrograms made with a suitable interval on the same night. Light observations on the same night separated by as much as $0^d.20$ were, however, made by Martin and Plummer and showed practical constancy near the median magnitude, a circumstance that is very unlikely in the case of a period of the order of one day.

In an eclipsing system with such a mass function the total mass will be a minimum when the masses of primary and secondary are equal. For this case the total is approximately $30\odot$, whereas, for a secondary one-half as massive as the primary, the total mass will be of the order $100\odot$.

Little can be said with certainty in regard to the secondary except that its integrated photographic light cannot well be more than one-half that of the primary, since the spectrograms give no evidence of the secondary's spectrum. This fact might tell us something of the relative masses, had we means of knowing whether this difference in total brightness results only from a difference in size. If the eclipses are partial, the surface brightness of the two stars would be different because of the inequality of the two minima. The explanation of the difference in total light for the two may therefore rest to some extent upon a difference in surface brightness, and hence on different physical conditions. In this case no safe assertion would be possible except that the minimum total mass cannot be less than thirty times that of the sun.

The curve *a* in Figure 1 and the broken straight line representing the velocity of the center of mass are based on the elements. Because of the large uncertainty, the circles representing the velocities have radii equivalent to 20 km/sec.

Whether the star is an eclipsing binary or not, it merits careful photometric observation, because in the one case photometric elements are required for combination with the spectroscopic elements, and in the other, data are needed to help unravel the relationship to the radial-velocity curve.

CARNEGIE INSTITUTION OF WASHINGTON
MOUNT WILSON OBSERVATORY
June 1933

APPROXIMATE SPECTROSCOPIC ELEMENTS FOR AG VIRGINIS, RW CORONAE BOREALIS, AND AK HERCULIS[1]

By ROSCOE F. SANFORD

ABSTRACT

Radial velocities of the three variables AG Virginis, RW Coronae Borealis, and AK Herculis give curves consistent with an eclipse of the brighter by the fainter star at primary minimum. On the assumption that $m_1 = 2m_2$ and that the inclination (i) of the orbit planes is 90°, the total masses are 0.93, 0.46, and 0.56⊙; and the distances of the centers, 2.10, 1.80, and 1.36×10^6 km, respectively. These values are quite in keeping with those for other stars for which complete solutions are available.

This note presents the approximate orbital elements of three short-period variable stars based upon spectrograms obtained mostly during the last two seasons. Table I gives the magnitude range, type of variation, and period (except for the first) taken from Prager's[2] latest compilation, and the spectral class and co-ordinates for 1900 from the *Henry Draper Catalogue*.

TABLE I

Designation	H.D.	Sp.	Mag.	Type of Var.	1900		Period
					α	δ	
AG Virg.....	104350	A0	8.6– 9.3 pg.	W U Maj.	11^h56^m0	+13°24′	$0^d.64265$
RW Cor B...	139815	A8	9.3–10.0	β Lyrae?	15 35.2	29 57	0.7264171
AK Herc.....	155937	F8	8.3– 8.9	W U Maj.	17 9.5	+16 29	0.42152207

The spectra of all three stars are characterized by a few very poorly defined lines, mostly of hydrogen, as might be expected for variables of very short period having these spectral classes and types of light variation. Axial rotation of the stars in periods identical with their orbital periods, a condition imposed by the small values of the distances of their centers, probably also plays a part in

[1] *Contributions from the Mount Wilson Observatory, Carnegie Institution of Washington*, No. 483.

[2] Katalog und Ephemeriden Veränderlicher Sterne für 1933: *Kleinere Veröffentlichungen der Universitäts-Sternwarte zu Berlin-Babelsberg*, No. 11, 1932.

TABLE II

Plate	Date	G.M.T.	Phase	Vel.
	AG Virginis			
				km/sec.
γ 18300	1931 June 28	16^h12^m	0^d503	+ 67
C 5759	30	15 54	.562	+ 38
γ 18670	1932 Jan. 24	20 26	.532	+ 84
18671	24	21 39	.583	+ 35
18672	24	22 59	.639	− 22
18673	25	0 12	.046	− 70
18674	25	1 5	.083	−106
C 5962	Feb. 23	20 35	.335	+ 7
5963	23	21 38	.378	+ 42
5964	23	22 44	.424	+ 39
5970	24	23 09	.156	− 43
5982	March 23	18 37	.334	− 4
5984	23	22 45	.506	+ 64
6000	April 21	18 53	.425	+ 62
γ 18843	May 22	16 32	.480	+ 51
18904	June 21	16 00	.254	− 49
19376	Dec. 16	1 05	.260	− 80
19380	17	1 07	.619	− 14
C 6212	1933 Feb. 12	0 15	.386	+ 30
γ 19498	14	21 10	.045	− 59
19499	14	22 59	.114	− 83
19500	15	0 40	.191	− 87
19506	15	23 57	.518	+ 48
19517	March 3	19 32	.268	− 7
19576	April 4	15 54	.626	− 13
19577	4	17 53	.066	− 72
19578	4	20 02	0.156	−100
	RW Coronae Borealis			
C 2303	1923 June 22	19 14	0.659	+ 25
2380	Aug. 18	16 10	.145	− 93
5451	1930 May 13	18 19	.585	+ 33
5471	June 10	16 45	.190	− 80
γ 18202	1931 April 8	20 45	.168	− 68
18213	30	21 50	.420	+ 9
18301	June 28	18 2	.421	+ 26
18308	29	19 31	.031	− 17
C 5764	30	19 19	.296	− 21
5971	1932 Feb. 25	0 53	.537	+ 5
γ 18844	May 22	19 4	.398	+ 19
18846	22	22 49	.554	+ 48
C 6028	23	23 16	.121	− 54
C 6038	26	23 34	.228	− 45
γ 18911	June 22	20 33	.224	− 40
C 6067	24	19 49	.015	− 6
6074	25	20 15	.306	− 45
γ 19513	March 2	22 13	0.501	+ 47

TABLE II—*Continued*

Plate	Date	G.M.T.	Phase	Vel.
	AK Herculis			
				km/sec.
C 5447	1930 May 12	20^h19^m	$0^d.263$	+55
γ 18216	1931 May 1	19 52	.165	−82
18307	June 29	18 00	.074	−54
C 5762	30	18 00	.231	+10
5989	1932 March 29	23 26	.311	+50
6007	April 23	22 10	.389	+25
6031	May 24	22 02	.190	−25
γ 18910	June 22	18 40	.387	+57
C 6057	23	16 19	.024	−65
6059	23	18 44	.124	−85
6065	24	15 46	.158	−68
6068	24	20 59	.375	+52
6230	1933 March 6	1 11	.372	+29
γ 19579	April 4	21 46	.302	+42
19580	4	22 57	0.351	+36

γ = 60-inch reflector; C = 100-inch reflector

The formulae from which phases were reckoned are:

G.M.T.

AG Virg ..... Min. = J.D. 2426418.991 + $0^d.64265E$ (Dugan) (1)
RW Cor B ..... Min. = J.D. 2425365.6 + 0.7264171*E* (McLaughlin) (2)
AK Herc ..... Min. = J.D. 2422977.254 + 0.42152207*E* (Jordan) (3)

(1) By letter.
(2) *Astronomical Journal*, **39**, 85, 1929.
(3) *Publications of the Allegheny Observatory*, **7**, 142, 1929——.

producing poor definition. The accuracy with which the radial velocities (Table II) were determined was further limited by the use of short-focus cameras (dispersion 75 A per mm at $H\gamma$), in order to make short exposures and thus avoid too great an integration of the velocity variation which depends upon the orbital motion. In no case was the secondary's spectrum certainly observed. The interest attaching to variable stars of such short period nevertheless justifies the results, even though approximate.

No successful assemblage of the radial velocities of AG Virginis was possible with the period given by Prager. Professor Raymond Dugan, who is interested in the photometry of the star, kindly informed me that this period also fails to harmonize the existing photometric data, which seem to require a period of $0^d.64265$. This period

was therefore tried, and its validity, as well as that of the periods of the other two variables, may be judged by Figures 1–3, which show plots of the radial velocities with each observation represented by a circle having a radius equivalent to a velocity of 20 km/sec. because

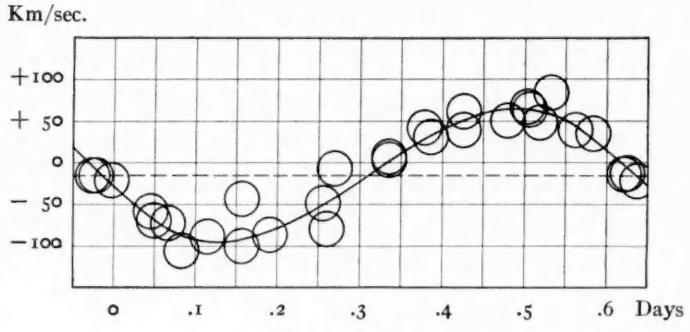

FIG. 1.—Velocity-curve of AG Virginis

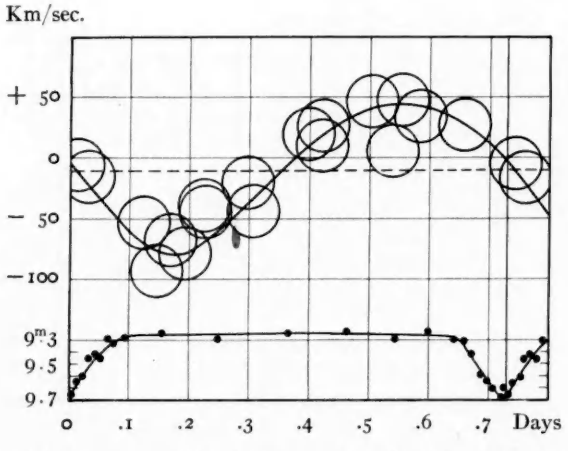

FIG. 2.—Velocity-curve of RW Coronae Borealis (above). Light-curve by Hoffmeister (below).

of the inherently large probable errors. All phases are referred to principal light minima given by the formulae following Table II. Orbital elements obtained by comparison with standard radial-velocity curves are given in Table III.

No light-curve with the period here used is available for AG Vir-

ginis. Curves by C. Hoffmeister[3] for RW Coronae Borealis and by F. C. Jordan[4] for AK Herculis are reproduced in Figures 2 and 3.

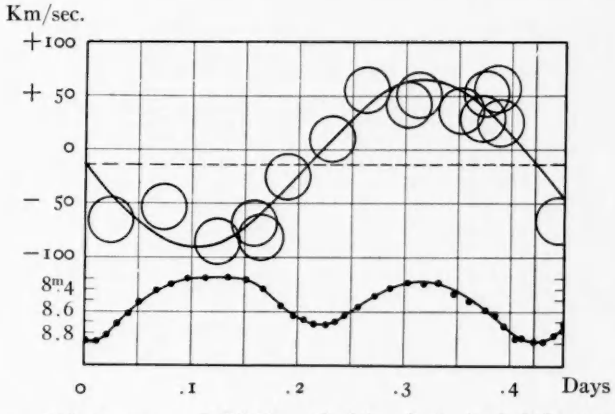

FIG. 3.—Velocity-curve of AK Herculis (above). Jordan's light-curve (below)

TABLE III

ELEMENTS

Star	AG Virginis	RW Cor. Borealis	AK Herculis
P	$0^d.64265$	$0^d.7264171$	$0^d.42152207$
T*	J.D. 2426418.979	J.D. 2425365.741	J.D. 2422977.254
ω	90°	160°	.....
e	0.10	0.12	0.00
K_1	80 km/sec.	61 km/sec.	78 km/sec.
γ	−16 km/sec.	−11 km/sec.	−13 km/sec.
$\frac{m_2^3 \sin^3 i}{(m_1+m_2)^2}$	0.0345⊙	0.0171⊙	0.0208⊙
$a_1 \sin i$	699,900	600,550	452,110 km
If $m_1=2m_2$ and $i=90°$			
$m_1+m_2=$	0.93⊙	0.46⊙	0.56⊙
$a_1+a_2=$	2,099,700	1,801,650	1,356,330 km

* T for AG Virginis and RW Coronae Borealis is the time of periastron passage, but for AK Herculis it is the time of light minimum.

Another light-curve for AK Herculis depending upon numerous observations has been given by J. Wasintynski.[5] This curve is also

[3] *Astronomische Nachrichten*, **201**, 407–414, 1915.

[4] *Publications of the Allegheny Observatory*, **7**, 142, 1929.

[5] *Warsaw Observatory Reprint*, No. 11, 1931.

of the β Lyrae type but appears to have changed since Jordan observed it both as to the position of the secondary minimum and as to the shape of the maxima.

The relation of each of the velocity-curves of Figures 1–3 (from the elements of Table III) to light minimum is that corresponding to the eclipse of the brighter component by the fainter.

The values for m_1+m_2 and a_1+a_2 given in Table IV depend on the assumption that $m_1=2m_2$ and $i=90°$. They are in reasonable agreement with results for other short-period eclipsing variables for which complete solutions have been obtained.

CARNEGIE INSTITUTION OF WASHINGTON
MOUNT WILSON OBSERVATORY
June 1933

SPECTROSCOPIC ORBITAL ELEMENTS FOR THE ECLIPSING VARIABLE CM LACERTAE[1]

By ROSCOE F. SANFORD

ABSTRACT

The light elements.—Wachmann found CM Lacertae to be an eclipsing variable with a period of $1^d.60469$ and with maximum, principal minimum, and secondary minimum equal to 8.14, 9.17, and 8.54 mag., respectively. Eclipse lasts 0.2 day. He does not state, however, whether he found evidence of totality.

Spectroscopic elements.—The radial velocities from fourteen spectrograms obtained in 1932 are well distributed in phase and confirm Wachmann's conclusion of variability by eclipse with the period mentioned. The observations are represented by circular motion with a minimum orbital velocity of 117.5 km/sec. for the primary and 159± km/sec. for the secondary, the latter value being much less reliable than that for the primary. The distances of the two components from the center of mass of the system are not less than 2,500,000 and 3,500,000 km. Their respective masses are at least two and one and one-half times the solar mass. The distance of the secondary and the two masses involve the uncertainties in the secondary's orbital speed.

Data are not available for deriving the photometric elements, and hence a complete solution of the orbit, which depends upon a knowledge of both the spectroscopic and the photometric elements, cannot yet be given.

According to A. A. Wachmann,[2] CM Lacertae[3] is an eclipsing binary with principal minima represented by

$$\text{J.D. } 2425922.284 + 1^d.60469E \text{ (G.M.T.)}.$$

He obtained the photographic magnitudes 8.14, 9.17, and 8.54 for maximum and principal and secondary minima, respectively. Eclipse lasts $0^d.2$, but whether total or not is not stated. No further details are available.

Fourteen well-distributed spectrograms (Table I), obtained between June and September, 1932, confirm the spectral classification (A2) given in the *Henry Draper Catalogue*. The velocities are variable and when assembled (Fig. 1) according to phases from Wachmann's formula reveal a velocity variation for the primary star that is well represented by circular elements. These elements (Table II) were derived by comparison of the plotted observation with stand-

[1] *Contributions from the Mount Wilson Observatory, Carnegie Institution of Washington*, No. 484.

[2] *Astronomische Nachrichten*, **244**, 303, 1931.

[3] BD +43°4106; H.D. 209147; α $21^h56^m.1$, δ +44° 4′ (1900).

ard curves and have not been further corrected by a least-squares solution.

TABLE I

RADIAL VELOCITIES OF CM LACERTAE

Plate	Date	G.M.T.	Phase	Vel. Prim.	Footnote
				km/sec.	
γ 18909	1932 June 21	23^h16^m	0^d686	− 65	(1)
18912	22	23 05	0.073	− 53	(1)
C 6062	23	21 25	1.003	+ 69	(1)
6069	24	21 40	0.409	−145	(2)
6076	25	23 08	1.470	+ 17	(2)
V 204	July 19	19 01	1.228	+106	.....
210	20	18 27	0.600	− 89	.....
γ 18951	21	17 12	1.548	− 7	(2)
18955	21	23 55	0.223	−103	(2)
19009	Aug. 15	22 32	1.096	+103	(1)
19012	16	16 23	0.236	−114	(1)
19017	16	22 52	0.506	−127	(1)
19020	17	19 10	1.352	+ 73	(1)
19125	Sept. 14	18 04	0.421	−135	(1)

γ = Series obtained with the 60-in. reflector and 1-prism spectrograph.

C = Series obtained with the 100-in. reflector and 1-prism spectrograph.

V = Series obtained with 3-prism ultra-violet spectrograph and 10-in. camera, for which the dispersion at $H\gamma$ is 39 A per mm.

(1) Dispersion = 35 ± A per mm at $H\gamma$.

(2) Dispersion = 73 A per mm at $H\gamma$.

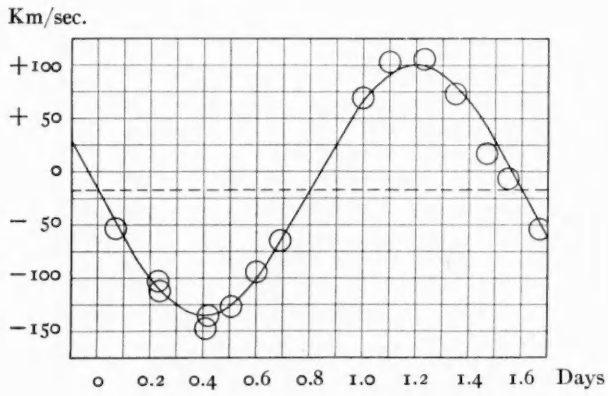

FIG. 1.—Velocity-curve of CM Lacertae

In some cases lines appeared to be double, as though two stars of about the same spectral class were present. In no case was this ap-

pearance entirely convincing; nor was the run of the separate values for the radial velocity of the secondary worthy of more confidence. The value adopted for K_2 in Table II is an attempt to be impartial to this very uncertain evidence.

The radial-velocity curve in Figure 1 and the broken line for the velocity of the system correspond to the elements of Table II. Zero

TABLE II

ELEMENTS FOR CM LACERTAE

$P = 1.60469$ (Wachmann)
$\gamma = -17.5$ km/sec.
$K_1 = 117.5$ km/sec.
$K_2 = 159 \pm$ km/sec.
T = J.D. 2425922.284 G.M.T.
= Epoch of primary minimum
$a_1 \sin i = 2{,}593{,}000$ km
$a_2 \sin i = 3{,}509{,}000 \pm$ km
$m_1 \sin^3 i = 2.0 \odot \pm$
$m_2 \sin^3 i = 1.5 \odot \pm$

phase or the time of principal minimum agrees very closely with the time when the primary star's velocity changes from recession to approach, that is, with the time of eclipse of the primary by the secondary. Hence the radial velocities confirm Wachmann's conclusion about variation by eclipse and prove the general accuracy of his period.

The complete solution of the orbit from spectroscopic and photometric elements awaits more precise data for the latter than are at present available.

CARNEGIE INSTITUTION OF WASHINGTON
MOUNT WILSON OBSERVATORY
June 1933

A PRELIMINARY TABLE OF LINES IN THE SPECTRUM OF δ CEPHEI

By C. J. KRIEGER

ABSTRACT

On four one-prism spectrograms of δ Cephei, the *wave-lengths* of 380 absorption lines were measured from λ 4000 to λ 4750.

The *intensities* of the lines at maximum and minimum phase were estimated on an arbitrary scale.

The *contributors* to the lines were identified, and are shown in Table I.

Elements definitely or probably present are: *H, C, Mg, Si, Ca, Sc, Ti, V, Cr, Mn, Fe, Ni, Sr, Y, Zr, Ba, La, Ce,* and *Eu.* A few other elements are possibly present. There are 68 lines which are probably unblended.

The *variation of intensity* of lines is studied, first, by means of the unblended lines of the various elements; second, by means of the important contributors to the blended lines. Many lines to which neutral *Ca, Ti, Cr, Fe,* or rare earths contribute are strengthened at minimum, while some lines to which *H* or ionized *Cr* and *Fe* contribute are weakened at minimum.

The purpose of the present study is to provide a preliminary list of absorption lines found in low-dispersion spectrograms of δ Cephei between λ 4000 and λ 4750, approximately. Unblended lines which may be used to advantage in a study of the radial velocity and of the physical conditions in the star's atmosphere should be distinguishable from blended lines unsuitable for these purposes. If a reasonably complete identification of the stellar lines is made, a discussion of the presence or absence of chemical elements and their relative abundance can be undertaken. It is possible that the present list might be of use in further, more detailed, studies of other Cepheid variables of which δ Cephei is the prototype.

I. OBSERVATIONS AND REDUCTIONS

The visual magnitude of δ Cephei ($\alpha = 22^h25^m.4$, $\delta = +57°54'$; 1900.0) varies from 3.6 to 4.3 in a period of $5.366396E - 0.84 \times 10^{-8}E^2$ days,[1] with the maximum epoch at J.D. 2393659.873. The

[1] *Kleine Veröffentlichungen der Universitätssternwarte, Berlin-Babelsberg,* **9,** 1930.

radial velocity varies within the same period from -35 to $+5$ km/sec.[2]

The spectral type varies from F2 to G4, the average of estimates by Shapley[3] and Miss Payne.[4] Whipple[5] estimates the temperature at maximum as 6800° and at minimum as 4800°. The average of five determinations[5] of the mean absolute visual magnitude is -1.8. The mass is about ten times that of the sun, and if, with Whipple, a mean radius of ten and one-half times that of the sun is assumed,[5] the mean surface of gravity of δ Cephei would be about 0.1 of its value at the surface of the sun, with a corresponding lower pressure of the atmosphere. Other determinations of the mean radius have led to larger values of R, and would give a smaller value for g.

Four Eastman Process plates taken at the Yerkes Observatory with the one-prism spectrograph attached to the 40-inch refractor were used for a study of the absorption lines in the spectrum of δ Cephei. The data concerning the plates are given in the accompanying table.

Plate	Date 1931, U.T.	Phase	Observers
IR 9903.....	Oct. 9, 5^h21^m	$3^d.763$	Morgan, Struve, Sullivan
9928.....	21, 8 10	5.148	Struve, Sullivan
9931.....	22, 0 12	0.450	Struve
9955.....	Nov. 16, 3 17	4.113	Struve, Swings, Sullivan

The spectra on plates 9928 and 9931 are good, and those on plates 9903 and 9955 are fair. Plates 9903 and 9955 were taken near minimum light and will be referred to as "minimum plates," while plates 9928 and 9931, taken near maximum light, will be referred to as "maximum plates." The dispersion is about 25 A per millimeter at $H\gamma$.

For the measurement of the wave-lengths a Gaertner comparator was used. About eighty iron and titanium comparison lines were measured at the same time. The plates were reduced by the Hart-

[2] T. S. Jacobsen, *Lick Observatory Bulletin*, **12**, 138, 1926.

[3] H. Shapley, *Astrophysical Journal*, **44**, 273, 1916.

[4] C. H. Payne, *The Stars of High Luminosity*, Appen. B, 1930.

[5] F. L. Whipple, *Lick Observatory Bulletin*, **16**, 1, 1932.

mann formula in two sections, λλ 3969.26–4337.92 and λλ 4337.92–4681.91, and were then corrected by drawing error-curves obtained by a representation of the comparison lines.

The lines used for calculating the radial velocity[6] are as shown in the accompanying list. Allowance was made for the annual and

λ 4045.818	λ 4340.467	λ 4541.520
4063.621	4351.770	4563.757
4071.758	4374.860	4571.970
4101.738	4395.036	4576.360
4163.647	4400.118	4583.847
4202.572	4404.754	4588.210
4226.945	4443.799	4589.960
4233.264	4450.490	4592.060
4246.850	4481.230	4616.720
4271.766	4491.410	4620.520
4294.103	4501.269	4629.330
4307.862	4508.291	4657.180
4320.800	4515.343	4670.400
4325.766	4520.231	
4337.915	4533.966	

diurnal motion of the observer, and the radial velocities reduced to the sun were found to be as tabulated.

Plate	Km/Sec.
9903	+ 1.5
9928	−28.9
9931	−31.6
9955	+ 2.4

These values are in satisfactory agreement with those found by Jacobsen.[7] The probable error of the radial velocity for one plate is about ± 1 km/sec., varying somewhat with the quality of the plate.

The forty-five lines tabulated thought to be practically unblended were measured on three or four plates. In the first column the number of plates on which the line was measured is given, in the second column is the mean of the calculated wave-lengths, in the third column are the differences between the calculated and the

[6] E. B. Frost, O. Struve, and C. T. Elvey, *Publications of the Yerkes Observatory*, **7**, Part II, 1932.

[7] *Loc. cit.*

standard wave-lengths ($C-S$). Twenty-five algebraic signs are positive, seventeen negative, and three zero. The algebraic sum of the forty-five residuals is +0.53 A, indicating a small systematic error,

No.	λ Meas.	Δλ	No.	λ Meas.	Δλ	No.	λ Meas.	Δλ
4.....	4028.41	+.06	4.....	4213.69	+.04	4.....	4491.42	+.01
4.....	4034.42	−.07	3.....	4220.39	+.05	4.....	4501.39	+.12
3.....	4036.74	−.03	4.....	4254.38	+.04	4.....	4508.31	+.02
4.....	4059.78	+.06	4.....	4260.44	−.05	4.....	4515.34	0
3.....	4062.42	−.03	3.....	4269.26	−.04	4.....	4520.19	−.05
4.....	4074.79	0	4.....	4312.92	+.04	4.....	4541.47	−.05
4.....	4107.46	−.03	4.....	4375.84	−.09	4.....	4554.12	+.08
4.....	4147.62	−.06	4.....	4383.53	−.02	4.....	4563.79	+.02
4.....	4157.79	+.01	4.....	4386.85	+.01	4.....	4576.44	+.13
4.....	4167.31	−.08	4.....	4413.61	+.01	4.....	4602.94	−.01
3.....	4175.64	0	3.....	4416.78	−.03	3.....	4620.53	+.01
3.....	4176.53	−.04	4.....	4425.59	+.16	4.....	4703.09	+.02
3.....	4188.76	+.02	4.....	4450.51	+.02	4.....	4714.54	+.12
4.....	4210.32	−.04	4.....	4466.62	+.06	4.....	4731.47	−.02
4.....	4211.91	+.06	4.....	4470.94	+.06	4.....	4736.85	+.06

at least with respect to this group of forty-five unblended lines. The principal reason is that the corrections for radial velocity had been made from another group of forty-three lines, most of which were later found to be blended. The probable error for the wave-length of a line, measured on three or four plates, is found to be ±0.04 A.

The intensities of the measured lines were estimated on an arbitrary scale from 0 to 6, defined as follows:

0 not visible
1 visible with difficulty
2 visible as a well-defined narrow line
3 easily measured, moderately strong, and wide line
4 wide and strong
5 very wide and strong
6 the widest and strongest lines in the spectrum

Both the width and the central intensity of a line were taken into account in the estimates. Blends consisting of unresolved faint lines were often estimated with difficulty, as the central intensity is likely to be small compared with the width, and a fair compromise was attempted. The notation "wide" or "blend" was usually included in the original measuring sheets. It is hoped that the adopted intensities, together with the wave-lengths, will make it possible to locate any line in the spectrum of δ Cephei (Pl. I). A difference of one

unit of intensity or less between the maximum and minimum plates is not necessarily significant. If, however, several unblended lines of the same atom show variations in the same sense, actual variation of the intensity becomes probable. An analysis of microphotometer tracings of spectrograms at different phases would be very valuable.

II. IDENTIFICATIONS

Identifications were made on the basis of the coincidence of laboratory and stellar wave-lengths, the simultaneous presence of the stronger members[8] in the multiplets, and a comparison with the spectrum of the sun,[9] the chromosphere,[10] and α Persei.[11]

The identification of stellar lines is readily possible when one or more lines in a multiplet are unblended, but it becomes uncertain when all lines in a multiplet are blended with other lines. The coincidences themselves of the stronger lines make the presence of the multiplet merely probable. In such cases the decision was made from their observed presence or absence in the sun and in α Persei.

The presence of unclassified lines of iron and of the rare earths can be established only to a lesser degree of certainty. The principal criteria were coincidences in wave-length, and the intensity in the laboratory, the sun, the chromosphere, and α Persei. Even after due consideration of the available facts, the decision reached is tentative and subject to modification. Classification of the lines of the rare earths and of the unclassified lines of iron would throw new light on the problem.

III. DESCRIPTION OF TABLE I

Table I shows the measured lines in the spectrum of δ Cephei, arranged in numerical order from λ 3997.27 to λ 4805.46 in column 1. The wave-lengths, in view of the probable error of $\pm$0.04 A for a line measured on three or four plates, are given to two decimal places,

[8] H. N. Russell, *Proceedings of the National Academy of Sciences*, **11**, 314, 1925.

[9] C. E. St. John, etc., *Revision of Rowland's Preliminary Table of Solar Spectrum Wavelengths*, Carnegie Institution of Washington, 1928.

[10] D. H. Menzel, *Publications of the Lick Observatory*, **17**, 1931.

[11] T. Dunham, Jr., *Contributions from the Princeton University Observatory*, No. 9, 1929; also unpublished tables for wave-lengths shorter than λ 4146, kindly placed at my disposal.

PLATE I

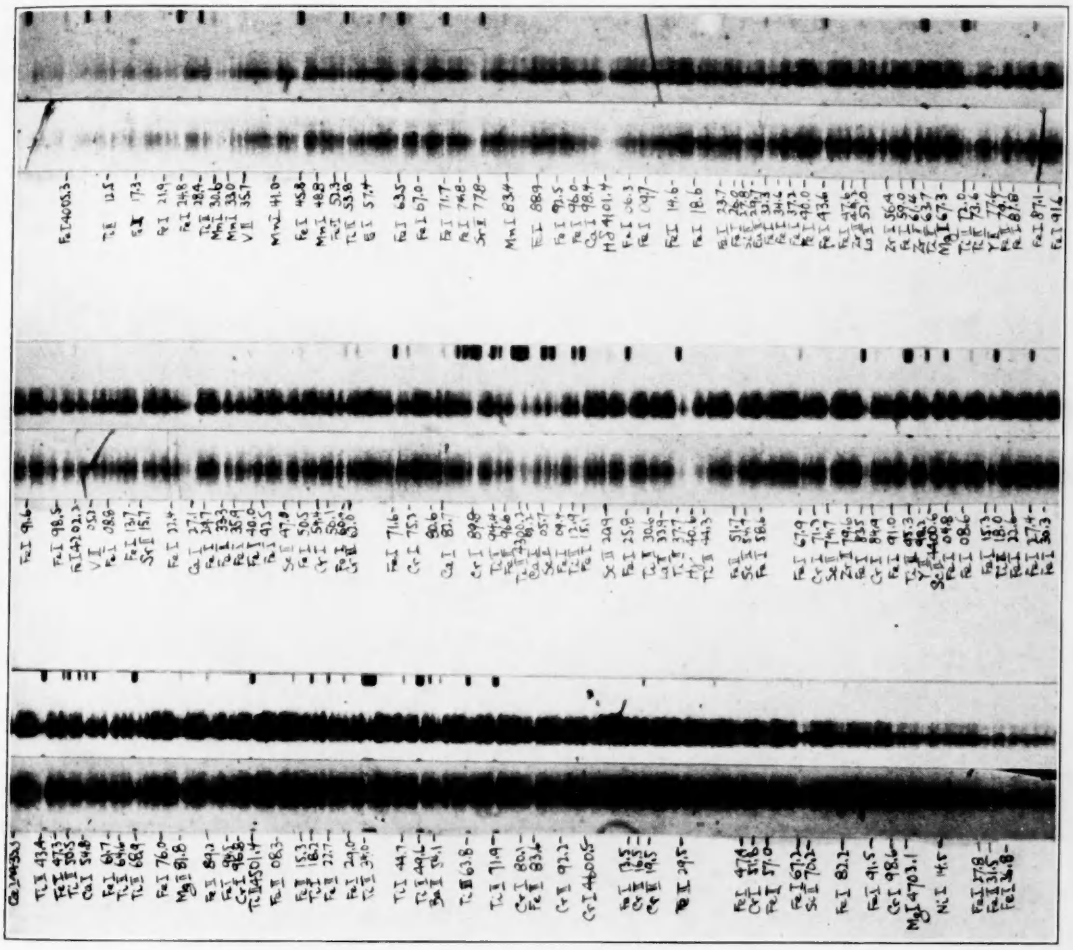

SPECTRUM OF δ CEPHEI

a) 1931 Nov. 16. Phase $4^{d}05$. Near minimum
b) 1931 Oct. 21. Phase $5^{d}15$. Near maximum

and are the averages of the wave-lengths calculated for the individual plates on which the line was measured. Column 2 shows the number of plates used for the determination of the wave-length. Column 3 gives the intensity of the line near maximum (the average of the intensities estimated on plates IR 9928 and 9931), while in column 4 the intensity of the line near minimum is listed (the average of the intensities estimated on Plates IR 9903 and 9955). The laboratory wave-lengths are shown in column 5, the elements are in column 6, and the extent to which each laboratory line contributes to the stellar line is shown in column 7:

+++	denotes the principal contributor
++	denotes an important contributor
+	denotes a minor contributor
[No symbol]	denotes a very slight or doubtful contributor
−	denotes an insignificant or absent contributor

The standard wave-lengths are taken from various sources.[12] Miss Moore's *Multiplet Table of Astrophysical Interest*[13] will furnish the multiplet designation, etc.

Plate I, enlarged about twenty times, shows the spectrum of δ Cephei near maximum (plate IR 9928; phase 5.148) and near minimum (plate IR 9954; phase 4.046; Nov. 16, 1931; 1^h40^m U.T.). Most of the stronger and some of the fainter lines have been indicated by their wave-lengths and their principal contributors to facilitate identification on the enlargement. Changes in the intensities of lines from maximum to minimum phase may be studied conveniently on the enlargement.

[12] St. John, etc., *op. cit.;* Menzel, *op. cit.;* A. S. King, *Astrophysical Journal*, **68**, 194, 1928; *ibid.;* **72**, 221, 1930; K. Burns and F. M. Walters, Jr., *Publications of the Allegheny Observatory of the University of Pittsburgh*, **6**. No. 11, 159, 1929; C. E. Moore, *A Multiplet Table of Astrophysical Interest*, Princeton University Observatory, 1933.

[13] *Op. cit.*

TABLE I

λ Delta Cephei	No. of Plates	Intensity		λ Lab.	Element	Cont.
		Max.	Min.			
3997.27	2	3.5	.....	6.97	*Fe* I	+
				7.12	*V* II	++
				.40	*Fe* I	++
				.49	⊙	+
3999.06	2	3	.....	8.65	*Ti* I	+
				.96	*Zr* II	+++
				9.23	*Ce* II	+
4000.43	3	2.5	3	0.25	*Fe* I	+
				.45	*Dy* II	+
				.47	*Fe* I	+++
4001.88	1	3	.....	1.67	*Fe* I	++
				.67	*Ce* II	+
				2.08	⊙	++
4003.07	1	1	.....	2.95	*V* II	+++
4003.91	2	1	.....	3.77	*Fe* I	++
				.77	*Ce* II	+
				.80	*Ti* I	+
				4.02	⊙	++
4005.26	3	4	4	5.25	*Fe* I	+++
				.55	*Tb* II	.....
				.71	*V* II	+
4006.61	1	2	.....	6.32	*Fe* I	++
				.64	*Fe* I	+++
				.77	*Fe* I	++
4009.78	1	1	.....	9.72	*Fe* I	+++
4012.49	4	3.5	3.5	2.38	*Ce* II	.....
				.40	*Ti* II	+++
				.52	*Cr* II	+
4013.71*	2	1	.....	3.64	*Fe* I	++
				.78	*Fe* I	+++
4014.54*	2	1	.....	4.49	*Sc* II	++
				.53	*Fe* I	+++
4015.56	4	1.5	2	5.40	*Ti* I	+
				.50	*Ni* II	++
				.61	⊙ = *Er* II?	+++
4017.28	4	1	2.5	7.10	*Fe* I	+
				.15	*Fe* I	++
				.47	⊙	++
				.56	*Ni* I	+

TABLE I—*Continued*

λ Delta Cephei	No. of Plates	Intensity		λ Lab.	Element	Cont.
		Max.	Min.			
4018.23....	3	2	1	8.10	*Zr* II	++
				.11	*Mn* I	++
				.27	*Fe* I	+++
				.36	*Zr* II	++
4019.14....	1	0	1	9.05	*Ce* II	.....
				.06	*Ni* I	++
4020.22....	1	0	1.5	0.19	⊙	++
				.28	⊙	++
				.40	*Sc* I	+
				.90	*Co* I	.....
4021.86....	4	2	2.5	1.62	*Fe* I	+
				.87	*Fe* I	+++
				.87	*Ti* I	+
4023.30....	3	2	1	3.30	*Zr* II	++
				.38	*V* II	+++
				.69	*Sc* I	.....
4024.78....	4	4	4.5	4.43	*Zr* II	+
				.57	*Ti* I	+
				.72	*Fe* I	+++
				5.13	*Ti* II	++
4028.41....	4	3	3.5	8.35	*Ti* II	+++
4029.56*...	3	1	1	9.64	*Fe* I	+++
				.67	*Zr* II	++
4030.61*...	3	3	3	0.19	*Fe* I	.....
				.37	*Cr* II	.....
				.49	*Fe* I	+
				.53	*Ti* I	++
				.76	*Mn* I	+++
4031.78.....	4	1.5	2	1.34	*Ce* II	+
				.70	*La* II	+
				.72	*Nd* II	.....
				.77	*Ti* I	+++
				.80	*Mn* I	++
				.97	*Fe* I	+
4032.95....	4	3	2	2.46	*Fe* I	+
				.64	*Fe* I	++
				3.07	*Mn* I	+++
4034.42....	4	2	2	4.49	*Mn* I	+++
4035.67....	4	2.5	2	5.62	*V* II	+++
				.73	*Mn* I	++

TABLE I—*Continued*

λ Delta Cephei	No. of Plates	Intensity		λ Lab.	Element	Cont.
		Max.	Min.			
4036.74	3	1	1	6.77	*V* II	+++
4040.63*	2	1	.....	0.22	*Zr* II	.....
				.64	*Fe* I	+++
				.76	*Ce* II	++
				.79	*Nd* II	+
4041.46*	2	1.5	.....	1.28	*Fe* I	++
				.37	*Mn* I	+++
4042.73	4	1.5	2.5	2.58	*Ce* II	++
				.91	*Sa* II	+
				.92	*La* II	++
4043.85	3	1	1	3.90	*Fe* I	+++
				.98	*Fe* I	++
4044.65	2	.5	.5	4.62	*Fe* I	+++
				.83	*Pr* II	−
4045.80	4	4	4.5	5.40	*Co* I	+
				.61	*Zr* II	+
				.82	*Fe* I	+++
				.98	*Dy* II	.....
				6.08	⊙	+
4047.42	1	0	1	7.32	*Fe* I	+++
				.65	*V* I	.....
				.79	*Sc* I	.....
4048.82*	3	2.5	3	8.66	*Zr* II	+
				.76	*Mn* I	+++
				.79	*Cr* I	.....
				9.34	*Fe* I	++
				.39	*Ti* I	.....
4050.39	2	1	0	0.31	*Zr* II	+++
				.58	*Dy* II	+
				.68	*Fe* I	+
4052.31*	3	2	3	1.92	*Fe* I	++
				2.00	*Cr* II	+
				.29	*Fe* I	+++
				.46	*Fe* I	++
				.50	⊙	++
				.65	*Fe* I	+
				.72	*Fe* I	.....
4053.75	4	3.5	3.5	3.27	*Fe* I	.....
				.43	*Cr* II	+
				.84	*Ti* II	+++
				4.08	*Cr* II	+

TABLE I—*Continued*

λ Delta Cephei	No. of Plates	Intensity		λ Lab.	Element	Cont.
		Max.	Min.			
4055.00	4	2	3.5	4.54	*Sc* I	.....
				.83	*Fe* I	+
				.88	*Fe* I	++
				5.02	*Ti* I	+++
				.04	*Zr* I	.....
				.05	*Fe* I	++
				.55	*Mn* I	++
4056.32	4	2	2.5	6.20	*Ti* II	+
				.35	*Fe* I	+++
				.54	*Pr* II	.....
4057.44	4	2.5	2.5	7.36	*Fe* I	++
				.63	*Mg* I	+++
4058.21	1	.5	0	8.19	*Co* I	.....
				.22	*Fe* I	+++
4058.83	4	1.5	1.5	8.77	*Fe* I	+++
				.94	*Mn* I	++
4059.78	4	1	1	9.72	*Fe* I	+++
4061.10	4	1	1	1.10	*Fe* I	+++
				.10	*Nd* II	.....
4062.42	3	1.5	1	2.45	*Fe* I	+++
4063.52	4	3.5	4	3.30	*Fe* I	+
				.53	*Mn* I	+
				.60	*Fe* I	+++
4064.41	2	.5	.5	4.05	*Cr* II	.....
				.22	*Ti* I	+
				.40	*Ti* II	+++
				.46	*Fe* I	++
				.58	*Sa* II	.....
				.76	*Fe* II	++
4065.30	4	1	2	5.01	*Y* II	.....
				.11	*Ti* I	++
				.40	*Fe* I	+++
4067.03	4	3.5	5	6.59	*Fe* I	+
				.97	*Fe* I	+++
				7.03	*V* II	.....
				.04	*Ni* II	.....
				.28	*Fe* I	++
4067.93	3	1.5	.5	7.98	*Fe* I	+++
				8.03	*Mn* I	.....

TABLE I—*Continued*

λ Delta Cephei	No. of Plates	Intensity		λ Lab.	Element	Cont.
		Max.	Min.			
4069.13	2	0	1.5	8.84	*Ce* II	.....
				9.07	⊙	+++
				.27	*Nd* II	++
4070.66	3	1	1	0.28	*Fe* I	++
				.28	*Mn* I	.....
				.77	*Fe* I	+++
				.96	*Cr* II	.....
4071.71	4	3	3	1.53	*Fe* I	.....
				.75	*Fe* I	+++
4072.64	3	1	.5	2.52	*Fe* I	++
				.63	*Cr* II	+++
4073.73	4	2	1.5	3.48	*Ce* II	+
				.76	*Fe* I	+++
				.77	*Ce* II	+
4074.79	4	1.5	2.5	4.79	*Fe* I	+++
4075.84	3	1	1	5.66	*Cr* II	.....
				.71	*Ce* II	+
				.85	*Ce* II	+
				.85	*Sa* II	+
				.95	*Fe* I	+++
4076.69*	3	1.5	1	6.49	*Fe* I	++
				.63	*Fe* I	+++
				.81	*Fe* I	++
				.88	*Cr* II	.....
4077.82*	3	4	5	7.03	*Zr* II	.....
				.34	*La* II	.....
				.39	*Y* I	.....
				.58	*Cr* II	.....
				.71	*Sr* II	+++
				.97	*Dy* II	.....
				8.36	*Fe* I	++
				.47	*Ti* I	+
4079.27	2	1	1	9.24	*Fe* I	+++
				.24	*Mn* I	++
				.43	*Mn* I	++
4080.12	2	0	3	9.85	*Fe* I	++
				0.20	*Fe* I	+++
				.22	*Cr* I	+
				.22	*Nd* II	.....

TABLE I—*Continued*

λ Delta Cephei	No. of Plates	Intensity		λ Lab.	Element	Cont.
		Max.	Min.			
4081.13	1	0	1	0.88	*Fe* I	++
				1.22	*Ce* II	+
				.24	*Zr* I	.....
				.27	*Fe* I	++
4082.20	2	.5	1	2.12	*Fe* I	++
				.23	*Fe* I	.....
				.40	*Sc* I	+
				.44	*Fe* I	+
				.46	*Ti* I	++
4083.35	4	2	4	2.95	*Mn* I	++
				3.23	*Mn* I	.....
				.24	*Ce* II	.....
				.34	*Pr* II	.....
				.55	*Fe* I	++
				.64	*Mn* I	++
				.76	*Fe* I	.....
4084.48	1	0	.5	4.51	*Fe* I	+++
4085.25	4	1	1	5.01	*Fe* I	+
				.25	*Fe* I	++
				.25	*Ce* II	.....
				.30	*Fe* I	++
4086.89	1	1	0	6.72	*La* II	+++
				7.09	*Fe* I	+
4088.86	4	1	3	8.57	*Fe* I	++
				.73	*Fe* II	+++
				.85	*Cr* II	.....
				.85	*Ce* II	.....
				9.22	*Fe* I	++
4090.40	3	.5	2.5	0.07	*Fe* I	++
				.52	*Zr* II	+
				.59	*V* I	.....
				.96	*Fe* I	++
				.96	*Ce* II	.....
4092.50	4	2	3	2.28	*Fe* I	++
				.40	*Co* I	++
				.42	*V* I	.....
				.51	*Fe* I	++
				.65	*Ca* I	++
				.69	*V* I	.....
4094.76	3	.5	1.5	4.42	⊙	++
				.70	⊙	.....
				.94	*Ca* I	+++

TABLE I—*Continued*

λ Delta Cephei	No. of Plates	Intensity		λ Lab.	Element	Cont.
		Max.	Min.			
4096.01	4	1	1.5	5.98	*Fe* I	+++
				6.11	*Fe* I	++
				.22	*Fe* I	+
4096.96	3	.5	1.5	6.62	*Zr* II	+
				7.08	*Fe* I	+++
4098.39	4	2.5	3.5	8.18	*Cr* I	.....
				.18	*Fe* I	++
				.55	*Ca* I	++
4099.96	1	0	.5	9.80	*V* I	++
				0.00	*Fe* I	.....
				.17	*Fe* I	++
4101.43	4	6	5	0.74	*Fe* I	++
				1.27	*Fe* I	++
				.68	*Fe* I	++
				.74	*Hδ*	+++
4103.07	2	0	2	2.94	*Si* I	++
				3.31	*Dy* II	++
4104.16	4	1	1.5	4.12	*Fe* I	++
				.14	*Fe* I	++
4105.03	1	0	.5	4.78	*V* I	−
				.94	*Fe* I	+
				5.17	*V* I	+++
4106.32	4	1.5	3	6.27	*Fe* I	++
				.44	*Fe* I	++
4107.46	4	2	2	7.49	*Fe* I	+++
4108.38	1	0	.5	8.40	*Cr* I	++
				.55	*Ca* I	++
4109.65	4	2	2.5	9.05	*Fe* I	++
				.46	*Nd* II	+
				.59	*Cr* I	+
				.78	*V* I	+
				.81	*Fe* I	+++
				0.02	*Zr* II	.....
4110.87	3	1.5	.5	0.54	*Co* I	++
				.87	*Cr* I	+
				1.00	*Cr* II	.....
				.04	*Cr* II	+++
				.36	*Cr* I	.....
				.79	*V* I	+

TABLE I—*Continued*

λ Delta Cephei	No. of Plates	Intensity		λ Lab.	Element	Cont.
		Max.	Min.			
4113.02....	4	2	1.5	2.57	*Cr* II	.....
				.97	*Fe* I	+++
				3.23	*Cr* II	.....
4114.63*...	2	2	4	4.45	*Fe* I	+++
				.94	*Fe* I	+
				5.18	*V* I	++
4116.81....	3	.5	2.5	6.48	*V* I	+
				.70	*V* I	++
				.82	*Nd* II	++
				.96	*Fe* I	+
				7.01	*Ce* II	
4118.60....	4	3.5	3.5	8.15	*Ce* II	.....
				.54	*Fe* I	+++
				.78	*Co* I	++
				.89	*Fe* I	+
4119.86....	4	1.5	2	9.40	*Fe* I	++
				.92	*Ce* II	+
				0.21	*Fe* I	++
4121.48....	4	2	2	1.33	*Co* I	+++
				.81	*Fe* I	++
4122.60....	4	2	1	2.52	*Fe* I	++
				.67	*Fe* II	+++
4123.70....	4	1	1.5	3.23	*La* II	+
				.56	*V* I	+
				.76	*Fe* I	+++
				.88	*Ce* II	.....
4124.80....	4	2.5	2	4.79	*Ce* II	+++
				.95	*Y* II	++
4126.05....	4	2	2.5	5.63	*Fe* I	++
				.88	*Fe* I	++
				6.09	*Cr* I	.....
				.18	*Fe* I	+++
4127.77....	4	3.5	3	7.61	*Fe* I	++
				.62	*Cr* I	.....
				.80	*Fe* I	++
				8.05	*Si* II	+++
				.08	*V* I	++
4129.65....	2	0	2	9.47	⊙	+
				.64	*Eu* II	−
				.73	*Eu* II	+++

TABLE I—*Continued*

λ Delta Cephei	No. of Plates	Intensity		λ Lab.	Element	Cont.
		Max.	Min.			
4130.82....	4	2	2	0.35	*Gd* II	.....
				.68	*Ba* II	++
				.71	*Ce* II	.....
				.88	*Si* II	+++
				1.10	*Ce* II	.....
4132.34....	4	3.5	4	1.95	*Fe* I	+
				2.02	*V* I	.....
				.06	*Fe* I	+++
				.44	*Cr* II	.....
				.54	⊙	+
				.91	*Fe* I	++
4133.71....	3	1	.5	3.36	*Nd* II	.....
				.80	*Ce* II	++
				.87	*Fe* I	+++
4134.58....	4	2.5	4	4.34	*Fe* I	++
				.43	*Fe* I	++
				.50	*V* I	.....
				.68	*Fe* I	+++
4137.22....	4	2	4	7.00	*Fe* I	+++
				.42	⊙	++
				.64	*Ce* II	+
4138.43....	2	1	0	8.36	*Fe* II	+++
4140.07....	4	2	3	9.93	*Fe* I	+++
				0.41	⊙	++
4141.72....	1	0	.5	1.72	*La* II	.....
				.86	*Fe* I	+++
4142.21*...	3	2.5	2	2.31	*Ni* I	++
				2.39	*Ce* II	++
				.48	*Ti* I	+
				.95	⊙	.....
4143.60*...	3	4	4	3.13	*Pr* II	.....
				.41	*Fe* I	++
				.51	*Fe* I	+
				.87	*Fe* I	+++
4144.99....	3	.5	1	4.52	*Ce* II	+
				.99	*Ce* II	+++
4146.02....	4	1.5	2	6.00	*Cr* II	.....
				.07	*Fe* I	+++
				.45	*Cr* II	.....

TABLE I—*Continued*

λ Delta Cephei	No. of Plates	Intensity		λ Lab.	Element	Cont.
		Max.	Min.			
4147.62	4	2	2.5	7.68	*Fe* I	+++
4149.22	4	3	3	9.20	*Zr* II	+++
				.36	*Fe* I	++
4150.89	2	.5	.5	0.25	*Fe* I	++
				.97	*Ti* I	+
				.97	*Zr* II	+++
4152.03	4	2.5	3	1.95	*Fe* I	++
				.95	*La* II	+++
				.98	*Ce* II	+
				2.18	*Fe* I	++
				.19	*Sa* II	.....
4153.93*	2	1.5	.....	3.84	*Cr* I	.....
				.90	*Fe* I	+++
4154.70*	2	2	.....	4.50	*Fe* I	++
				.81	*Fe* I	++
4156.40	4	4	3.5	6.23	*Nd* II	.....
				.24	*Zr* II	++
				.31	⊙	++
				.67	*Fe* I	+
				.80	*Fe* I	++
4157.79	4	2	1.5	7.78	*Fe* I	+++
4158.98	4	2.5	2	8.79	*Fe* I	++
				9.19	⊙	++
4160.31	3	.5	1	0.25	⊙	.....
				.37	*Ti* II	+++
4161.43	4	4	3.5	1.08	*Fe* I	.....
				.21	*Zr* II	++
				.49	*Fe* I	.....
				.54	*Ti* II	++
				.81	*Sr* II	+
4163.65	4	3	2.5	3.62	*Cr* I	+
				.65	*Ti* II	++
				.67	*Fe* I	+
4165.48	4	1.5	3	5.39	*Fe* I	+++
				.61	*Ce* II	++
4167.31	4	3	4	7.39	*Mg* I	+++

TABLE I—*Continued*

λ Delta Cephei	No. of Plates	Intensity		λ Lab.	Element	Cont.
		Max.	Min.			
4168.71....	2	.5	.5	8.62	*Fe* I	++
				.95	*Fe* I	++
4169.68....	3	.5	1.5	9.62	⊙(=*CH*?)	+
				.76	*Fe* I	+++
4170.87....	4	2.5	1.5	0.64	*Cr* II	.....
				.90	*Fe* I	+++
				1.02	*Ti* I	.....
4171.97....	3	2.5	2	1.91	*Ti* II	+++
				.92	*Cr* II	.....
				2.14	*Fe* I	+
4172.68....	1	.5	0	2.27	*Pr* II	.....
				.62	*Cr* II	.....
				.64	*Fe* I	++
				.75	*Fe* I	+++
4173.61....	3	2.5	1	3.32	*Fe* I	+
				.48	*Fe* II	++
				.55	*Ti* II	+++
				.92	*Fe* I	+
4174.92....	1	.5	0	4.92	*Fe* I	+++
4175.64....	3	1	.5	5.64	*Fe* I	+++
4176.53....	3	1	.5	6.57	*Fe* I	++
4177.61....	4	2.5	2.5	7.54	*Y* II	++
				.60	*Fe* I	++
4179.06....	4	3	3	8.87	*Fe* II	++
				9.41	*Cr* II	++
				.43	*V* I	.....
4181.84....	4	2.5	2.5	1.75	*Fe* I	+++
				.98	⊙	++
4183.36....	2	1	0	3.43	*V* II	+++
4184.20....	4	2	2	4.00	⊙	++
				.25	*Gd* II	.....
				.33	*Ti* II	++
				.90	*Fe* I	.....
4187.09....	4	2.5	4	6.60	*Ce* II	+
				.81	*Dy* II	.....
				7.05	*Fe* I	+++

TABLE I—*Continued*

λ Delta Cephei	No. of Plates	Intensity		λ Lab.	Element	Cont.
		Max.	Min.			
4187.81	2	2	0	7.81	*Fe* I	+++
4188.76	3	1	.5	8.74	⊙	+++
4190.10	1	.5	0	0.13	*Cr* I	+
				.29	*Ti* II	+++
4191.56	4	3	3	1.29	*Cr* I	.....
				.45	*Fe* I	+++
				.68	*Fe* I	++
				.75	*Cr* I	.....
4193.51	2	0	1.5	3.10	*Ce* II	+
				.28	*Ce* II	++
				.88	*Ce* II	++
4195.38	4	2	2	4.83	*Dy* II	−
				5.33	*Fe* I	+++
				.62	*Fe* I	+
4196.48	4	2	2.5	6.21	*Fe* I	+
				.53	*Fe* I	++
				.56	*La* II	++
4198.45	4	3	4	8.25	*Fe* I	.....
				.31	*Fe* I	++
				.64	*Fe* I	++
4199.08	2	1	0	9.10	*Fe* I	+++
				.28	*Y* II	.....
4200.02	2	0	1	9.97	*Fe* I	+++
4200.92	4	1	2	0.79	*Ti* I	.....
				.92	*Fe* I	+++
4202.24	4	3	3	2.03	*Fe* I	++
				.34	*V* II	++
4203.94	4	1	1.5	3.59	*Fe* I	++
				.59	*Cr* I	.....
				.98	*Fe* I	+++
				4.05	*La* II	++
				.27	*Cr* I	.....
4205.20	4	2.5	2.5	4.69	*Y* II	+
				.91	*Eu* II	.....
				5.05	*Eu* II	+
				.09	*V* II	++
				.47	*Mn* II	.....
				.54	*Fe* I	++

TABLE I—*Continued*

λ Delta Cephei	No. of Plates	Intensity		λ Lab.	Element	Cont.
		Max.	Min.			
4207.02....	4	2	3.5	6.70	*Fe* I	++
				7.13	*Fe* I	++
				.34	*Cr* II	+
4208.78....	4	2	2.5	8.60	*Fe* I	+++
				.96	*Zr* II	++
4210.32....	4	2	1.5	0.36	Fe I	+++
4211.91....	4	2	1.5	1.85	*Zr* II	+++
4213.69....	4	2	1.5	3.65	*Fe* I	+++
4215.70....	4	4.5	4.5	5.52	*Sr* II	+++
				.78	*Cr* II	.....
				6.18	*Fe* I	++
4217.49....	4	2	2	7.08	*Cr* II	.....
				.26	⊙(=*CH*?)	+
				.55	*Fe* I	+++
				.60	*Cr* I	.....
4219.38....	4	1.5	1.5	9.36	*Fe* I	+++
				.42	⊙	++
4220.39....	3	1	1	0.34	*Fe* I	+++
4222.37....	4	2.5	3	2.22	*Fe* I	+++
				.60	*Ce* II	+
4224.26....	4	2	2	4.17	*Fe* I	+++
				.51	*Fe* I	++
4225.46....	4	2	1	5.23	*V* II	+
				.34	*Pr* II	.....
				.45	*Fe* I	+++
4227.06*...	3	4	5	6.42	*Fe* I	.....
				.73	*Ca* I	+++
				7.43	*Fe* I	++
4229.68....	4	1	2.5	9.52	*Fe* I	++
				.75	*Fe* I	+++
				.82	*Cr* II	.....
4231.58....	1	.5	0	1.59	*Zr* II	+++
				.69	*Fe* I	++
4233.29....	4	3.5	4	2.72	*Fe* I	+
				3.16	*Fe* II	+++
				.25	*Cr* II	.....
				.61	*Fe* I	++

TABLE I—*Continued*

λ Delta Cephei	No. of Plates	Intensity		λ Lab.	Element	Cont.
		Max.	Min.			
4235.92....	4	2	3	5.71	*V* II	.....
				.95	*Fe* I	+++
4237.13....	1	0	.5	6.76	*Sa* II	.....
				.81	*V* II	.....
				7.08	*Fe* I	++
				.18	*Fe* I	++
4238.48....	4	2	2	8.02	*Fe* I	++
				.40	*La* II	++
				.81	*Fe* I	++
4239.98....	4	2	3	9.73	*Mn* I	.....
				.85	*Fe* I	++
				.85	*Nd* II	.....
				.91	*Ce* II	.....
				0.38	*Fe* I	++
				.46	*Ca* I	+
4242.48....	4	2.5	2.5	2.39	*Cr* II	++
				.59	*Fe* I	++
				.74	*Fe* I	++
4243.64....	3	.5	1	3.45	⊙	++
				.55	⊙	+
				.82	*Fe* I	++
4245.23....	4	1	1	5.26	*Fe* I	+++
				.36	⊙	+
4247.03....	4	2.5	3	6.83	*Sc* II	++
				7.43	*Fe* I	++
4248.53....	4	1	1.5	8.22	*Fe* I	++
				.67	*Ce* II	++
4250.48....	4	3	4	0.13	*Fe* I	++
				.79	*Fe* I	++
4252.55....	4	1.5	1.5	2.46	*Nd* II	+
				.63	*Cr* II	+++
4254.38....	4	2.5	2	4.34	*Cr* I	+++
4256.14....	4	1	3	5.79	*Ce* II	+
				.84	*Fe* I	+
				6.32	*Dy* II	++
				.42	*Sa* II	++
4258.32....	4	2.5	4	8.03	*Zr* II	.....
				.16	*Fe* II	++
				.32	*Fe* I	+++

TABLE I—*Continued*

λ Delta Cephei	No. of Plates	Intensity		λ Lab.	Element	Cont.
		Max.	Min.			
4260.44....	4	3	3.5	0.49	*Fe* I	+++
4261.96....	4	2	2.5	1.81	*Cr* II	.....
				.90	*Cr* II	+++
				2.09	*Gd* II	.....
4267.02....	1	0	.5	6.97	*Fe* I	+++
4267.96....	2	.5	.5	7.83	*Fe* I	+++
				8.11	⊙(=*CH*?)	+
4269.26....	3	2	1	9.30	*Cr* II	+++
4271.64....	4	3.5	3.5	1.17	*Fe* I	++
				.76	*Fe* I	+++
4273.50....	4	2	2	3.31	*Fe* II	++
				.31	*Ti* I	.....
				.52	*Zr* II	+++
4274.82*...	2	1	2	4.79	*Cr* I	+++
4275.62*...	2	1	1	5.55	*Cr* II	++
				.65	*La* II	++
4276.92....	1	0	.5	6.67	*Fe* I	++
				7.34	*Zr* II	+
				.54	⊙	++
4278.26....	3	1	.5	8.23	*Fe* I	++
				.23	*Ti* I	++
4280.63....	3	1	4	9.49	*Fe* I	++
				.70	*Sa* II	.....
				.87	*Fe* I	.....
				.95	*Sc* II	.....
				.96	*Sa* II	.....
				0.34	*Cr* II	.....
				.41	*Cr* I	++
				.50	*Gd* II	.....
				.79	*Sa* II	.....
				1.08	*Cr* II	.....
				.10	*Mn* I	+
4282.70....	4	3	4	2.41	*Fe* I	++
				3.01	*Ca* I	++
4284.32....	3	1	.5	4.20	*Cr* II	+++
				.54	*Nd* II	.....
4285.60....	1	.5	0	5.44	*Fe* I	+++

TABLE I—*Continued*

λ Delta Cephei	No. of Plates	Intensity		λ Lab.	Element	Cont.
		Max.	Min.			
4288.03....	4	2	2	7.88	*Ti* II	++
				8.01	*Ni* I	+
				.15	*Fe* I	+
4289.82....	4	4.5	3.5	9.36	*Ca* I	++
				.73	*Cr* I	++
				.93	*Ce* II	.....
				0.23	*Ti* II	++
4291.36....	1	0	.5	0.88	*Fe* I	+
				.93	*Ti* I	.....
				1.47	*Fe* I	+++
4294.39....	4	3	3	4.10	*Ti* II	++
				.13	*Fe* I	+
				.77	*Sc* II	++
4296.55....	4	2.5	2.5	6.56	*Fe* II	+++
				.68	*Ce* II	.....
4297.98....	3	.5	1.5	7.75	*Cr* I	.....
				.76	*Pr* II	.....
				8.03	*Fe* I	+++
4299.21*...	3	2	3	8.99	*Ca* I	++
				9.24	*Ti* I	+
				.25	*Fe* I	+++
				.36	*Ce* II	.....
				.65	*Ti* I	+
4300.18*...	3	2.5	4	0.05	*Ti* II	+++
				.33	*Ce* II	+
				.55	*Ti* I	.....
4302.20*...	2	2.5	.....	1.93	*Ti* II	++
				2.19	*Fe* I	++
				.52	*Ca* I	+++
4303.22*...	2	1.5	.....	3.18	*Fe* II	+++
4305.73....	4	2.5	3	5.45	*Fe* I	++
				.46	*Sr* II	+
				.71	*Sc* II	++
				.91	*Ti* I	++
4307.95....	4	2.5	2.5	7.74	*Ca* I	+
				.89	*Ti* II	++
				.91	*Fe* I	+++
4309.44....	4	2	2.5	9.38	*Fe* I	+++
				.61	*Y* II	+

TABLE I—*Continued*

λ Delta Cephei	No. of Plates	Intensity		λ Lab.	Element	Cont.
		Max.	Min.			
4312.92....	4	2	2	2.88	*Ti* II	+++
4314.16*...	2	2	.....	4.09	*Sc* II	+++
				.52	*Nd* II	.....
4315.06*...	2	1.5	.....	4.98	*Ti* II	++
				5.09	*Fe* I	+++
4316.99....	4	1.5	2.5	6.80	*Ti* II	+++
				7.30	*Zr* II	++
4318.80....	4	1.5	2	8.64	*Ti* I	+
				.65	*Ca* I	+++
				.94	*Sa* II	+
4320.85....	4	3	3.5	0.73	*Ce* II	.....
				.73	*Sc* II	+++
				.95	*Ti* II	++
4323.55....	2	0	1	3.33	*Sa* II	.....
				.52	*Cr* I	+++
4325.12*...	2	1	2	5.00	*Sc* II	+++
4325.82*...	2	2	2	5.77	*Fe* I	+++
4326.93....	3	.5	1	6.71	*Mn* II	.....
				.76	*Fe* I	++
				7.11	*Fe* I	+++
				.14	*Gd* II	.....
4330.57....	4	2	3	0.25	*Ti* II	++
				.71	*Ti* II	+++
4333.91....	4	1	2	3.77	*La* II	+++
				.91	*Pr* II	.....
				4.20	*Sa* II	.....
4337.68....	4	3.5	3.5	7.05	*Fe* I	++
				.32	*Ti* II	+
				.59	*Cr* I	+
				.92	*Ti* II	++
4339.44....	1	0	.5	9.44	*Cr* I	+++
				.53	*Zr* II	+
				.74	*Cr* I	+
4340.59....	4	6	4.5	0.46	*H*γ	+++
4344.30....	4	3	4	4.31	*Ti* II	+++
				.53	*Cr* I	.....

TABLE I—*Continued*

λ Delta Cephei	No. of Plates	Intensity		λ Lab.	Element	Cont.
		Max.	Min.			
4346.49*	1	0	.5	6.55	*Fe* I	+++
4347.88*	2	.5	.5	7.81	*Sa* II	++
				.85	*Fe* I	+++
4351.70	4	3	4	0.83	*Ti* II	.....
				1.06	*Cr* I	++
				.54	*Fe* I	++
				.77	*Cr* I	+
				.77	*Fe* II	+++
				.94	*Mg* I	++
4352.93	3	1	.5	2.74	*Fe* I	+++
				.75	*Ce* II	.....
				.89	*V* I	++
4354.74	4	2	3	4.60	*Sc* II	+++
				5.10	*Ca* I	++
4358.57	4	1	2	8.17	*Nd* II	.....
				.51	*Fe* I	+++
				.72	*Y* II	++
4359.71	4	1	1	9.59	*Ni* I	.....
				.64	*Cr* I	+++
				.74	*Zr* II	++
4367.89	4	3	3	7.58	*Fe* I	+
				.67	*Ti* II	+
				.91	*Fe* I	+++
4369.62	4	2	2	9.41	*Fe* II	++
				.70	*Ti* I	.....
				.78	*Fe* I	+++
4371.21	4	1.5	2	0.95	*Zr* II	+
				1.30	*Cr* I	+++
4374.72	4	3.5	3	4.46	*Sc* II	++
				.82	*Ti* II	+
				.95	*Y* II	++
4375.84	4	1	1	5.93	*Fe* I	+++
4379.57	4	1	2	9.24	*V* I	++
				.77	*Zr* II	++
4383.53	4	2	1.5	3.55	*Fe* I	+++

TABLE I—*Continued*

λ Delta Cephei	No. of Plates	Intensity		λ Lab.	Element	Cont.
		Max.	Min.			
4384.93....	4	3	3.5	4.73	*V* I	++
				.80	*Sc* II	+
				.98	*Cr* I	++
				5.39	*Fe* II	++
4386.85....	4	2	1	6.84	*Ti* II	+++
4388.26....	4	1	1	7.89	*Fe* I	++
				8.41	*Fe* I	+++
4391.00....	4	2	3	0.89	*Sa* II	.....
				.96	*Fe* I	+++
				1.02	*Ti* II	++
4393.95....	4	1	1	3.93	*Ti* I	++
				4.06	*Ti* II	++
4395.30....	4	3	3	5.04	*Ti* II	+++
				.24	*V* I	+
				.86	*Ti* II	++
4398.15....	4	2	2.5	8.03	*V* II	++
				.31	*Ti* II	++
4400.01*...	2	3	.....	9.77	*Ti* II	++
				0.38	*Sc* II	++
				.59	*V* I	+
4401.39*...	2	1	.....	1.30	*Fe* I	++
				.33	*Zr* II	.....
				.45	*Fe* I	+
				.55	*Ni* I	++
4403.20....	4	1	1	3.19	⊙	+++
				.33	*Zr* II	++
4404.81....	4	2.5	3	4.75	*Fe* I	+++
				5.04	*Fe* I	+
4408.58*...	3	3	4	7.66	*V* I	.....
				.68	*Ti* II	+
				.72	*Fe* I	++
				8.21	*V* I	+
				.42	*Fe* I	++
				.52	*V* I	++
				.84	*Pr* II	−
				9.13	*Fe* I	.....
				.23	*Ti* II	+
				.53	*Ti* II	+
4410.83....	4	1	1	0.50	*Ni* I	++
				1.10	*Ti* II	++

TABLE I—*Continued*

λ Delta Cephei	No. of Plates	Intensity		λ Lab.	Element	Cont.
		Max.	Min.			
4412.11	4	1	1	1.94	*Ti* II	++
				2.28	*Cr* I	++
4413.61	4	1	1	3.60	⊙	+++
4415.29	4	3	3	4.89	*Mn* I	+
				5.13	*Fe* I	+++
				.55	*Sc* II	++
4416.78	3	1	.5	6.81	*Fe* II	+++
4417.99	4	2.5	4	7.72	*Ti* II	+++
				8.33	Ti II	++
4420.58	3	.5	1.5	0.53	*Sa* II	+
				.66	*Sc* II	++
				1.13	*Sa* II	+
4422.60	4	2	3	2.58	*Fe* I	+++
				.60	*Y* II	++
4424.16	1	0	.5	3.85	*Fe* I	++
				4.28	*Cr* I	+++
				.37	*Sa* II	+
4425.59	4	1	2	5.43	*Ca* I	+++
4427.38	4	2	2.5	7.10	*Ti* I	+
				.31	*Fe* I	+++
				.92	*Ti* II	.....
4430.31	4	1.5	3	9.90	*La* II	++
				0.62	*Fe* I	++
4431.90	1	0	.5	1.35	*Sc* II	++
				2.09	*Ti* II	++
4433.63	3	.5	1	3.22	*Fe* I	++
				.78	*Fe* I	++
4435.29	4	2.5	4	4.95	*Ca* I	++
				5.15	*Fe* I	+
				.47	*Eu* II	.....
				.60	*Eu* II	.....
				.67	*Ca* I	++
4443.44	4	5	6	2.35	*Fe* I	++
				.84	*Fe* I	.....
				.99	*Zr* II	.....
				3.20	*Fe* I	++
				.80	*Ti* II	++
				4.56	*Ti* II	++

TABLE I—*Continued*

λ Delta Cephei	No. of Plates	Intensity		λ Lab.	Element	Cont.
		Max.	Min.			
4447.34	4	2.5	3	6.85	*Fe* I	++
				7.14	*Fe* I	++
				.73	*Fe* I	+++
4450.51	4	2	2	0.49	*Ti* II	+++
4453.01	2	0	1	2.74	*Sa* II	++
				3.32	*Ti* I	++
4454.78	4	2	3.5	4.39	*Fe* I	++
				.66	*Fe* I	.....
				.77	*Ca* I	+++
				.79	*Zr* II	++
				5.32	*Ti* I	+
				.32	*Mn* I	+
				.82	*La* II	.....
				.88	*Ca* I	++
4459.19	4	1.5	1	9.05	*Ni* I	++
				.13	*Fe* I	+++
				.36	*Cr* I	+
4461.70	4	3	4	1.21	*Zr* II	+
				.21	*Fe* I	+
				.66	*Fe* I	+++
				.97	*Fe* I	++
				2.03	*Mn* I	+
4464.58	4	2	2.5	4.47	*Ti* II	++
				.68	*Mn* I	++
4466.62	4	1	2	6.56	*Fe* I	+++
4468.86	4	3	3.5	8.49	*Ti* II	+++
				9.15	*Ti* II	+
				.38	*Fe* I	++
4470.94	4	2	2.5	0.88	*Ti* II	+++
4472.83	4	2	2.5	2.79	*Mn* I	++
				.93	*Fe* II	+++
4476.04	4	2	2	6.02	*Fe* I	+++
				.08	*Fe* I	++
4479.90	2	0	1.5	9.36	*Ce* II	.....
				.61	*Fe* I	++
				.98	⊙	+
				0.13	*Fe* I	++

TABLE I—*Continued*

λ Delta Cephei	No. of Plates	Intensity		λ Lab.	Element	Cont.
		Max.	Min.			
4481.20*...	3	2	1	1.13	*Mg* II	++
				.27	*Ti* I	+
				.33	*Mg* II	++
4482.31*...	2	1	1	2.18	*Fe* I	++
				.26	*Fe* I	+++
				.40	*Ti* II	.....
				.69	*Ti* I	.....
				.75	*Fe* I	+
4484.12....	4	1	1.5	3.90	*Ce* II	+
				.95	*Co* I	.....
				4.24	*Fe* I	+++
4485.56....	3	.5	1	5.42	*Zr* II	.....
				.68	*Fe* I	+++
4487.03....	1	0	.5	6.91	*Ce* II	+++
4489.24....	4	2.5	3	8.33	*Ti* II	+
				.91	*Fe* I	+
				.91	*V* I	.....
				9.10	*Ti* I	+
				.21	*Fe* II	+++
				.74	*Fe* I	+
4491.42....	4	2	2.5	1.41	*Fe* II	+++
4494.48....	4	1.5	3	4.41	*Zr* II	+
				.57	*Fe* I	+++
4496.81....	4	1	2.5	6.16	*Ti* I	+
				.86	*Cr* I	+++
				.96	*Zr* II	+
4499.16....	1	0	1	8.90	*Mn* I	++
				9.15	⊙	+++
				.50	*Sa* II	.....
4501.39....	4	3	3.5	1.27	*Ti* II	+++
4504.88....	1	0	.5	4.85	*Fe* I	+++
4506.70....	2	0	1	6.74	*Ti* II	+++
4508.31....	4	2	1.5	8.29	*Fe* II	+++
4515.34....	4	2	2	5.34	*Fe* II	+++
4518.16....	4	1	2.5	8.03	*Ti* I	+++
				.30	*Ti* II	++

TABLE I—*Continued*

λ Delta Cephei	No. of Plates	Intensity		λ Lab.	Element	Cont.
		Max.	Min.			
4520.19....	4	2	2.5	0.24	*Fe* II	+++
4522.72....	4	2.5	3.5	2.60	*Eu* II	.....
				.64	*Fe* II	+++
				.80	*Ti* I	++
4524.96....	4	1.5	2	4.72	*Ti* II	++
				.95	*Ba* II	+
				5.14	*Fe* I	+++
4526.75....	4	1.5	1.5	6.48	*Cr* I	++
				.57	*Fe* I	+
				.94	*Ca* I	++
				7.32	*Ti* I	++
				.35	*Ce* II	+
4528.98....	4	3	2.5	8.62	*Fe* I	++
				9.46	*Ti* II	++
				.55	*Fe* I	.....
4531.12....	4	2	3	0.98	*Co* I	++
				1.16	*Fe* I	+++
4533.98....	4	3	2.5	3.25	*Ti* I	++
				.97	*Ti* II	+++
				4.17	*Fe* II	+
				.78	*Ti* I	++
4535.84....	4	1	2	5.58	*Ti* I	++
				.72	*Cr* I	+
				.92	*Ti* I	++
				6.00	*Ti* I	++
4539.80....	1	.5	0	9.76	*Ce* II	+++
				.79	*Cr* I	++
				0.50	*Cr* I	+
4541.47....	4	1.5	1.5	1.52	*Fe* II	+++
4544.74....	4	2	3.5	3.96	*Sa* II	.....
				4.01	*Ti* II	++
				.62	*Cr* I	++
				.69	*Cr* II	.....
				.70	*Ti* I	+++
				5.15	*Ti* II	+
				.96	*Cr* I	++
4547.26....	1	0	.5	6.94	*Ni* I	+
				7.03	*Fe* I	+++
				.23	*Ni* I	.....
				.85	*Fe* I	++

TABLE I—*Continued*

λ Delta Cephei	No. of Plates	Intensity		λ Lab.	Element	Cont.
		Max.	Min.			
4549.57	4	3	3.5	9.48	*Fe* II	++
				.64	*Ti* II	+++
4552.38	4	1	1.5	2.25	*Ti* II	+
				.45	*Ti* I	+++
				.54	*Fe* I	+
4554.12	4	1.5	2	4.04	*Ba* II	+++
4555.88	4	2	2	5.09	*Cr* II	.....
				.50	*Ti* I	+
				.90	*Fe* II	+++
				6.10	*Fe* I	+
				.13	*Fe* I	+
4558.66*	3	2	2	8.66	*Cr* II	+++
				.84	*Cr* II	.....
4560.20*	1	.....	.5	0.09	*Fe* I	++
				.27	*Ce* II	++
4563.79	4	2	2	3.77	*Ti* II	+++
4565.78	4	1	2	5.52	*Cr* I	++
				.60	*Co* I	+
				.68	*Fe* I	+++
				.74	⊙	.....
4568.58	3	.5	1.5	8.30	*Ti* II	++
				.79	*Fe* I	+++
4571.93	4	3	3.5	1.11	*Mg* I	++
				.30	*Cr* II	.....
				.68	*Cr* I	.....
				.98	*Ti* II	+++
				2.28	*Ce* II	.....
				.87	*Cr* II	+
4574.83	2	0	1.5	4.73	*Fe* I	+++
				.90	*La* II	++
4576.44	4	1.5	1	6.31	*Fe* II	+++
4580.12	4	1	2.5	0.07	*Cr* I	++
				.08	*La* II	++
				.40	*V* I	.....
				.46	*Ti* II	+
4581.56	1	0	.5	1.41	*Ca* I	++
				.53	*Fe* I	+++
				.62	*Co* I	.....

TABLE I—*Continued*

λ Delta Cephei	No. of Plates	Intensity		λ Lab.	Element	Cont.
		Max.	Min.			
4583.60....	4	3	3.5	3.45	*Ti* II	++
				.84	*Fe* II	++
4585.93....	4	1	1.5	5.87	*Ca* I	+++
				.98	⊙	.....
4588.28....	4	1	1	8.21	*Cr* II	+++
				.40	*Cr* II	+
4589.95....	4	1.5	1	9.89	*Cr* II	+
				.96	*Ti* II	+++
				.96	*Cr* II	+
4592.18....	4	2	2.5	2.06	*Cr* II	++
				.53	*Ni* I	++
				.66	*Fe* I	++
4594.01....	4	1	1	3.94	*Ce* II	++
				.99	*Eu* II	.....
				4.10	*V* I	++
4595.79....	4	1	1.5	5.30	*Sa* II	.....
				.36	*Fe* I	++
				.70	*Fe* II	+
				6.06	*Fe* I	++
4598.04....	4	1	2	7.76	⊙	+
				.88	⊙ = *Gd* II?	+
				8.14	*Fe* I	+++
4600.48....	4	2	3	0.11	*Cr* I	+
				.21	*V* II	++
				.36	*Ni* I	++
				.75	*Cr* I	+++
4602.94....	4	1	1	2.95	*Fe* I	+++
4605.46....	3	1	2	4.99	*Ni* I	++
				5.36	*Mn* I	.....
				.60	⊙	++
				.79	*La* II	.....
4607.62....	3	.5	1.5	7.34	*Sr* I	+
				.66	*Fe* I	+++
4609.49....	1	0	.5	9.27	*Ti* II	+++
4611.29....	4	1.5	1.5	1.19	*Fe* I	.....
				.28	*Fe* I	+++

TABLE I—*Continued*

λ Delta Cephei	No. of Plates	Intensity		λ Lab.	Element	Cont.
		Max.	Min.			
4613.53	4	1.5	2.5	3.22	*Fe* I	++
				.33	*Cr* I	.....
				.40	*La* II	++
				.95	*Zr* II	+
4616.46	4	2	3.5	6.11	*Cr* I	++
				.67	*Cr* II	++
4618.90*	3	1.5	2	8.76	*Fe* I	.....
				.82	*Cr* II	+++
				9.29	*Fe* I	++
4620.53*	3	1	1	0.52	*Fe* II	+++
4622.71	1	0	.5	2.46	*Cr* I	++
				3.10	*Ti* I	++
4625.44	2	1	.5	5.06	*Fe* I	++
				6.16	*Cr* I	++
4629.46	4	2.5	3.5	9.33	*Fe* II	+++
				.34	*Ti* I	+
4632.80	1	0	.5	2.82	*Fe* I	+
				.92	*Fe* I	+++
4634.10	2	1	0	4.09	*Cr* II	+++
4636.36	1	0	.5	6.34	*Ti* II	+++
4637.83	4	1	1	7.52	*Fe* I	++
				.77	*Cr* I	.....
				8.01	*Fe* I	++
4640.23	1	0	.5	9.66	*Ti* I	+
				.94	*Ti* I	+
				0.29	⊙	+++
4643.56	2	0	1	3.46	*Fe* I	+++
				.70	*Y* I	.....
4646.03	2	1	0	6.17	*Cr* I	+++
4647.42	2	0	5	6.80	*Cr* I	.....
				7.44	*Fe* I	+++
				.96	⊙	+
				8.12	*Cr* I	.....
4648.93	1	.5	0	8.66	*Ni* I	+++
				.86	*Cr* I	.....

TABLE I—*Continued*

λ Delta Cephei	No. of Plates	Intensity		λ Lab.	Element	Cont.
		Max.	Min.			
4651.79....	3	.5	2	1.28	*Cr* I	++
				2.16	*Cr* I	+++
4654.58....	4	1	2	4.50	*Fe* I	++
				.64	*Fe* I	+++
4656.96....	4	2	3.5	6.47	*Ti* I	++
				.98	*Fe* II	++
				7.20	*Ti* II	++
4663.34....	4	1	2.5	2.55	*La* II	.....
				.76	*Ti* II	++
				3.36	*Cr* I	+
				.71	*Fe* II	++
4667.16....	4	2	4	6.75	*Fe* II	++
				7.45	*Fe* I	+++
				.59	*Ti* I	+
4670.17....	4	2	3	0.18	⊙	+++
				.40	*Sc* II	++
4673.29....	1	.5	0	3.16	*Fe* I	+
				.27	*Fe* I	+++
4678.76....	4	1	1.5	8.18	⊙	++
				.42	*Fe* I	.....
				.85	*Fe* I	+++
				9.23	*Fe* I	++
4680.26....	2	0	1.5	0.20	*Zn* I	+
				.30	*Fe* I	+++
				.48	*Fe* I	+
4682.17....	4	1	1.5	1.91	*Ti* I	++
				2.12	*Fe* I	++
				.31	*Y* II	++
4691.47....	4	1	1	1.42	*Fe* I	+++
				.60	⊙	+
4698.60....	4	1.5	3	8.48	*Cr* I	++
				.62	*Cr* I	++
				.74	*Cr* II	+
4703.09....	4	2	1.5	3.07	*Mg* I	+++
4708.46....	4	3	3.5	8.05	*Cr* I	++
				.65	*Ti* II	+++
				9.09	*Fe* I	+

TABLE I—*Continued*

λ Delta Cephei	No. of Plates	Intensity		λ Lab.	Element	Cont.
		Max.	Min.			
4714.54....	4	2	2	4.42	*Ni* I	+++
4727.76....	3	.5	2	7.40	*Fe* I	++
				.46	*Mn* I	+
				8.55	*Fe* I	++
4731.47....	4	1.5	1.5	1.49	*Fe* II	+++
4733.79....	3	.5	1	3.59	*Fe* I	+++
				4.11	*Fe* I	+
4736.85....	4	2.5	3	6.79	*Fe* I	+++
4762.59....	2	2	.....	2.38	*Mn* I	++
				.41	*C* I	+
				.63	*Ni* I	+
				.77	*Ti* II	++
4763.91....	1	.....	3	3.90	*Ti* II	++
				.95	*Ni* I	++
4771.70....	2	1	2	1.47	⊙	+
				.70	*Fe* I	++
				.72	*C* I	++
4779.87....	2	2	2	9.99	*Ti* II	++:
4783.43....	2	2	2	3.43	*Mn* I	+++
4786.62....	2	1	2	6.51	*V* I	.....
				.54	*Ni* I	++
				.57	*V* II	+
				.81	*Fe* I	++
4805.46....	1	2	.....	5.11	*Ti* II	++
				.18	*Cr* II	+
				.42	*Ti* I	+++

NOTES TO TABLE I

4013.71–4014.54. Blend 4014.14 (4) on pl. 9955. Not measured on pl. 9903.
4029.56–4030.61. Blend 4030.17 (4) on pl. 9903.
4040.63–4041.46. Blend 4040.97 (5) on pls. 9903 and 9955.
4048.82. Two separate lines, 4048.03 (2) and 4049.53 (3), on pl. 9955.
4052.31. Two separate lines, 4051.91 (1) and 4052.71 (1), on pl. 9931.
4076.69–4077.82. Blend 4076.98 (6) on pl. 9903.
4114.63. Two separate lines, 4114.31 (2) and 4115.19 (2), on pl. 9955.
4142.21–4143.60. Blend 4142.93 (5) on pl. 9903.
4153.93–4154.70. Blend 4154.28 on pls. 9903 (4) and 9955 (3).
4227.06. Two separate lines, 4226.69 (3) and 4227.36 (1), on pl. 9928.
4274.82–4275.62. Blend 4275.19 (3) on pl. 9903.
4299.21–4300.18. Blend 4299.88 (5) on pl. 9903.

4302.20–4303.22. Blend 4302.84 (4) on pls. 9903 and 9955.
4314.16–4315.06. Blend 4314.65 (4) on pls. 9903 and 9955.
4325.12–4325.82. Blend 4325.50 (4) on pls. 9931 and 9903.
4346.49–4347.88. Blend 4347.24 (2) on pl. 9903.
4400.01–4401.39. Blend 4400.57 on pls. 9903 (5) and 9955 (4).
4408.58. Two separate lines, 4407.98 (1) and 4409.27 (1), on pl. 9928.
4481.20–4482.31. Blend 4481.76 (4) on pl. 9903.
4558.66–4560.20. Blend 4559.08 (2) on pl. 9928.
4618.90–4620.53. Blend 4619.54 (4) on pl. 9903.

IV. THE ELEMENTS REPRESENTED IN δ CEPHEI

H (1) — *Hγ* and *Hδ* are among the strongest lines in the spectrum. *Hγ* is probably unblended, while *Hδ* is blended with neutral iron lines.

C I (6) — The multiplet $3s^3P^o-4p^3P$ near λ 4770 is probably present, but is blended.

Mg I (12) — Several lines are present, of which λ 4167.39 (I 3, 4) and λ 4703.07 (I 2, 1.5) are unblended.

Mg II — The pair at λ 4481.13 and λ 4481.33 (I 2, 1) is present and is slightly blended with *Ti* I.

Al II (13) — Stellar lines are measured near λ 4585.82, λ 4588.19, and λ 4589.75. The evidence is uncertain, since the stellar lines are blended and since λ 4026.5 is absent. The group near λ 4227, $4^3D-9^3F^o$, if it were present, would be masked by *Ca* I λ 4226.73. In view of the high excitation potential, *Al* II is probably absent.

Si I (14) — λ 4102.94 may contribute to λ 4103.07, which is blended with *Dy* II. Probably present.

Si II — The pair λ 4128.05 and λ 4130.88, 2^2D-3F, is probably present, but is blended.

Ca I (20) — Several multiplets are present. λ 4425.43 (I 1, 2) is unblended.

Ca II — The H and K lines are beyond the range of the spectrum.

Sc I (21) — While five stellar lines fall near laboratory lines, they are blended and the evidence is uncertain.

Sc II — Several multiplets are present. λ 4325.00 (I 1, 2) is unblended on two plates.

Ti I (22) — Several multiplets are present, but all lines are blended.

Ti II — Most multiplets falling within the measured range are represented. Unblended lines are tabulated here.

Ti II

λ	*I*		λ	*I*	
	Max.	Min.		Max.	Min.
4028.35	3	3·5	4506.74	0	1
4312.88	2	2	4563.77	2	2
4386.84	2	1	4609.27	0	·5
4450.49	2	2	4636.34	0	·5
4470.88	2	2.5	4779.99	2	2
4501.27	3	3·5			

V I (23) The multiplets $a^6D - y^6D^o$ and $a^6D - y^6F^o$ are probably present. All lines are blended.

V II Four multiplets are represented. Unblended lines are λ 4036.77 (I 1, 1); λ 4183.43 (I 1, 0).

Cr I (24) A number of multiplets are present. Unblended lines are the ultimate lines of the multiplet $a^7S - z^7P^o$, λ 4254.34 (I 2.5, 2) and λ 4274.79 (I 1, 2). λ 4289.73 is blended. Another unblended line is λ 4646.17 (I 1, 0).

Cr II Many multiplets are identifiable. Unblended lines are λ 4269.30 (I 2, 1); the pair at λ 4558.66 and λ 4558.84 (I 2, 2), of which the former is the stronger, and λ 4634.09 (I 1, 0).

Mn I (25) A number of multiplets are represented. Unblended lines are λ 4034.49 (I 2, 2) and λ 4783.43 (I 2, 2).

Mn II The evidence is very uncertain. Strong laboratory lines such as λ 4206.43, λ 4251.77, and 4259.26 are absent. λ 4282.50 falls between a strong *Fe* I line, λ 4282.41, and a *Ca* I line, λ 4283.01. λ 4326.71 may be a contributor to λ 4326.93.

Fe I (26) The lines of neutral iron dominate the spectrum. Lines of intensity 3 in the sun are usually visible in δ Cephei. The greater number of neutral iron lines are, however, blended. A list of unblended *Fe* I lines is given here.

Fe I CLASSIFIED—UNBLENDED

λ	I		λ	I		λ	I	
	Max.	Min.		Max.	Min.		Max.	Min.
4062.45	1.5	1	4175.64	1	.5	4325.77	2	2
4074.79	1.5	2.5	4176.57	1	.5	4375.93	1	1
4084.51	0	.5	4187.81	2	0	4383.55	2	1.5
4107.49	2	2	4199.97	0	1	4466.56	1	2
4147.68	2	2.5	4210.36	2	1.5	4504.85	0	.5
4157.78	2	1.5	4260.49	3	3.5	4602.95	1	1
4174.92	.5	0	4266.97	0	.5	4736.79	2.5	3

Fe I UNCLASSIFIED—UNBLENDED

λ	I		λ	I	
	Max.	Min.		Max.	Min.
4059.72	1	1	4285.44	.5	0
4213.65	2	1.5	4346.55	0	.5
4220.34	1	1			

Fe II — Represented by several multiplets. A fairly large percentage of lines are unblended:

λ	I		λ	I	
	Max.	Min.		Max.	Min.
4138.36.....	1	0	4520.24.....	2	2.5
4416.81.....	1	.5	4541.52.....	1.5	1.5
4491.41.....	2	2.5	4576.31.....	1.5	1
4508.29.....	2	1.5	4620.52.....	1	1
4515.34.....	2	2	4731.49.....	1.5	1.5

Co I (27) — The evidence is rather uncertain, since no unblended lines are found. The stronger *Co* I lines, such as λ 4118.78 and λ 4121.33, may well be contributors to the stellar lines λ 4118.60 and λ 4121.48, respectively.

Ni I (28) — A small number of neutral nickel lines are probable contributors. λ 4714.42 (I 2, 2) is unblended.

Ni II — The lines λ 4015.50 and λ 4067.04 are possibly present, but are blended.

Zn I (30) — λ 4680.20, if present, is blended with *Fe* I. Two other strong laboratory lines, λ 4722.16 and λ 4810.54, fall outside the useful range of the spectrum.

Sr I (38) — λ 4607.34, a strong ultimate line, may be faintly present in λ 4607.62, and may tend to decrease the wave-length of the *Fe* I line at λ 4607.66.

Sr II — λ 4077.71 and λ 4215.52 are probably the principal contributors to the respective stellar lines. λ 4161.81 and λ 4305.46 are blended with other strong lines.

Y I (39) — The evidence is very weak. Probably absent.

Y II — λ 4177.54 is an important contributor to the stellar line λ 4177.61 but is blended. The situation is similar with respect to λ 4374.95, which is blended with *Sc* II and *Ti* II. Several other blended lines are present.

Zr I (40) — Probably absent.

Zr II — Represented by a fair number of lines which are blended, except λ 4211.85 (I 2, 1.5).

Ba II (56) — λ 4554.04 is a strong, unblended line (I 1.5, 2).

La II (57) — Probably present as a contributor in a number of stellar lines such as λ 4031.70, λ 4086.72, λ 4333.77, and λ 4429.90. The evidence for the presence of the rare earths is very uncertain. While there are numerous coincidences of laboratory and stellar lines, the lack of classified multiplets would make identification almost impossible, if

many lines in the sun, the chromosphere, and α Persei had not been attributed to the rare earths.

Ce II (58)	Numerous coincidences, all blended except λ 4486.91 (I 0, .5).
Pr II (59)	Several coincidences, all blended.
Nd II (60)	Several coincidences, all blended.
Sa II (62)	Several coincidences, all blended.
Eu II (63)	Several coincidences, all blended. The lines at λ 4129.73 and λ 4205.05 are possible contributors to the stellar lines at λ 4129.65 and λ 4205.20.
Gd II (64)	A few coincidences, all blended.
Dy II (66)	Several coincidences, all blended.
Er II (68)	λ 4015.61, unidentified in the sun, may be *Er* II. May contribute to stellar line λ 4015.56.
	Numerous unidentified solar lines coincide with stellar lines. Two are unblended: λ 4188.74 (I 1, .5) and λ 4413.60 (I 1, 1).

P. Swings and O. Struve[14] have concluded that the bands of *CH* and *CN* disappear at spectral class F8. Swings,[15] on microphotometer tracings of the Yerkes Observatory series of single-prism spectrograms of δ Cephei, has measured the absorption due to *CN* molecules at λ 4192.574 and λ 4197.102, and that due to *CH* molecules in the region λ 4310.4 to λ 4312.7.

The writer, when measuring all visible lines objectively without regard to their identifications, did not record as individual lines such strong lines of *CN*, unblended in the sun, as λ 4180.81 (2N), λ 4189.57 (2), λ 4192.57 (2N), and λ 4197.10 (2). A stellar line was measured at λ 4193.51, which is strengthened at minimum (I 0, 1.5). It lies almost 1 A to the red of the strong *CN* line λ 4192.57, although several faint *CN* lines are listed in this neighborhood in the sun.

Similarly, the writer did not record as individual lines such strong lines of *CH* as λ 4293.12 (3), λ 4310.38 (2), λ 4311.17 (2), λ 4311.45 (2), λ 4311.72 (2N), λ 4312.09 (2), λ 4313.63 (2Nd?). There remain coincidences, as λ 4279.72 (2Nd?) and λ 4280.97 (1) with a stellar line at λ 4280.63 which shows unusual variation (I 1, 4).

While these lines have not been observed individually on the spectrograms, it is quite probable that, if present, they would produce a

[14] P. Swings and O. Struve, *Physical Review*, **39**, 142, 1932; P. Swings, *Monthly Notices of the Royal Astronomical Society*, **92**, 140, 1931.

[15] *Loc. cit.*

weakening in the continuous background more easily observed on microphotometer tracings, as shown by Swings.

Three unidentified solar lines recently attributed by Richardson[16] to *CN* bands—λ 4169.62, λ 4217.26, and λ 4268.11—are listed as possible minor contributors to lines in δ Cephei.

V. VARIATION IN INTENSITY OF LINES

The accompanying list shows the average intensity of unblended lines at maximum and minimum, grouped according to elements. The number of unblended lines used is given in column 2.

Element	No. of Lines	I		Element	No. of Lines	I	
		Max.	Min.			Max.	Min.
H (1)	1	6	4.5	*Ti* II (22)	11	1.6	1.8
Mg I (12)	2	2.5	2.8	*V* II (23)	2	1	.5
Ca I (20)	1	1	2	*Cr* II (24)	3	1.7	1
Cr I (24)	3	1.5	1.3	*Fe* II (26)	10	1.6	1.4
Mn I (25)	2	2	2	*Zr* II (40)	1	2	1.5
Fe I (26)	26	1.3	1.3	*Ba* II (56)	1	1.5	2
Ni I (28)	1	2	2	*Ce* II (58)	1	0	.5
Sc II (21)	1	1	2				

Two unidentified solar lines are of average intensity 1 and 0.8 at maximum and minimum respectively.

The evidence from these few unblended lines shows no outstanding variation of intensity with phase, with the exception of *H*, *Ca* I, *Sc* II, *Cr* II.

In the accompanying table those blended lines showing a variation of $1\frac{1}{2}$ units or more are listed, with their probable contributors in order of their importance, in two groups: (A) lines strengthened at minimum; (B) lines strengthened at maximum.

Ca I contributes largely to λ 4435.29 and λ 4454.78.

Ti I is an important contributor to four lines.

Cr I is listed as a contributor to ten lines, and is an important contributor to seven lines.

Cr II contributes to seven lines, but is an important contributor to only one line, λ 4616.46.

[16] R. S. Richardson, *Astrophysical Journal*, **77**, 195, 1933.

λ	No. of Plates	I		Contributors
		Max.	Min.	
	A. Blended Lines Strengthened at Minimum			
4017.28	4	1	2.5	*Fe* I, ⊙, *Fe* I, *Ni* I
4020.22	1	0	1.5	⊙, ⊙, *Sc* I, *Co* I
4055.00	4	2	3.5	*Ti* I, *Fe* I, *Fe* I, *Mn* I, *Fe* I, *Sc* I, *Zr* I
4067.03	4	3.5	5	*Fe* I, *Fe* I, *Fe* I, *V* II, *Ni* II.
4069.13	2	0	1.5	⊙, *Nd* II, *Ce* II
4080.12	2	0	3	*Fe* I, *Fe* I, *Cr* I, *Nd* II
4083.35	4	2	4	*Mn* I, *Fe* I, *Mn* I, *Ce* II, *Pr* II, *Mn* I, *Fe* I
4088.86	4	1	3	*Fe* II, *Fe* I, *Fe* I, *Cr* II, *Ce* II
4090.40	3	.5	2.5	*Fe* I, *Fe* I, *Zr* II, *V* I, *Ce* II
4103.07	2	0	2	*Si* I, *Dy* II
4106.32	4	1.5	3	*Fe* I, *Fe* I
4114.63	2	2	4	*Fe* I, *V* I, *Fe* I
4116.81	3	.5	2.5	*V* I, *Nd* II, *V* I, *Ce* II, *Fe* I
4129.65	2	0	2	*Eu* II, ⊙, *Eu* II
4134.58	4	2.5	4	*Fe* I, *Fe* I, *Fe* I, *V* I
4137.22	4	2	4	*Fe* I, ⊙, *Ce* II
4165.48	4	1.5	3	*Fe* I, *Ce* II
4187.09	4	2.5	4	*Fe* I, *Ce* II, *Dy* II
4193.51	2	0	1.5	*Ce* II, *Ce* II, *Ce* II
4207.02	4	2	3.5	*Fe* I, *Fe* I, *Cr* II
4229.68	4	1	2.5	*Fe* I, *Fe* I, *Cr* II
4256.14	4	1	3	*Dy* II, *Sa* II, *Ce* II, *Fe* I
4258.32	4	2.5	4	*Fe* I, *Fe* II, *Zr* II
4280.63	3	1	4	*Fe* I, *Cr* I, *Mn* I, *Sa* II, *Fe* I, *Sc* II, *Sa* II, *Cr* II, *Gd* II, *Sa* II, *Cr* II
4300.18	3	2.5	4	*Ti* II, *Ce* II, *Ti* I
4417.99	4	2.5	4	*Ti* II, *Ti* II
4430.31	4	1.5	3	*La* II, *Fe* I
4435.29	4	2.5	4	*Ca* I, *Ca* I, *Fe* I, *Eu* II, *Eu* II
4454.78	4	2	3.5	*Ca* I, *Fe* I, *Zr* II, *Ca* I, *Mn* I, *Ti* I, *La* II, *Fe* I
4479.90	2	0	1.5	*Fe* I, *Fe* I, ⊙, *Ce* II
4494.48	4	1.5	3	*Fe* I, *Zr* II
4496.81	4	1	2.5	*Cr* I, *Zr* II, *Ti* I
4518.16	4	1	2.5	*Ti* I, *Ti* II
4544.74	4	2	3.5	*Ti* I, *Ti* II, *Cr* I, *Cr* I, *Ti* II, *Sa* II, *Cr* II
4574.83	2	0	1.5	*Fe* I, *La* II
4580.12	4	1	2.5	*Cr* I, *La* II, *Ti* II, *V* I
4616.46	4	2	3.5	*Cr* I, *Cr* II
4647.42	2	0	5	*Fe* I, ⊙, *Cr* I, *Cr* I
4651.79	3	.5	2	*Cr* I, *Cr* I
4656.96	4	2	3.5	*Ti* I, *Fe* II, *Ti* II
4663.34	4	1	2.5	*Ti* II, *Fe* II, *Cr* I, *La* II
4667.16	4	2	4	*Fe* I, *Fe* II, *Ti* I
4680.26	2	0	1.5	*Fe* I, *Zn* I, *Fe* I
4698.60	4	1.5	3	*Cr* I, *Cr* I, *Cr* II
4727.76	3	.5	2	*Fe* I, *Fe* I, *Mn* I
	B. Blended Lines Strengthened at Maximum			
4173.61	3	2.5	1	*Ti* II, *Fe* II, *Fe* I, *Fe* I

Fe I appears in twenty-nine lines, and is an important contributor to twenty-six lines.

Ce II contributes to twelve lines, and is an important contributor to two lines.

Sa II contributes possibly to three lines, of which λ 4256.14 and λ 4280.63 are exceptionally strengthened at minimum.

Eu II contributes to two lines, and is probably largely responsible for the variation of λ 4129.65.

In addition to these forty-six blended lines showing a variation in intensity of $1\frac{1}{2}$ units or more, there are numerous lines with a variation of 1 unit which may be found by an inspection of Table I. An important fact is that the greater number of lines showing a variation in intensity are stronger at minimum rather than the opposite.

It would appear that there are two distinct groups of lines which may be responsible for the strengthening of blended lines at minimum. First, lines of neutral *Ca*, *Ti*, *Cr*, and *Fe;* second, lines of the rare earths. The first group comprises elements whose lines are usually stronger in the sun-spot spectrum. The second group contains elements whose lines are often strengthened in the chromosphere. Examples are *Ce* II, λ 4193.12 and λ 4193.28, of intensity −1d? and −1 in the sun, and of intensity 2N in the chromosphere, disregarding the influence of the *CN* lines nearby. The *Eu* II line at λ 4129.73, of intensity 1 in the sun, is of intensity 6 in the chromosphere. The behavior of these lines in the sun and in the chromosphere is closely paralleled by their behavior in δ Cephei at maximum and minimum.

Considering as a whole blended and unblended lines, the changes in the spectrum of δ Cephei appear closely linked with the variations of temperature and perhaps of pressure in its atmosphere.

The variation of line intensities has been studied by several different investigators. References to important papers may be found in Miss Payne's monograph,[17] chapter xiv, and in Whipple's paper,[18] page 13. There is, in general, satisfactory qualitative agreement as to the variation in intensity of the stronger lines, estimated visually by the writer on the original spectrograms, as compared with measurements of line breadth or depth on microphotometer tracings. The latter method is, of course, superior to visual estimates, at least for the stronger lines, and is to be employed for quantitative studies.

[17] *Loc. cit.* [18] *Loc. cit.*

It is a pleasure to express my gratitude to Dr. Otto Struve, who suggested the problem and placed at my disposal the spectrograms and facilities of the Yerkes Observatory. I am indebted to Miss C. E. Moore, who kindly read the manuscript and made numerous valuable suggestions concerning notation and identifications, and to Mr. W. A. Ulrich and Misses V. Gregg and V. Wolken, who assisted very ably in the preparation of the manuscript. Publication of this study was made possible, in part, by a grant from the Society of Sigma Xi, to whom grateful acknowledgment is made.

ST. LOUIS UNIVERSITY
ST. LOUIS, MO.
April 12, 1933

THE HYDROGEN LINE WIDTHS IN 5 κ DRACONIS

By RALPH N. VAN ARNAM

ABSTRACT

Contours of $H\beta$, $H\gamma$, and $H\delta$ from twelve spectrograms of 5 κ Draconis, in which double emission components are superposed on the absorption contour of $H\beta$, fail to show correlation between intensity of emission and width of absorption wings. This is taken as added evidence in support of the hypothesis that these lines originate at different levels in the star.

The rotational hypothesis of the production of emission lines in B-type spectra postulates the existence of a very extensive atmosphere or rotating nebulous shell of gas above the photospheres of B stars. This mechanical interpretation of the doubling and broadening of bright lines, which are believed to be produced by recombination above the reversing layer of the star, was proposed by Otto Struve[1] as a consequence of his earlier work on stellar rotation. As developed by Struve and his collaborators,[2] the rotational hypothesis appears to give a satisfactory explanation for most of the characteristics of the bright lines in early type spectra. It meets with some difficulty in accounting for the relative intensities of the double components of emission and the actual disappearance of these lines at times in certain peculiar Be spectra. In this connection the suggestions of atmospheric pulsation combined with rotation advanced by D. B. McLaughlin[3] are of interest.

If we are to believe that the emission lines originate in a different layer of gas from that which gives rise to the absorption lines and that the former are superposed upon the latter in the spectrum, it is difficult to see why there should be any relation between the intensities or widths of the two types of lines. In a recent paper Struve[4] points out that the establishment of this lack of correlation between the contours of the emission and absorption lines is a necessary con-

[1] *Astrophysical Journal*, **73**, 94, 1931; *Zeitschrift für Astrophysik*, **4**, 177, 1932.

[2] Struve and Schwede, *Physical Review*, **38**, 1195, 1931; Struve and Swings, *Astrophysical Journal*, **75**, 161, 1932.

[3] *Publications of the American Astronomical Society*, **7**, 31, 1931.

[4] *Astrophysical Journal*, **76**, 309, 1932.

dition which his rotational hypothesis must satisfy. From the study of a considerable number of $H\beta$ and $H\gamma$ contours from Be spectra he shows that their absorption wings are closely akin to those of the same lines in B stars which are rotationally broadened but in which emission is absent.

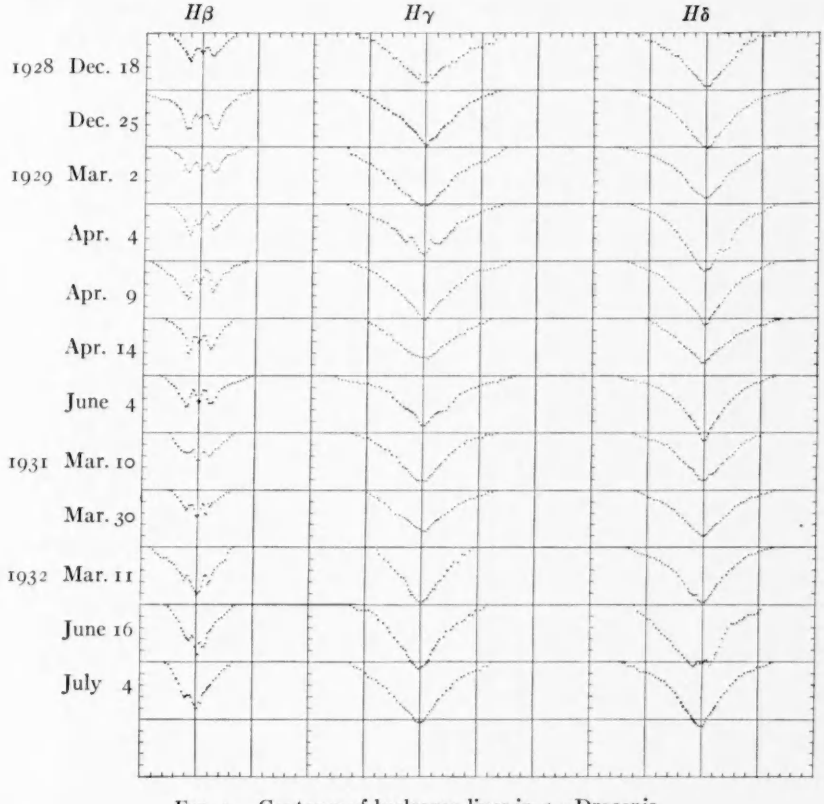

FIG. 1.—Contours of hydrogen lines in 5 κ Draconis

It now becomes of interest to study the widths of the absorption wings of the Balmer hydrogen series in B stars the spectra of which are not only complicated by emission, but in which the emission is known to be changing in intensity with the passing of time. Such a star is 5 κ Draconis.[5]

Using the Yerkes thermoelectric microphotometer, I have ob-

[5] R. H. Baker, *Publications of the Observatory of the University of Michigan*, **3**, 29, 1923; Curtiss and Petrie, *ibid.*, **4**, 171, 1932; Struve, *Popular Astronomy*, **33**, 596, 1925.

tained the contours of three hydrogen lines on twelve spectrograms of this star. Many other plates in the Yerkes collection were unsatisfactory for the purpose, either because of lack of standardization or because of unsuitable emulsion. In Figure 1 I show these contours arranged in chronological order.

The dots represent individual measures. No attempt was made to smooth out the inevitable errors due to imperfections in the plates

TABLE I

LINE WIDTHS IN A.U. AT 10 PER CENT ABSORPTION

Date	$H\beta$	$H\gamma$	$H\delta$
1928 Dec. 18	16.0	19.0	15.5
Dec. 25	21.0	17.5	17.5
1929 Mar. 20	15.0	22.5	16.5
Apr. 4	16.0	18.0	16.5
Apr. 9	21.0	17.5	17.5
Apr. 14	15.0	15.5	14.5
June 4	17.0	16.5	16.0
1931 Mar. 10	16.0	15.0	13.5
Mar. 10	12.5	14.0	14.5
1932 Mar. 31	21.0	13.0	15.5
June 16	17.0	16.5	18.0
July 4	16.5	18.0	17.0

and in the microphotometer tracings. The ordinates represent percentages of absorption of the continuous spectrum with 10 per cent divisions in the scale. The abscissae represent angstrom units measured from the center of the line. Each scale division corresponds to four A.U. for $H\beta$ and two for $H\gamma$ and $H\delta$.

A cursory inspection of the $H\beta$ contours indicates the dying-out of the double-emission line with time. In view of this it seemed unnecessary to obtain the emission contours by extrapolation of the absorption wings. Moreover, the diminution in the intensity of the emission agrees with the recent work of M. K. Jessup,[6] who finds a minimum for $H\beta$ emission in 1932. Emission is absent, or nearly so, in the $H\gamma$ and $H\delta$ contours.

In Table I, I show the measured line widths in A.U. derived from the contours at 10 per cent absorption of the continuous spectrum.

[6] *Astrophysical Journal*, **76**, 75, 1932.

Since the absorption wings become asymptotic to the level of the continuous spectrum and very uncertain on the traces, an attempt at measurement of widths at the continuous spectrum would be quite inconclusive.

An inspection of the measures or of the contours themselves shows the absence of any definite trend in the line widths and no correlation with the intensity of the emission. It appears that this result gives added confirmation of Struve's conclusion, obtained from a study of Be spectra in which the emission is fairly constant in intensity. The non-correlation between the emission intensities and absorption line widths is strong evidence that these lines originate in different layers in the star.

YERKES OBSERVATORY
June 19, 1933

REVIEWS

Amateur Telescope Making. Edited by ALBERT G. INGALLS. 3d rev. and enlarged ed. Pp. 500+xii. New York: Scientific American Publishing Co., 1933. $3.00.

The authors and editors are to be commended on this splendid work. It is an excellent reference book and encyclopedia of telescope making.

A few minor errors and omissions may be noted. On page 40 the author gives instructions for making the declination circle as follows: "Every tenth division is made larger than the others and numbered, starting with zero at the middle of the strip and increasing to 180 either way." This is not strictly correct. The circle should be numbered from 0 to 90 and back to 0 on each half. A working drawing, with proper dimensions, of a simple pill-box observatory, or some other type, would be of help to any beginner. There is no mention made of the different types of observing ladders which are very necessary for reflecting telescopes, especially the Newtonian. Photographs and descriptions of parts of the 100-inch telescope are perhaps out of place in this book. A chapter or two might have been devoted to some of the astronomical observations done by active amateurs of today. The book list does not contain any works on the moon and planets.

Part XI, "Miscellany," contains a wealth of information. This, together with Part II, ought to enable anyone to grind a mirror without difficulty. The discussion of equatorial mountings shows the ingenuity of the amateurs in the use of inexpensive materials.

The book should be in the hands of every amateur whether or not he intends making a telescope.

R. N. BUCKSTAFF

Mirrors, Prisms and Lenses. By J. P. C. SOUTHALL. New York: Macmillan Co., 1933. 8vo. Pp. xxiv+806. Figs 329. $4.50.

This is the third edition of a college textbook on geometrical optics, the second edition of which appeared in 1923. Two new chapters dealing largely with physiological optics have been added, increasing the size of the book to some 806 pages. Numerous problems for college students are given at the end of each chapter.

F. E. ROSS